PANIC

PRELIMINARY DESIGN REPORT

Code :	PANIC-GEN-SP-01
Issue/Rev. :	0/1
Date :	22 October 2007
No. of pages :	183

Approval control

Prepared by	Vianak Naranjo Harald. Baumeister Werner Laun Ulrich Mall Matthias Alter Clemens Storz Jens Helmling M. Concepción Cárdenas Vázquez José Miguel Ibáñez Mengual Matilde Fernández Josef W. Fried	**MPIA** **MPIA** **MPIA** **MPIA** **MPIA** **MPIA** **CAHA** **IAA** **IAA** **IAA** **MPIA**
Revised by	Josef W. Fried Julio Rodríguez	**MPIA** **IAA**

Max-Planck-Institut für Astronomie (MPIA)

Instituto de Astrofísica de Andalucía (IAA)

Changes record

Issue	Date	Section	Page	Change description
0/0	17/10/07	All	All	First writing
0/1	22/10/07	All	All	Wording Revising

Applicable documents

Nº	Document title	Code	Issue
1	O2000 User's Manual		2.6 Oct 2005
2	PANIC SCIENTIFIC REQUIREMENTS	PANIC-GEN-RQ-00	02

Reference documents

Nº	Document title	Code	Issue
RD1	PANIC SCIENTIFIC REQUIREMENTS	PANIC-GEN-RQ-00	0/2
ORD2	Signal to Noise cases	PANIC-OPT-TN-00	00
ORD3	Second Pixel Scale study	PANIC-OPT-TN-03	02
ORD4	Glass Catalogue	PANIC-OPT-TN-04	00
ORD5	Tolerance analysis	PANIC-OPT-TN-05	00
ORD6	Optical AIV, Preliminary Design AIV	PANIC-OPT-TN-06	00
RD7	Fruchter, A. S., Hook, R. N., 1997, "A method for the Linear Reconstruction of undersampled Images", PASP; astro-ph/9808087,		

List of acronyms and abbreviations

2MASS	Two Micron All Sky Survey
ADC	Analog Digital Converter
AGB	Asymptotic Giant Branch
AIV	Assembly-Integration-Verification
AR	Anti-Reflection
CA	Calar Alto
CAHA	Centro Astronómico Hispano Alemán
CAN	Controller Area Network
CDR	Critical Design Review
CDS	Correlated Double Sampling
COMBO	Classifying Objects by Medium-Band Observations
CPU	Central Processor Unit
CSE	CircumStellar Enveloppe
D	Distortion
DAC	Digital Analog Converter
DHS	Data Handling Software
DMA	Direct Memory Access
DRS	Data Reduction Software
EE	Ensquared Energy length square side
EFL	Effective focal length
EMC	ElectroMagnetic Compatibility
EN	Eurpäische Norm
EPICS	Experimental Physics and Industrial Control System
ESD	Electrostatic Discharge
FEA	Finite Elements Analysis
FIFO	First In First Out
FOV	Field of View
FPA	Focal Plane Assembly
FPGA	Field Programmable Gate Array
FWHM	Full Width Half Maximum
GEIRS	Generic Infrared Software

GEIRS	Generic InfraRed detector readout Software
GRB	Gamma Ray Burst
GUI	Graphical User Interface
H2RG	HAWAII-2RG
HW	Hardware
IAA	Instituto de Astrofísica de Andalucía
ICS	Instrument Control Software
IEC	International Electrotechnical Commission
IQ	Image Quality
L0	Lens number 0 of the PANIC optics system
L1	Lens number 1 of the PANIC optics system
L2	Lens number 2 of the PANIC optics system
L3	Lens number 3 of the PANIC optics system
L4	Lens number 4 of the PANIC optics system
L5A	Lens number 5 of the PANIC optics system in the 0.45"/px scale
L5B	Lens number 5 of the PANIC optics system in the 0.25"/px scale
L61B	Lens number 7 of the PANIC optics system in the 0.25"/px scale
L6A	Lens number 6 of the PANIC optics system in the 0.45"/px scale
L6B	Lens number 6 of the PANIC optics system in the 0.25"/px scale
L7A	Lens number 7 of the PANIC optics system in the 0.45"/px scale
L7B	Lens number 8 of the PANIC optics system in the 0.25"/px scale
L8A	Lens number 8 of the PANIC optics system in the 0.45"/px scale
L8B	Lens number 9 of the PANIC optics system in the 0.25"/px scale
LAS	Large Area Survey
M1	First folding mirror inside the instrument
M2	Second folding mirror inside the instrument
M3	Third folding mirror inside the instrument
MBE	Molecular Beam Epitaxy
MOCON	Motion Controller
MPIA	Max Planck Institute for Astronomy
MSPS	Mega Sample Per Second
N/A	Non Applicable
NIR	Near InfraRed

ORD	Optics' Reference Document
OT	Observation Tool
PANIC	**PA**noramic **N**ear **I**nfrared camera for **C**alar Alto
PC	Personal Computer
PCB	Printed Circuit Board
PCI	Peripheral Component Interconnect
PCS	PANIC Control System
PDCS	PANIC Detector Control System
PDR	Preiliminary Design Review
POD	Preliminary Optical Design
PSF	Point Spread Function
PWM	Puls Width Modulation
QSO	Quasi Stellar Object
RC	Ritchey-Chrétien
RESMOD	Resolver Module
RMS	Root Mean Square
ROC	Radius of Curvature
ROE	ReadOut Electronics
S1	Telescope Primary mirror
S2	Telescope Secondary mirror
SDSS	Sloan Digitized Sky Survey
SED	Spectral Energy Distribution
SMD8	Stepper Motor Driver for 8 Axis
SRAM	Static Random Access Memory
SW	Software
TBC	To be confirmed
TBD	To be decided
TNO	Trans Neptunian Object
UKIDSS	United Kingdom Infrared Deep Sky Survey
UML	Unified Modeling Language
UNIMOD	Universal Module
WFCAM	Wide Field Camera (UKIRT)

CONTENTS

LIST OF FIGURES

LIST OF TABLES

1. PANIC GENERAL

1.1 Introduction

The greatest strength of the Calar Alto observatory is its up-to date instrumentation. Whereas the 3.5m telescope is well equipped with modern instruments, the 2.2m telescope is lacking modern instrumentation; an exception is the lucky imager Astralux, but this is a special purpose instrument for a limited range of applications.

A survey on instrumentation wanted for Calar Alto at MPIA and IAA came independently to the same result, i.e. a NIR (0.9 to 2.5 microns) imager for the 2.2m telescope. It is obvious that an instrument with a single 2x2 k detector is not state of the art, so a mosaic of 4 detectors was envisaged. Science applications would obviously be wide field (>1 square degree) imaging and surveys, but a collection of ideas at IAA and MPIA showed that there are many very interesting applications also for single pointed observations. The Calar Alto Instrumentation Committee recommended to build such an instrument. In October 2006 the project PANIC (**Pa**noramic **N**ear **I**nfrared Camera for **C**alar Alto) was started. It is a joint project between IAA and MPIA.

One may argue that an instrument like PANIC should be installed at the 3.5m telescope. Obviously the 3.5m telescope is more powerful; however, observation time is much more readily available at the 2.2m telescope, so the disadvantage in light collecting power by a factor of (2.2/3.5)**2 = 0.4 can be compensated by integration time. Omega 2000 at the 3.5m telescope is clearly a competing instrument. However, Omega 2000 does not have a cold entrance pupil and hence has a high thermal background in the K-bands. It is expected that PANIC, which will have a cold stop, will be more sensitive than Omega2000, and since PANIC has a four times larger FOV it will be more efficient by factors of a few than Omega2000 in the K-bands.

PANIC will not be the first instrument of its kind. Competing instruments at telescopes < 4m are WFCAM at UKIRT, NEWFIRM at Kitt Peak 4m telescope, and WIRCAM at CFHT. In the southern hemisphere, VISTA (4m telescope) has a 64 Mpixel camera that will cover 2154 square arcmin, its operation shall start mid 2008. It is obvious that because of these competing instruments the development of PANIC should be fast. However, the proposed science cases for PANIC show that interesting science can be done with it, even if it is not unique.

1.2 General Requirements

The general requirements that were clear from the start are:

- Detector size 4096x4096 pixel
- Spectral range NIR, i.e. minimum YJHK
- Image scale 0.45 arcsec/pixel
- 2.2m telescope

Additional obvious requirements are

- Instrument must not exceed limits set by the telescope in size and weight
- Flexure of the instrument must not degrade optical quality
- Power dissipation should be kept as low as possible, goal < 200W
- The standard guiding unit on the telescope can not be used since it would vignette the field of PANIC. So PANIC must have its own guiding system.

1.3 Design Aspects

These requirements have direct consequences on the design of PANIC:

- The optical train is much longer than the maximum allowable length of the instrument along the optical axis. This requires a folded design. The lateral dimension is not critical.
- The weight limit is a very severe one. According to the original ZEISS documentation, the weight limit is 300kg at the focus. This has led us not to follow the commonly used design with two nested tanks, rather our design uses one super-isolated tank with one small tank to cool the detector. However, both CAFOS and WFI at the twin telescope on LaSilla exceed this limit without any degradation in telescope performance. Including the guider unit, CAFOS weighs 400kg and has a torque of 1860Nm. We take these values as safe limits.
- The operating temperature of the detectors is in the range 77-80K, the optimum temperature has to be found by experiment. From experience with other Rockwell detectors we expect that the operating temperature should be stable to ± 0.1K.
- The cooling system should require as little attention as possible. Since liquid Nitrogen cooling requires only refilling, we decided to use nitrogen cooling. We are aiming at holding times longer than 24 hours, although Calar Alto would accept refilling twice a day.
- We try to benefit from experience gained with Omega2000 as much as possible:

- Mechanical detail solutions, such as lens holders and filter wheel mechanics, will be taken over with minimal changes
- The read-out electronics is a further development of the older MPIA ROE, using newer and cheaper ICs. Furthermore the new ROE will read out 132 channels, compared to 36 in Omega2000.
- The control electronics will use modules which are standard at MPIA/CAHA and are in use not only in Omega2000, but also in several other instruments on Calar Alto. This will reduce not only the time required for development but also has obvious advantages for documentation, spare parts stock and know-how on Calar Alto.

1.4 Additional Features

While designing PANIC, several additional features were proposed which go beyond the basic requirements. The ones we followed up are:

- Extend the spectral range to 0.82 microns, so PANIC will cover all spectral bands from the z to K. The z-band has been included for convenience of the observers, in order to allow z-band observations to complement NIR observations without changing instrumentation or waiting for another instrument to be mounted. The applications of PANIC, however, are in the NIR.

- The use of narrow band (bandwidth = 1% of central wavelength) filters. This requires that the angle of incidence of the beam does not exceed a certain value. Our optical design takes this into account.

- A second pixel scale of 0.25 arcsec/pixel. This image scale will allow higher spatial resolution and will be very useful under good seeing conditions which prevail frequently since the median seeing at Calar Alto is 0.89 arcsec in the R band which corresponds to 0.65 arcsec in the K band. An optics wheel to exchange some parts of the optics allows to change between the two image scales. A major difficulty imposed by the optics is the high mechanical precision required in positioning this wheel – 0.45 microns (see mechanics section). However, close to the date of submitting the PDR documents, it finally turned out that PANIC with 2 image scales well exceeds the 400kg limit. We estimate the difference in mass between a single and two pixel scale instrument to 80-100 kg. This is so because not only additional hardware is need but also a larger cryostat with thicker walls, requiring additional Nitrogen because of increased heat input. We are currently testing the performance of the telescope with additional weights. A design with only one pixel scale is also presented; this clearly avoids the weight problem and exceeds the torque only slightly, and the mechanical tolerances are relaxed.

2. SCIENCE CASES

We list below potential scientific cases that would benefit from the panoramic imaging mode of this camera. More details for some of them can be found in the Phase A document, section 2. A (non-exhaustive) compilation of science cases that would benefit from the other TBC observing modes is also given.

2.1 Extragalactic Astronomy

2.1.1 Extragalactic Surveys

Cosmic evolution in the z range 1.5 – 2.0 can be studied through surveys of specific areas in the sky in the clean windows of z and J bands, which enormously reduce the background sky contained in the OH lines originated in the high levels of the atmosphere, as compared with the corresponding broad band filters. Photometric redshifts would then be systematically derived in the so called redshift desert.

A wide-field survey covering the SDSS area not contained in the UKIDSS LAS would provide highly resolved NIR images of the local galaxy population, including studies of bars, lopsidedness, population gradients and bulge/disk decomposition. Rare objects, as T+ dwarfs and $z \geq 6$ QSOs could be other science goals.

The NIR part of COMBO-17+4 could be completed in 12.5 clear nights.

A deep NIR photometric survey, for sample selection and characterization, would be also of interest as a previous step for the exploitation of the EMIR NIR multi-object spectrograph, a common-user instrument for Grantecan.

Characterization of distant galaxies will also benefit from a high-resolution imaging mode.

2.1.2 GRBs

2.1.2.1 GRBs at high redshift

The detection of GRBs at redshifts beyond $z > 7$ is currently one the major astrophysical challenges, due to its deep implications in the reconstruction of the history of the Universe. However, at redshifts $z > 5$ the Lyman-α blanketing prevents the detection of their optical afterglows, so near-IR observations are required for their identification. The determination of photometric redshifts is viable with simultaneous multiband observations carried out with medium-class telescopes like the 2.2m Calar Alto telescope.

2.1.2.2 GRB host galaxies

A dedicated multicolour imaging program running at the 2.2m would allow, for the first time, to compile a homogeneous large sample of GRB host galaxies and to apply statistical methods to construct the SED of GRB host galaxies brighter than $R < 24$ using photometric points. From the fit of the SED we would infer information about the following quantities: the photometric redshift, the age of the dominant stellar population, the extinction A_V, the galaxy-type, the favoured IMF, the total stellar mass of the host galaxy and the host galaxy environment.

2.1.3 Mapping of nearby galaxies

It is well known that at NIR wavelengths the effects of extinction are mitigated, while galaxy phenomena are hidden at shorter wavelengths. The following studies could be performed:

2.1.3.1 Morphological characterization

Multiple nuclei, bars, and boxy/peanut-shaped bulges become visible at NIR wavelengths. The wide field of PANIC is also particularly suitable for mapping the outer parts of galaxies, where flaring or warping occur. Extremely low surface brightness halo structures in nearby galaxies could be traced using red giants. A high-resolution imaging mode will provide access to nuclear parts of galaxies, e.g. photometric cusps used to measure the mass of the black hole.

2.1.3.2 Star formation and stellar populations

Studying dust-embedded star formation in nearby galaxies. Mapping in [SIII] 0.9069, 0.9532 μm, Paschen & Brackett series, H2, [FeII], CO band head, and their corresponding continua, would allow to study the excitation mechanisms in regions of active star formation, as well as detection of the shock effects and possible impact on the dust attenuation law. They could also be an interesting supplement to Spitzer data. It will be also possible to detect intermediate age populations in spiral arms by identifying AGB stars; their stellar photometry is of crucial importance for understanding and quantifying the importance of the AGB star contribution to the integral light of (unresolved) stellar populations in distant galaxies. Global progression of star formation throughout galaxies could be characterized obtaining accurate maps of the old stellar population mass and comparing them with star formation measurements.

2.1.3.3 Magnetic field

Polarimetric observations of nearby galaxies allow determining the large scale distribution of the magnetic field. At a nuclear level information on the geometry of the narrow and broad band line regions could be inferred. Polarimetric studies of extragalactic star forming regions will provide information on the dust distribution as well as on the energizing mechanism of the magnetic field in the thermal structure of the nebulae.

2.1.4 Distance scale

A measure of the near-IR period-luminosity relation of Cepheids in nearby galaxies as a function of the metallicity would improve the accuracy of extragalactic distance scales.

2.1.5 Searches for high-redshift quasars

A by product of large area multiband imaging could come the detection of high redshift ($z > 7$) quasars, based on the position of the Lyman−α break between the z and K-bands at $z > 7$. The high redshift quasar candidates would be subject of specifically planned spectroscopic observations.

2.1.6 Clusters and Superclusters of galaxies

Broad band observations of clusters and superclusters of galaxies would allow to search for objects with strong IR excess and/or the selection of candidates to supermassive starbursts in clusters at intermediate redshift making use of deep narrow band filter imaging matching their redshifted Hα line.

2.2 Galactic Astronomy

2.2.1 Galactic survey

A proper motion survey is proposed, using 2MASS as the first epoch, over a quarter of the sky, which will not be covered by any NIR imager. The larger depth of the survey would allow obtaining a better star/galaxy separation and photometry for all 2MASS objects and proper motion down to ≈ 10 mas·yr^{-1}.This catalogue would allow searching for population II very low-mass stars and brown dwarfs. This project is completed by the case explained in 2.3.4.

2.2.2 Galactic plane and bulge

The wide field of PANIC will allow mapping selected areas of the galactic plane and bulge. NIR imaging permits a detailed exploration of the large-scale structure of the Milky Way and the Galactic components in hidden areas of the Milky Way. There are still controversial or totally unknown parameters in the description of the detailed stellar structure, e.g. concerning the radial and vertical distribution of the Galactic disc, and its specific morphology. Halo streams across the galactic plane would be traced using colour-selected M-stars, as has recently been demonstrated to have spectacular effect by 2MASS.

2.3 Stellar evolution, star formation, exoplanets

2.3.1 Accretion disks of young stars

NIR monitoring of young stars, most of them low mass stars, show variations due mainly to changes of the innermost parts of the disk. Simultaneous zJHK photometry would allow studying the variability of the disk (H and K bands, and maybe the J band) at the same time that the stellar photosphere is monitored in the z band. Hot stellar spots, thought to induce the changes observed in the inner disk, leave also a fingerprint on the H and K bands that would be removed before that data are fitted by theoretical models of the disks. Polarimetric measures can provide in these systems information on the geometry of the system, since light becomes polarized after dispersion/reflection in structures like the inner cavities of the disk, etc.

2.3.2 Search for post-AGBs

Post-AGB stars are enshrouded by a dusty CSE which becomes optically thinner at NIR wavelengths. NIR emission is primarily emitted from the reddened photosphere and from light scattered by dust grains. Polarimetry would also allow discriminating between the faint polarised scattered light from the dusty envelope and the bright unpolarized emission from the central star. This enables the imaging of material that would normally be lost under the wings of the stellar PSF. It is possible to obtain information on the grain size distribution, extinction, equator-to-pole ratio density contrast and structure of the CSE via modelling the observations. This case would benefit from a high-resolution imaging mode.

2.3.3 Measures of stellar sizes

Lunar occultations in the IR allow to derive very high angular resolution (~1 mas) information to be used for: close binaries resolution, direct measure of stellar diameters, resolving objects with extended envelopes (T Tauris, carbon stars, etc). Narrow band filters will complement broad band ones as they allow a better resolution of diffraction fringes for bright stars. Fast read-out mode should be implemented for these applications.

2.3.4 Low mass objects, exoplanets

The wide field provided by this camera will allow performing efficient searches of faint brown dwarfs, and, specially, objects with planetary masses, either isolated or far from their parent star in open clusters.

2.3.4.1 Probing the IMF down to ~ 1-Jupiter mass. A deep star forming region survey.

The closest (not farther than 300 pc) and densest star forming regions will be surveyed, in order to detect 1-Jupiter mass objects and to extend the IMF of those regions to that limit. The different regions should also provide a wide range of initial conditions: stellar density, presence of hot stars, total mass, and/or age. The long integration times will be split into several epochs, along a few years, in the way of a photometric monitoring. This variability survey could detect new eclipsing binaries, transiting planets, stellar variability (rotational periods), etc.

2.3.4.2 Testing the brown dwarf ejection scenario: a survey around Bok globules.

Since in large star forming regions there is a problem in distinguishing the early brown dwarf halo from mass segregation due to interactions, it is advantageous to study the distribution of brown dwarfs around more isolated and much less massive systems containing only a few objects, like Bok globules.

A dozen Bok globules would be observed in three bands: J, H, and Ks, depending on sensitivity and contaminant rejection potential. Escaping brown dwarfs detections will be confirmed by spectroscopic and astrometric follow up.

2.3.5 X-ray binary counterparts

Identification of counterparts of X-rays binaries can be performed at NIR wavelengths, particularly of massive ones, so that high extinction areas towards the galactic disk and/or centre can be searched. Ellipsoidal variations due to perturbations in the shape of the donor star can be detected, and multiwavelength photometric data can be modelled to infer whether the emission is due to the companion star, accretion disc or a possible relativistic jet. This scientific case would also benefit from a polarimetric mode since the IR emission from X-ray binaries can be intrinsically polarised because of light scattered within the system or because there is a significant synchrotron emission at high frequencies from a compact jet.

2.3.6 Asteroseismology

Phase shifts between different colours increases significantly toward the infrared for non-radial pulsating stars. Time series analysis extended to the NIR increases dramatically the pulsation modes identification, allowing real asteroseismology of main sequence stars.

2.3.7 Supernovae searches

The large FOV of PANIC will allow observing large portions of individual clusters of galaxies, or even whole ones at the same time, boosting the rate of supernova detections. Once detected, multiband light curves (YJHK) could be constructed, a relevant issue for the calculation of the total SN luminosity.

2.3.8 Active stars

Photometric time series extended to the NIR constrain the theoretical models of active stars showing photospheric solar-like activity cycles and give information about differential rotation and temporal and/or spatial correlations between inhomogeneities at different atmospheric levels.

2.4 Solar system

2.4.1 Trans-Neptunian's, minor bodies

A survey to study NIR colors and short-term variability of a good sample of TNOs, centaurs and other minor planets could be performed with PANIC, together with a search for very slowly moving objects in the largest possible fraction of the sky, at least ± 30 degrees above the ecliptic. For that goal, the 2MASS archive would be used as the initial epoch.

2.4.2 Comets

The most visible and distinctive features of comets are the dust coma and tail: the refractory material reflects the solar radiation at every wavelength from the near-UV to the sub-mm range. Systematic observations of comets belonging to different families can be performed in order to follow the comet activity, the dynamical and compositional evolution of the dust coma and tail, and gas coma as a function of the heliocentric distance. In the case of the dust, by fitting the observed image with images synthetically generated by a dust dynamical model, it is possible to put constraints in the distribution of the dust size and terminal velocity. Making use of cometary images in several continuum filters, the dust colour can be measured as a function of the projected cometocentric distance as well as a function of the heliocentric distance. The dust colour, combined with similar measurement in the optical range, allow constraining the mineralogical composition of the dust grains. If polarimetry is also provided, most of the uncertainties arising from the dust colour analyses can be cleared up.

2.5 JUSTIFICATION FOR A SECOND PIXEL SCALE

The need of a smaller pixel scale is given by the fact that the average seeing at Calar Alto in the V band is 0.9" (S.F. Sanchez, J. Aceituno, U. Thiele, D. Perez-Ramirez, J. Alves, arXiv:0709.0813, "The night-sky at the Calar Alto Observatory"), that is, 0.67" in the K band. From Sanchez et al.'s Fig.5 one can compute that 51% of the nights have seeing ≤0.67" in the K band. During these nights the images will be undersampled. In order to avoid this situation, a smaller pixel scale has been proposed and the optical design has incorporated it.

Different kind of scientific projects that will profit from a such a pixel scale (0.25"/pixel):

- Morphological studies of extended objects (galaxies, planetary nebulae, etc) .

- Differential photometry with precision of millimagnitudes. Since the light will be spread over more pixels, differences in their response will be averaged; besides, partial aperture techniques can be easily applied.

- Detection of faint sources close to bright objects (low mass companions, objects with planetary masses, etc), because, if the point spread function is oversampled, the saturation level and saturation effects will be reached only after longer exposure times.

In order to compute the effect of the pixel size on the photometric precision, we have analyzed a set of 226 K-band images taken with Omega2000 for the Alhambra project (Mariano Moles et al.) on a certain field. Differential photometry was performed on a bright star of the field taking as a reference star the weighted average of another 7 stars on the same field. Figure 2-1 shows the brightness difference between the bright star and the reference star for different values of the seeing, that is, for different ratios of seeing/pixel_size, the pixel size of Omega2000 being 0.45". The scatter of the data-points decreases as the ratio of the seeing over the pixel size increases. The larger scatter is obtained for values of this ratio between 1 and 2 (a seeing below the pixel size cannot be measured, therefore 1 is a lower limit for this ratio). A pixel size half of the seeing value (or smaller) ensures the best photometric precision. Since a seeing of ≤0.67" is expected at Calar Alto for 51% of the nights, a pixel size < 0.33" should be available.

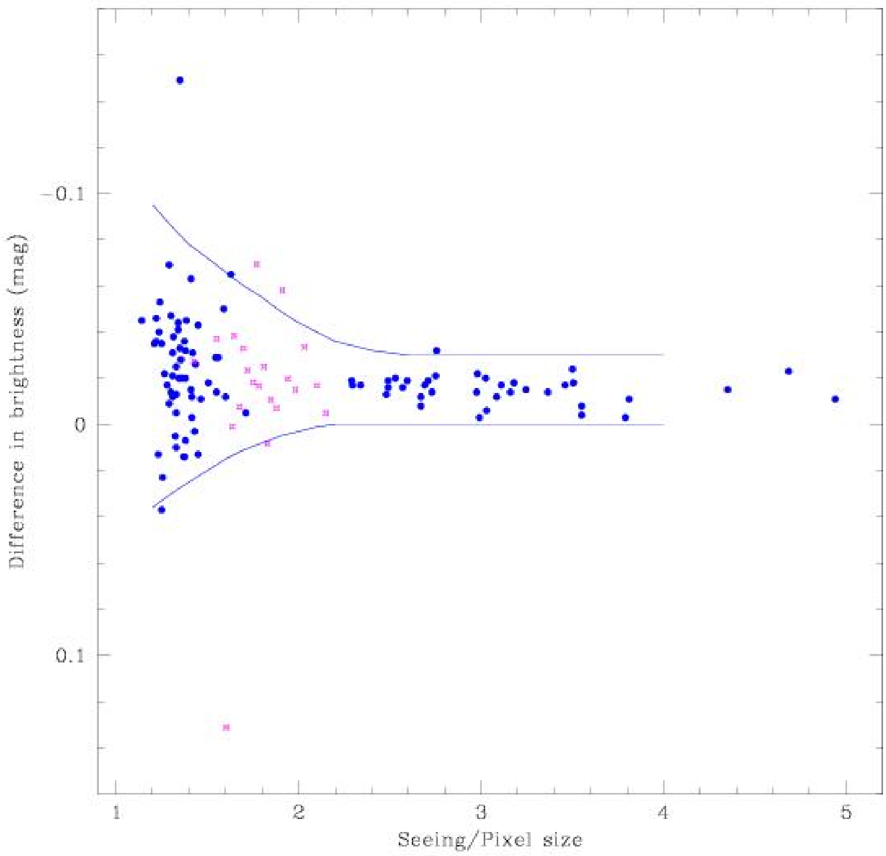

Figure 2-1 Improvement of the photometric precision if a small pixel size (compared to the seeing) is used.

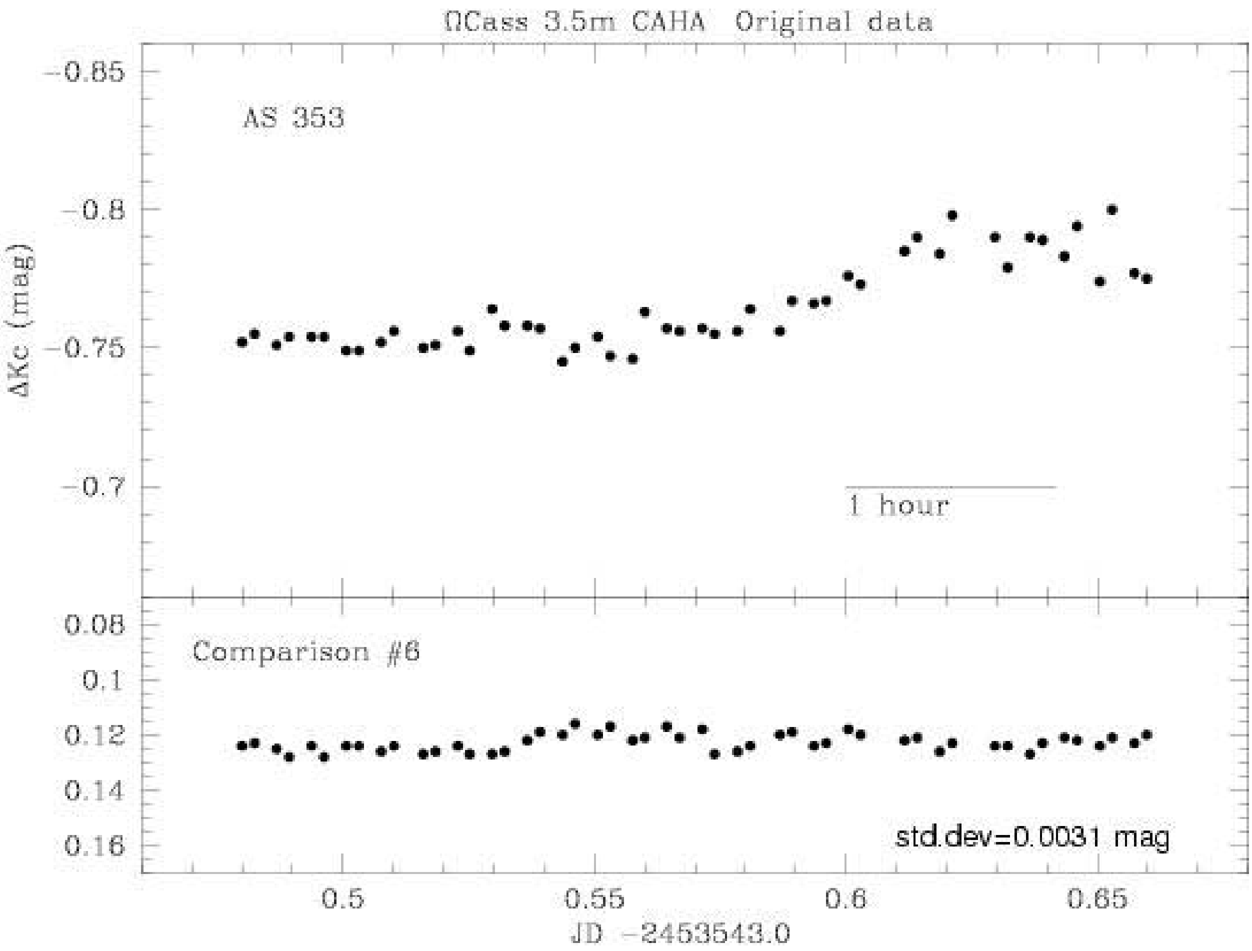

Figure 2-2 Observations done with the 3.5m telescope at Calar Alto, using the infrared camera Omega Cass and the 0.2"/pixel scale. The upper panel shows the light curve of a young, variable star and the lower panel shows the light curve of a reference star; the standard deviation of the second star is 3 millimagnitudes.

3. REQUIREMENTS AND DESIGN

3.1 Detectors

3.1.1 Summary

PANIC will use a mosaic of four 2k x 2k HAWAII-2RG arrays from Rockwell (now Teledyne) in order to cover a field of view of approximately 30 arcmin.

3.1.2 Requirements

The following section lists the technical requirements for the PANIC Science Detector based on the PANIC Scientific Requirements (Ref 01).

3.1.2.1 Number of pixels

The detector shall have a total of 4096 x 4096 pixels.

3.1.2.2 Spectral Range

The detectors should be responsive from 0.82 to 2.42 µm. In the worst case, a minimum spectral range from 0.95 to 2.42 µm shall be achieved.

3.1.2.3 Guiding

Since the actual autoguider at the Calar Alto 2.2m Telescope vignettes the FOV of PANIC, and it will have to be removed whenever PANIC is attached to the telescope, the detector shall support fast readout rates in order to implement a guiding mode using a subframe of the detector.

3.1.2.4 Flatness

The physical flatness of the detector should be better than ± 40 µm peak to valley from the best fit plane in order to avoid image degradation.

3.1.3 Introduction

The selection of the science detector was mostly based on cost, availability, and of course technical requirements. There were 3 options investigated: the 2K x 2K VIRGO detector from Raytheon, the 4K x 4K new development from Teledyne, and a mosaic of four HAWAII-2RG detectors also from Teledyne.

The HAWAII-4RG, Teledyne's new development, was discarded at an early stage of the project because of cost and risk. The capital cost of the project would have increased in approximately 0.4 MEuro, and the array was only at a design stage.

On the other hand, the VIRGO detector was more expensive than the HAWAII-2RG, and since MPIA has gained a lot of experience working with Teledyne detectors, it was decided to use a mosaic of four 2k x 2k HAWAII-2RG arrays. These arrays were also preferred because they have a special "guide mode" in which a programmable window may be read out continuously at high pixel rates for stable tracking of guide stars, allowing interleaved readout with the full frame science data.

3.1.4 Scope

This document presents the specifications of the NIR-Detectors for PANIC. In addition, the test procedures for the characterization process and the general handling of the detectors are described.

3.1.5 Specifications

The following specifications apply under normal operating conditions, and correspond to the ones given by Teledyne in their offer.

3.1.5.1 Science Detectors

PANIC will use a mosaic of four 2k x 2k HAWAII-2RG, MBE grown HgCdTe, AR coated, substrate-removed devices from Teledyne.

3.1.5.1.1 Number of pixels

Each detector shall have 2048 x 2048 pixels.

3.1.5.1.2 QE and Spectral Range

The detectors shall be responsive from 0.3 µm to 2.5 µm.

The QE shall be ≥ 75 % in all photometric bands (Y, J, H and K).

3.1.5.1.3 Uniformity of QE

The non-uniformity of QE shall be < 10 % (σ / mean in the QE histogram) in all bands.

3.1.5.1.4 Pixel Pitch

The pixel pitch shall be 18.0 µm, square format.

3.1.5.1.5 Number of Outputs

Each detector shall have 32 outputs that can be operated in parallel in order to reduce frame times.

3.1.5.1.6 Read Noise

The read noise shall be < 20 e- CDS @ 100 kHz.

3.1.5.1.7 Timing

In subarray mode, an area of 15″x 15″ of the detector shall be read out at a rate of 8 ms/frame, with a goal of 1 ms/frame for fast photometry. This specification was not given by Teledyne, it was rather defined by the PANIC team based on the scientific requirements.

3.1.5.1.8 Dark current

The dark current shall be < 0.1 e-/sec at operating temperature.

3.1.5.1.9 Pixel operability

The number of functional pixels shall be ≥ 95%.

3.1.5.1.10 Operating temperature

The operating temperature shall be 77 K ± 5 K.

3.1.5.1.11 Temperature fluctuation

The temperature fluctuation should be less than 0.1 K. This specification was not given by Teledyne, it was rather defined by the PANIC team.

3.1.5.1.12 Cool down and warm up

The cool down and warm up rates of the detectors shall be < 0.5 K/ min.

3.1.5.1.13 Physical flatness

The surface of each detector shall be flat to ± 40 µm peak to valley.

3.1.5.1.14 Storage temperature limits

The detectors shall be stored safely between 50 K and 310 K.

3.1.5.1.15 Detector identification

Each detector shall be identified by a unique serial number.

3.1.5.2 Mosaic Package

The mosaic package consists of an assembly plate made of molybdenum where the 4 detectors will be mounted to.

3.1.5.2.1 Flatness

The flatness over the surface of the whole array (4 detectors) shall be ± 40 µm peak to valley from the best fit plane.

3.1.5.2.2 Dead space

The dead space between the detectors shall be ≤ 3 mm (approx. 167 pix, which correspond to about 75 arcsec) from one active area edge to the other.

3.1.6 Design

3.1.6.1 Science Detectors

The science detectors are mounted into a molybdenum mosaic assembly plate. This mosaic integrates four HAWAII-2RG arrays as separate modules into one single thermal and vibration stable structure allowing precision alignment and physical flatness between all 4 detectors. The following figure shows a picture of the detectors mounted into the mosaic package, followed by a table with the major characteristics of these detectors.

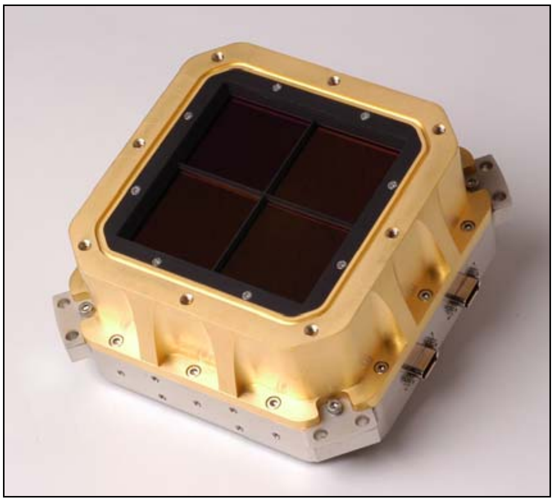

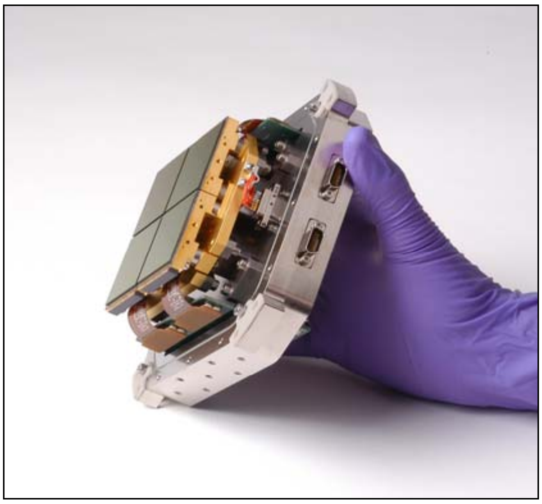

Figure 3.1.6-1. The mosaic assembly plate (left) and four H2RG's mounted into it (right). Courtesy of Teledyne Scientific and Imaging, LLC.

Table 3.1.6-1. H2RG Major Characteristics

Parameter	Specification
Total pixels	2048 x 2048
Pixel size	18 μm
Physical Flatness	± 40 μm PTV
Pixel readout rate	100 kHz to 5 MHz
Output ports	32 + 2 + "guide window"
Charge storage capacity	> 100000 e^-
Read noise (CDS)	≤ 20 e^-
Quantum efficiency	≥ 75 %
Dark current	< 0.1 e^-/sec
Spectral range	0.3 – 2.5 μm
Pixel operability	≥ 95 %
Operating temperature	≥ 65 K
Power dissipation	≤ 4 mW @ 100 kHz
Cost	$ 350000 each

The mosaic package and the science detectors are already ordered. A Bare Multiplexer and an Engineering Grade detector will also be available for test purposes.

3.1.6.2 Requirements verification

The following section presents the calculations needed to determine the feasibility of the critical technical requirements. So far, the most critical requirement regarding the detectors is the physical flatness of ± 40 µm peak to valley from the best fit plane and its effect on the optical quality.

Calar Alto 2.2 Telescope:

Focal ratio: $f/8$

Plate scale: 11.7″/mm

⇒ 1″ = 85 µm

PANIC Scale:

$$1'' = \frac{18\mu m}{0.45''} = 40\mu m$$

Then, the focal ratio at the detector is:

$$f/8 \cdot \frac{40}{85} = f/3.76$$

On the other hand,

$$\tan\alpha = \frac{D}{2}\cdot\frac{1}{f} = \frac{1}{2}\cdot\frac{1}{f/\#} = \frac{1}{2}\cdot\frac{1}{3.76} = 0.13$$

Then,

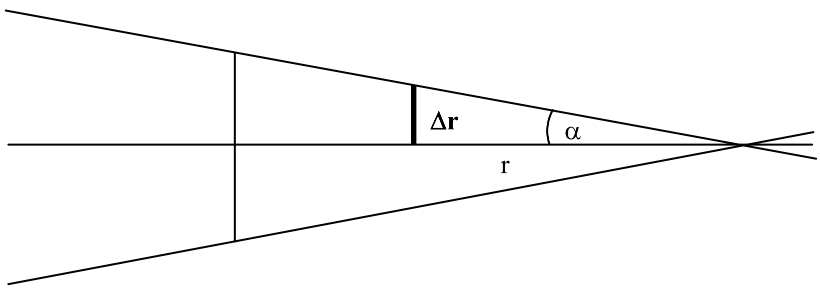

$$\tan\alpha = \frac{\Delta r}{r} \Rightarrow \Delta r = 0.13 \cdot r$$

Now, considering different "*r*" values:

r	0	10 µm	40 µm	100 µm
Δr	0	1.3 µm	5.3 µm	13 µm

With a physical flatness of ± 40 µm peak to valley from the best fit plane, the blurr will be of approximately 10 µm.

Considering also the seeing at Calar Alto (0.6″), at 40 µm the blurr is 24 µm. Adding this values leads to:

$$\text{Total blurr} = \sqrt{24^2 + 10^2} = 26\,\mu m$$

Which means that the optical quality is mostly dominated by the seeing, and not by the factor introduced by the physical flatness of the detectors.

3.1.7 Characterization

The detector characterization will be done at MPIA using the existing cryogenic test equipment for IR detectors and the real PANIC readout electronics. The final detector control system PDCS (computer and software) shall be used.

The cryogenic test equipment allows to change detector temperature, insert a filter, and blank off any light by cold light-tight baffles. This setup has also been used for other projects using HAWAII-2 detectors e.g. LUCIFER I & II, LINC-NIRVANA, Omega2000, etc.

Using the real PANIC readout electronics allows a fine tuning of all components in order to achieve best performance. For cross checks, a spare set of readout electronics will be available.

3.1.7.1 Tests

The standard parameters of the Omega2000 detector provide a good starting point for optimization.

3.1.7.1.1 Detector sensitivity and system gain

The system gain relates the output digital numbers (ADU) to the corresponding input electrons collected at the pixel unit cell. The system gain is expressed in units of electrons / ADU. With the knowledge of system gain and gain in the signal processing chain (pre-amp gain), the detector internal conversion gain (in units of µV / electron) can be determined.

Since system gain (G) and read noise (R) are constant, this leads to a linear correlation between variance of the signal (N^2) and the signal itself (S):

$$N^2 = \frac{S}{G} + \frac{R^2}{G^2}$$

A linear regression fit (y = mx + b) leads to:

$$m = \frac{1}{G} \quad ; \quad b = \frac{R^2}{G^2}$$

The actual MPIA detector readout software GEIRS supports a set of statistical functions that allow the data calculation from a stack of images for various integration times i.e. flux levels. Since PANIC detector readout software is based on GEIRS, these statistical functions will also be available.

3.1.7.1.2 Full well capacity

The full well capacity is estimated from the photon transfer plot (variance versus signal). The noise increases linearly with the flux signal. Once the signal level approaches the full well capacity, a noise roll-over is reached due to pixel saturation effects where the noise no longer obeys Poisson's statistics.

3.1.7.1.3 Read noise

- Spatial read noise measurement: Two CDS dark frames, each with minimum detector integration time, are subtracted from each other pixel-by-pixel. The standard deviation estimated from a defect free region of the resultant frame is divided by √2 and multiplied by the system gain to get the spatially averaged temporal read noise in electrons rms. This noise is referred as read noise in a CDS frame.

- Temporal noise: A series of dark frames are obtained with minimum detector integration time and without any time interval between individual frames. A noise frame (in ADU) is generated by measuring the noise in every pixel from all the dark frames on a pixel-by-pixel basis. The resultant noise frame is converted into electrons by multiplying by the system gain. The result is a histogram of the noise frame in electrons. The mean of the histogram is the temporal read noise. The standard deviation of the histogram shows the noise uniformity.

The actual MPIA detector readout software GEIRS supports a set of statistical functions to perform these tests. Since PANIC detector readout software is based on GEIRS, these statistical functions will also be available.

3.1.7.1.4 Linearity

The mean and/or median output signal vs. integration time is measured and plotted. The output signal in ADU is converted into electrons by multiplying it with the system gain.

A least-squares fit to the data from 10% to 80% of the full well gives the linearity behavior.

3.1.7.1.5 Persistence and cross-talk

Will not be measured at MPIA.

3.1.7.1.6 Quantum efficiency

This test will not be performed. Values will be taken from the manufacturer's data sheets.

3.1.7.1.7 Flatness

The flatness of each detector's surface will be measured by means of a triangulation method using an xy stage to map the detector area. MPIA owns such an xy stage, and it will be used to perform the measurements.

3.1.8 Handling, storage and transportation

The main purpose of this section is to describe a series of safe procedures that shall be followed when handling the science detectors during acceptance, delivery, inspection, storage, transportation, integration and maintenance.

3.1.8.1 Electrostatic Discharge

Detectors can be damaged by ESD. The science detectors shall be handled only in an ESD-protected area. MPIA counts with integration halls and dedicated labs in which ESD-protected conditions are fulfilled.

3.1.8.2 Clean room conditions

The detector should be handled under clean room conditions (class 10000). For assembly and integration, the detector should be handled in a laminar flow area.

3.1.8.3 Detector handling

The handling of the detectors is restricted to well trained persons. Only persons with permission from MPIA are allowed to handle the detectors.

The handling of the detectors is only allowed with sufficient ESD protection equipment.

The detectors shall **not** be cleaned. In case cleaning is necessary, contact the responsible person at MPIA.

Avoid any mechanical shock to the detectors and mosaic package.

3.1.8.4 Storage

The detectors must be stored in their original case under correct environmental conditions.

Temperature: the storage temperature must be between 50 K and 310 K (-220°C and 30°C).

Humidity: the case shall contain humidity absorbent materials.

Only qualified people shall have access to the storage cabinet.

3.1.8.5 Transportation

The detectors must be transported in its original case. The previous rules must also be fulfilled during transportation.

For transportation across countries, ensure that all custom regulations are fulfilled. Before shipping the detectors, contact the responsible person at MPIA.

3.2 Optics

3.2.1 Summary

This optics section contains a description of the PANIC Preliminary Optical Design. The report includes the optics requirements, the optics layout and image quality, a preliminary ghost analysis and stray light considerations, optical tolerances analysis and a preliminary AIV.

3.2.2 Introduction

PANIC shall be a wide-field infrared imager for the Ritchey-Chrétien (RC) focus of the Calar Alto (CAHA) 2.2 m telescope.

The camera optical design is a single optical train that images the sky onto the focal plane at an optical speed of f/3.74, with a plate scale of 0.45 arcsecond per 18 µm pixel. The detectors are four Hawaii 2RG of 2k x 2k made by Teledyne, mounted in a mosaic giving a field of view (FOV) of 31.9 arcmin x 31.9 arcmin.

The camera has been provided with a second smaller pixel scale of 0.25 arcsecond per pixel optimized for a 18 arcmin diameter FOV.

Special care has been taken in the selection of the standard IR materials used for the optics in order to include the z band and to maximize the instrument throughput. This cryogenic instrument has been optimized for Y, J, H and K bands.

The mains challenges of this design are: the correction of off-axis aberrations due to the wide-field available, the correction of chromatic aberration due to the wide spectral coverage, the introduction of narrow band filters (~1%) in the system minimizing the degradation in the filter pass-band, and the mechanical constrains in mass and torque at the Ritchey-Chrétien focus of the telescope.

The optical design produces an internal pupil available for a Lyot stop at the telescope image pupil placed at the primary mirror.

3.2.3 Scope

The Preliminary Optical Design is described in this optics section..

3.2.4 Simulations

The PANIC optical design has been developed using ZEMAX-EE (Version January 2007). The model includes the optical components of the 2.2 m telescope.

The optical surfaces are defined with respect to the optical axis, which is always parallel to the Z axis of the local frame of reference by the optical design program. The distance between optical surfaces is measured along the optical axis and it is defined by a thickness parameter.

3.2.5 OPTICS Requirements

This section summarizes the Requirements established/imposed by the science goals and the Technical Requirements that derivate of the operational conditions and design choices. A separate document describes the Science Requirements (RD1) for PANIC.

The Table 3.2-1 summarizes the General Specifications for PANIC.

Focal Station	*Cassegrain 2.2 m*
FOV	*30’ x 30’ for 0.45”/px*
Pixel scales	*0.45 arcsec/pixel* *0.25 arcsec/pixel*
Direct Imaging	*Over the whole FOV*
Pupil image available	*Cold stop*
Wavelength range	*0.95– 2.45 μm with IQ* *0.82-0.95 μm able to transmit*
IR Detector	*4 K x 4 K*
Gap between detectors	*Minimum*
Operating temperature	*80 K*
Filters	*Broad band: ¿z?YJHK* *Narrow band ~1%*
System focusing mechanism	*Telescope S2*

Table 3.2-1 Summary of the PANIC General Specifications

The optical system is a monobeam design all refractive, being the only mirrors of the system the ones used for folding and packaging. The design has not been required to have an internal collimated beam.

3.2.5.1 GENERAL REQUIREMENTS

3.2.5.1.1 Pixel scale

Parent requirement: 4.1.1. in RD1

The optimum scale shall be 0.45″/pixel.

3.2.5.1.2 Wavelength range

Parent requirement: 4.1.2. in RD1

PANIC shall work in the wavelength range 0.95 -2.42 µm and should work in the range 0.82 – 2.42 µm.

3.2.5.1.3 Image quality

Parent requirement: 4.1.3. in RD1

The image quality shall be such that an 80% of the energy is ensquared (EE) in a 0.9” (2 pixels) over the full FOV for each of the broad bands.

3.2.5.1.4 FOV

Parent requirements: 4.1.1. and 5.4.1. in RD1

PANIC when observing with the 0.45"/px scale shall have a FOV of at least 30 arcmin x 30 arcmin.

3.2.5.1.5 Pupil re-imaging quality

Parent requirement: 4.1.4. in RD1

A separate Technical Note (ORD2) describes in details the signal to noise study for PANIC and imposes the following requirements in the pupil quality:

3.2.5.1.5.1 System pupil

The PANIC pupil has to be placed at the telescope primary mirror (S1).

3.2.5.1.5.2 Accessible pupil image

The Optical design shall provide an accessible pupil image so that a suitable cold mask shall be used to minimize stray thermal radiation.

3.2.5.1.5.3 Pupil shape and dimension

The maximum degradation in the pupil re-imaging diameter shall be 3% which is less than a 10% loss in flux for K band.

The central obstruction of the S2 image at the re-imaging pupil plane shall be avoid.

It is not necessary to avoid the structure of the S2 spiders.

3.2.5.1.6 Stray light and Ghosts

Parent requirements: 4.1.5.1 and 4.1.5.2. in RD1

3.2.5.1.6.1 Image/Ghost ratio

The intensity ratio between a ghost image and its source shall be lower than 1e-4 (this means that for a point source at the detector and at the limit of saturation there shall not be a single ghost structure contributing more than 6 counts).

3.2.5.1.6.2 Individual Ghost diameter

The diameter of any individual ghost shall be larger than 10" in case the requirement of Image/Ghost ratio is not fulfilled.

3.2.5.1.6.3 Stray light

The total stray light shall be minimized.

3.2.5.1.7 Band passes

Parent requirements: 4.1.6.1., 4.1.6.2 and 4.1.6.3.in RD1

PANIC shall be designed to allow use of broad and narrow band filters.

3.2.5.1.7.1 Broad band filters

Filters shall be provided for Y, J, H and K bands. A z filter should also be provided if the 0.82 – 2.42 μm range is achieved.

3.2.5.1.7.2 Tolerance for narrow band filters

Parent requirement: 4.1.6.3. in RD1

Since the narrow band filters have widths, on average, of 1% of the central wavelength of the filter, the maximum shift allowed for this central wavelength shall be 0.3%.

3.2.5.1.8 Field distortion requirement

Parent requirement: 4.1.8. in RD1

Field distortion shall be less than 1.5 % from the field centre.

3.2.5.1.9 Transmission

Parent requirements: 4.1.6.1., 4.1.6.2 and 4.1.6.3.in RD1

There is no number requirement defined for the transmission of PANIC. There is only the goal to be as high as possible, to optimize the materials to maximize transmission in the 0.95-2.45 μm range and to work in the z band (from 0.82 μm).

3.2.5.1.10 Environmental conditions

Parent requirement: 5.3. in RD1

PANIC shall be designed to operate and have optical quality under cryogenic conditions (temperature 80 K and vacuum).

3.2.5.1.11 High-resolution mode

Parent requirements: 4.3. in RD1

Requirements 3.2.5.1.2., 3.2.5.1.5, 3.2.5.1.6, 3.2.5.1.7, 3.2.5.1.8, 3.2.5.1.9 and 3.2.5.1.10 apply to this mode.

3.2.5.1.11.1 Pixel scale

A second pixel scale of 0.25″/pixel shall be implemented in PANIC.

3.2.5.1.11.2 FOV

PANIC when observing with the 0.25"/px scale shall have a FOV of at least a circle with a diameter of 8 arcmin. The goal is a FOV with a diameter of the circle inscribed in the detector dimension which is a diameter of 17.76 arcmin.

3.2.5.1.11.3 Image quality

The image quality shall be such that an 80% of the energy is ensquared (EE) in a 0.75" (3 pixels) over the full FOV for each of the broad bands.

3.2.6 Optics Layout

3.2.6.1 PANIC General Optics layout

Figure 3.2.6-1 shows the location of PANIC in the telescope.

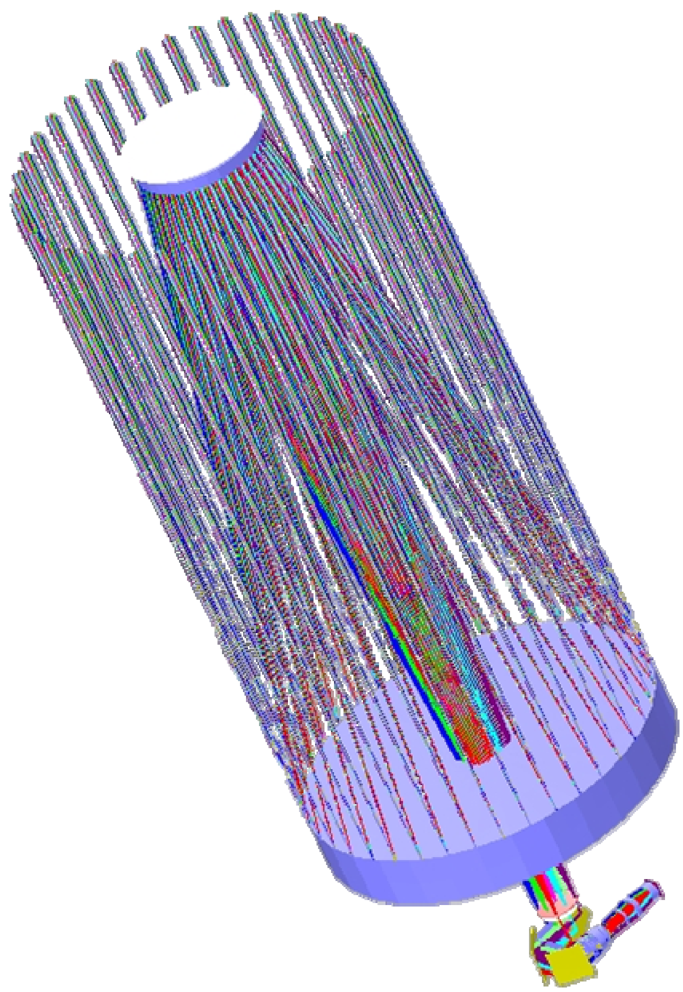

Figure 3.2.6-1 PANIC location in the RC focus of the 2.2 m telescope

Figure 3.2.6-2 shows the optics model solution for the two scales of PANIC.

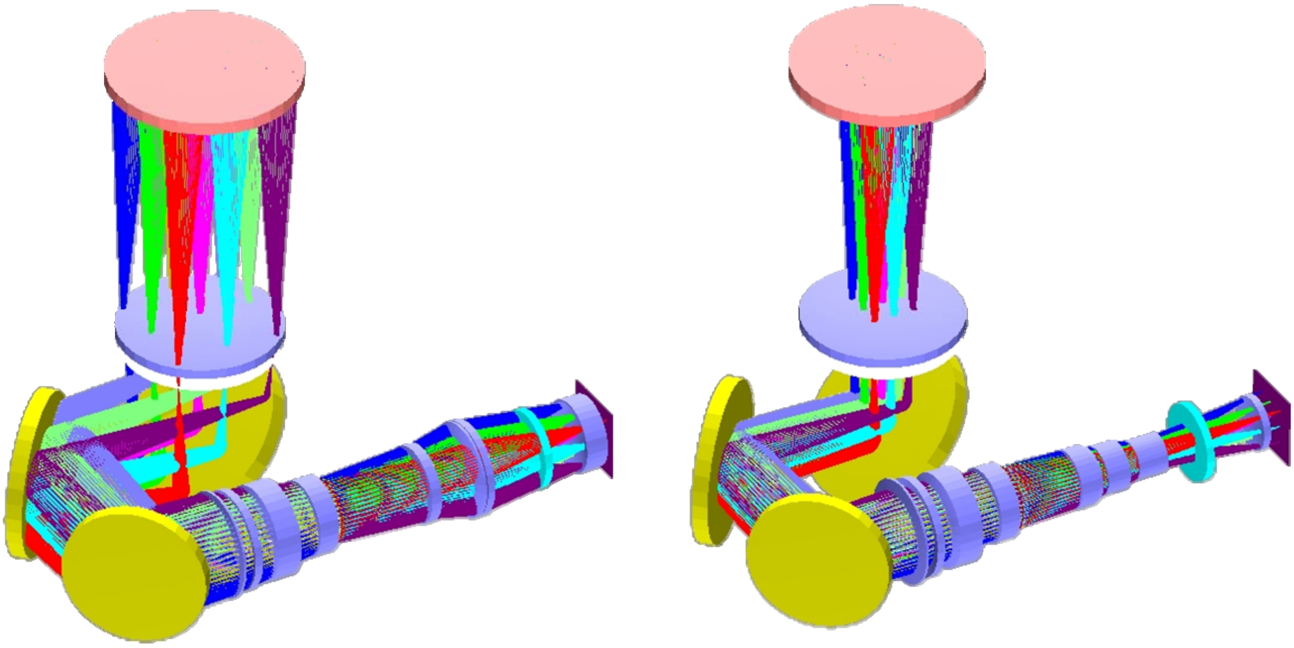

Figure 3.2.6-2 Optics layout of PANIC: left the 0.45"/px camera and right the 0.25"/px camera.

The PANIC optics design presented in this document has been modelled at cryogenic temperatures and vacuum. A separate Technical Note (ORD4) describes in details the models considered to obtain the glass catalogue at 80 K produced for PANIC.

The camera consists of two separate lens systems which will be alternatively inserted after the cold stop mask, keeping the total distance between the cold stop and the detector fixed and equal to 437.30 mm. A deep study has been made to evaluate the best solution for the implementation of that second pixel scale in PANIC and a separate Technical Note (ORD3) describes in details this second pixel scale study. Finally we decided to implement the classical solution which consist in a optics wheel that interchanges all the optics elements after the cold stop as it is shown in the next pages in this document.

The straight layout shown in the Figure 3.2.6-3 and Figure 3.2.6-16 shows a long instrument (≈1925 mm). Due to the mechanical constrains in length and weight it has been searched alternatives to make the system more compact and finally the packaging solution adopted, shown in the Figure 3.2.6-2, introduces three folding flat mirrors in the optical path between L0 and L1. From the optical performance point of view this packaging proposed has not effect.

The distances between mirrors have been fixed as shows the Table 3.2-4, which is an optimum mirror separation, with no possible interference and vignetting and optimizes the cold volume of the system.

In Table 3.2-2 it is shown the mass estimation for the lenses of PANIC calculated from the Zemax model. In the calculations are included the cryostat window and the lenses of the two pixel scales.

Element	Weight (Kg)
Window	2.93
L0 to L4	7.51
L5A to L8A	2.96
L5B to L8B	2.84
Total	16.24

Table 3.2-2 Mass estimation for the PANIC optics system

A raw estimation for the folding mirrors mass, shown in Table 3.2-3, could be made assuming circular mirrors with a clear aperture diameter and a thickness of the 10% of its diameter. Notice that this is only a first estimation and the final mirrors could be elliptical shape (see Figure 3.2.6-5) and with the minimum thickness needed to assure not degradation in the optical quality. That thickness will be determined for a FEA, taking into account also the holder design for that element. So the final mirrors weight surely will be less of this estimation.

Element	Weight (Kg)
M1	4.46
M2	3.64
M3	2.37
Total	10.47

Table 3.2-3 Raw mass estimation for the folding mirrors

3.2.6.2 0.45”/px camera

3.2.6.2.1 0.45”/px Optics Layout

Figure 3.2.6-3 shows the unfolded optics layout of the 0.45”/px scale of PANIC.

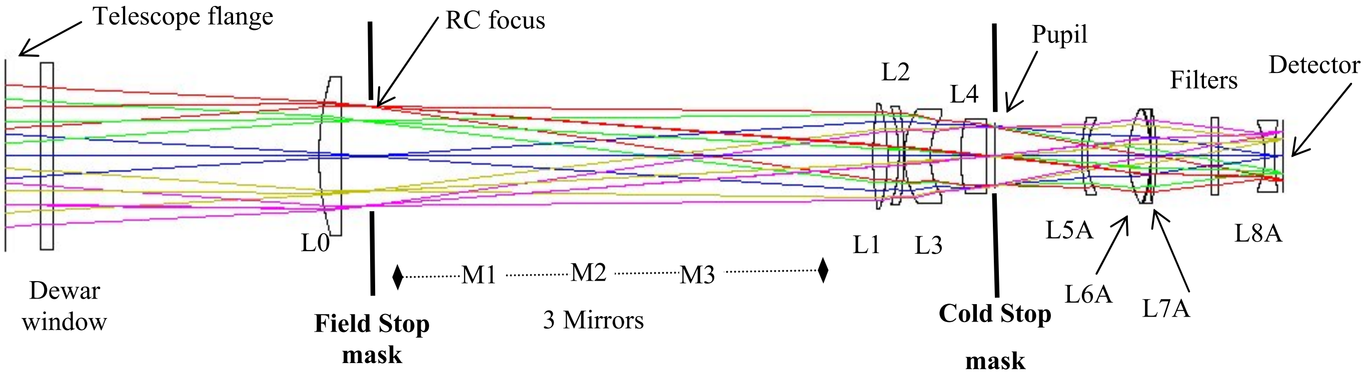

Figure 3.2.6-3 Optics layout of de PANIC the 0.45”/px camera

3.2.6.2.2 0.45"/px optical prescriptions

The prescription of the system is listed in Table 3.2-4 and Table 3.2-5. In Table 3.2-4 are listed all the common elements of the two pixel scales and in Table 3.2-5 here are listed the elements of the scale 0.45"/px that only belong to that pixel scale. The nominal length from the external part of the window to the detector is 1925.36 mm for both scales.

The curvature radius and thicknesses of the lenses are given at 80 K, working temperature of PANIC. For manufacturing and assembly, those parameters have to be replaced by warm parameters, using thermal expansion coefficients defined in ORD4.

Element	***Curvature radius (mm) at 80 K***	***Thickness or Separation (mm) at 80 K***	***Material***	***Aperture ∅ (mm)***
Telescope flange	*Plane*	*54.6*		*296.6*
Cryostat window	*Plane* *Plane*	*20.0*	*IR Fused Silica*	*291.2*
		411.8	*Vacuum*	*-*
L0	*424.9674* *Plane*	*33.6*	*IR Fused Silica*	*247.0*
Focal plane		*25.0*	*Vacuum*	
		145.0	*Vacuum*	
M1	*Plane*	*28.0 (TBD)*	*Zerodur® or BK7 (TBD)*	*276.3*
		255.0	*Vacuum*	
M2	*Plane*	*25.0 (TBD)*	*Zerodur® or BK7 (TBD)*	*248.7*
		275.0	*Vacuum*	
M3	*Plane*	*22.0 (TBD)*	*Zerodur® or BK7 (TBD)*	*219.0*
		125.0	*Vacuum*	
L1	*480.3027* *-281.1478*	*22.8*	CaF_2	*162.4*
		17.1	*Vacuum*	
L2	*-251.2363* *-431.1047*	*8.0*	*E-SF03*	*152.8*
		1.0	*Vacuum*	
L3	*144.1806* *121.4225*	*40.0*	*IR Fused Silica*	*146.1*
		46.8	*Vacuum*	
L4	*217.8809* *-6469.551*	*39.8*	BaF_2	*116.5*

Table 3.2-4 Prescriptions data of the common elements of the optical system at its nominal design temperature

Element	*Curvature radius (mm) at 80 K*	*Thickness or Separation (mm) at 80 K*	*Material*	*Aperture ∅ (mm)*
		148.2	*Vacuum*	
L5A	*246.6815* *121.6698*	*8.0*	*IR Fused Silica*	*118.4*
		64.7	*Vacuum*	
L6A	*163.4817* *-212.7252*	*34.0*	*S-FPL51*	*146.0*
		1.0	*Vacuum*	
L7A	*-229.7703* *-356.7755*	*8.0*	*E-SF03*	*144.6*
		168.1	*Vacuum*	
L8A	*-124.6153* *283.5234*	*14.6*	*S-FTM16*	*105.2*
		13.0	*Vacuum*	
Detector	*FLAT*			

Table 3.2-5 Prescriptions data of the elements that only belong to the 0.45"/px scale

3.2.6.2.3 0.45"/px descriptions

In this section we present all the footprint for the optical components in the 0.45"/px scale configuration from Figure 3.2.6-4 to Figure 3.2.6-10.

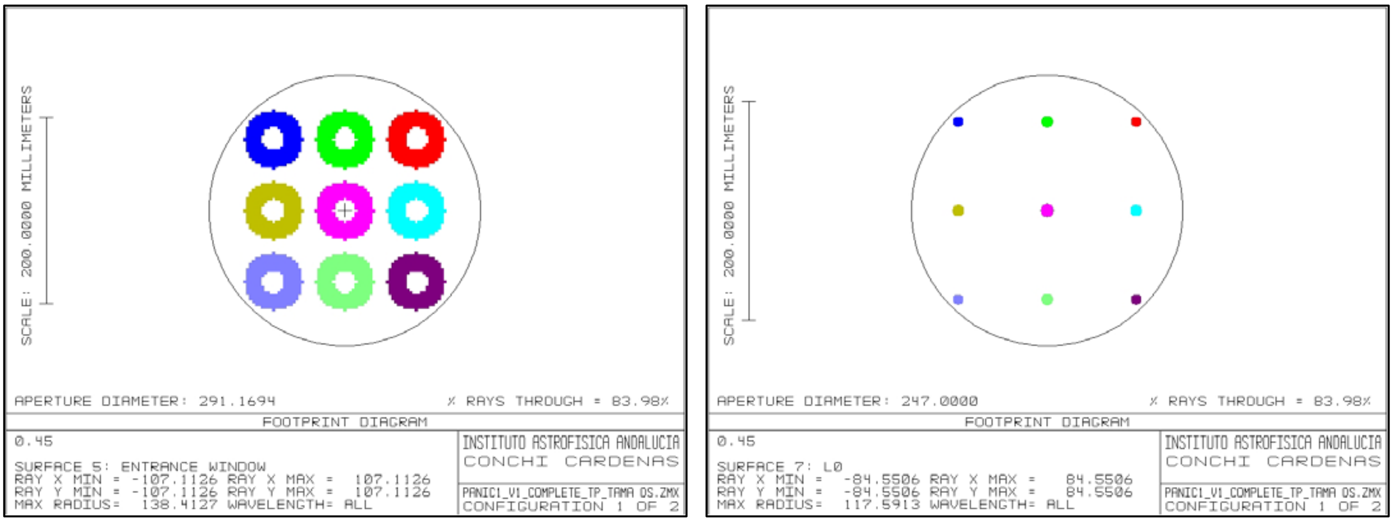

Figure 3.2.6-4 Footprint of the 0.45"/px camera FOV: on the Entrance window (left), on the L0 (right).

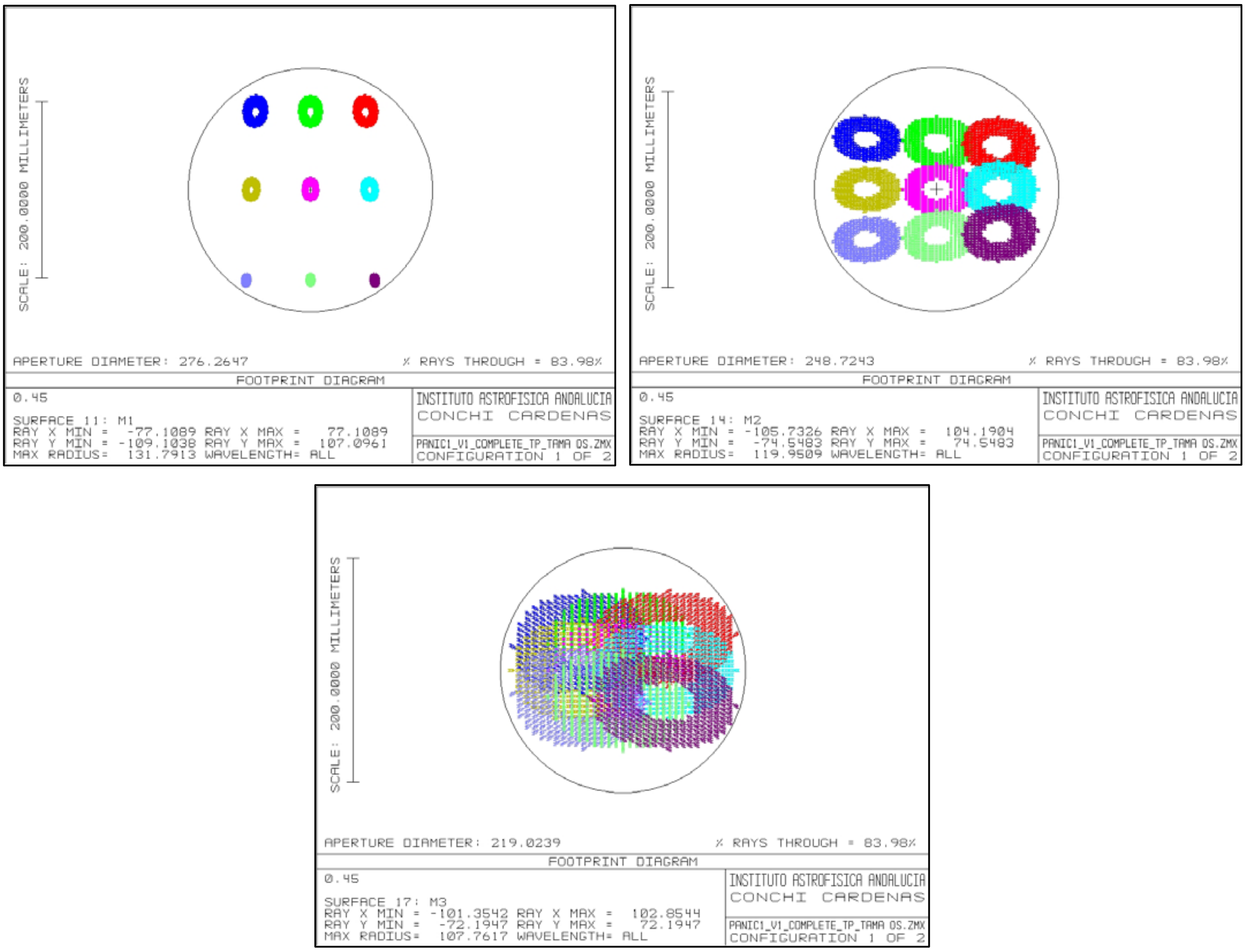

Figure 3.2.6-5 Footprint of the 0.45"/px camera FOV: on the M1 (left up), on the M2 (right up) and on the M3 (bottom).

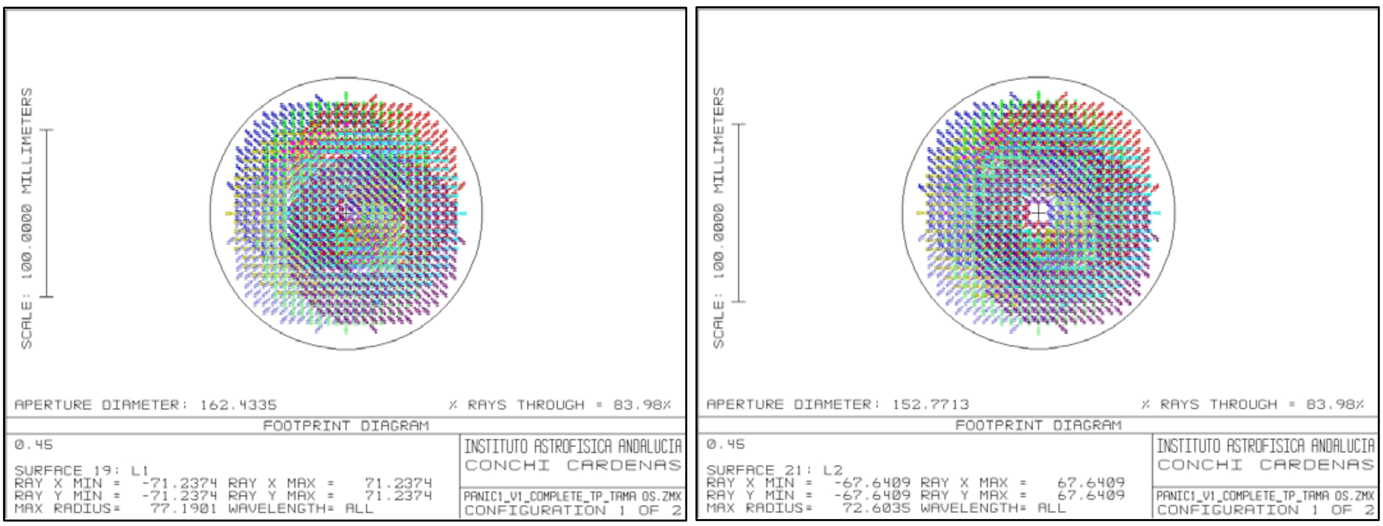

Figure 3.2.6-6 Footprint of the 0.45"/px camera FOV: on the L1 (left), on the L2 (right).

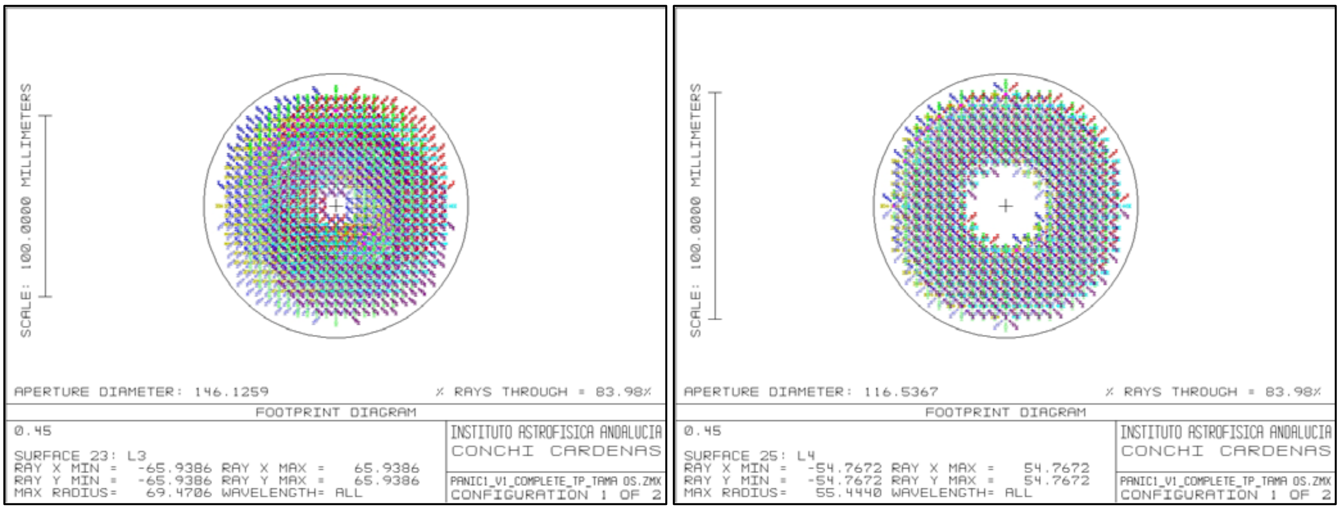

Figure 3.2.6-7 Footprint of the 0.45"/px camera FOV: on the L3 (left), on the L4 (right).

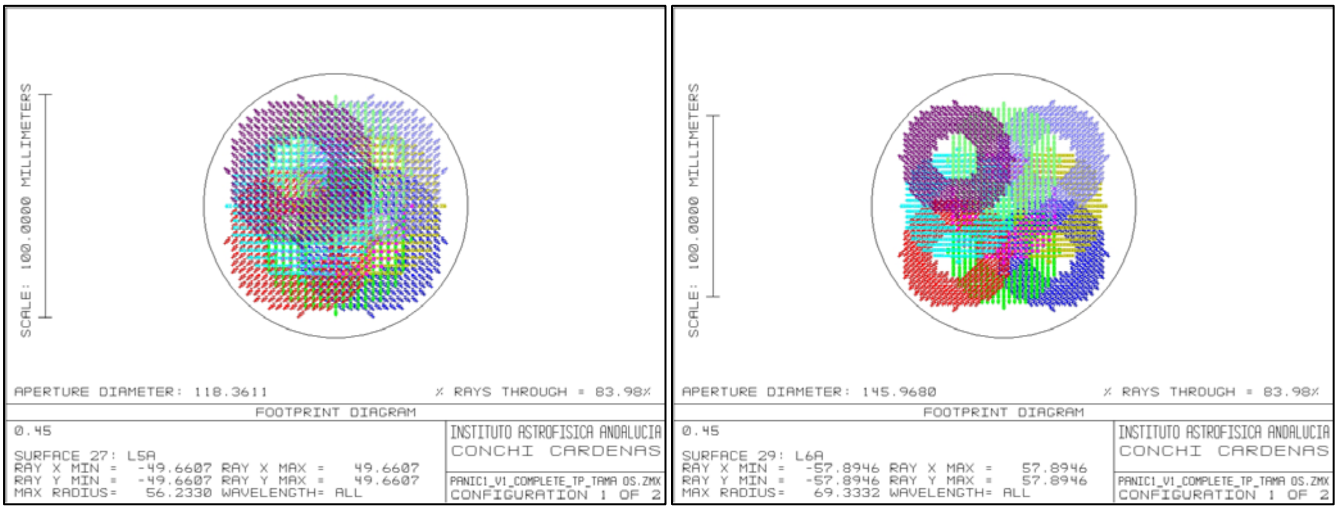

Figure 3.2.6-8 Footprint of the 0.45"/px camera FOV: on the L5A (left), on the L6A (right).

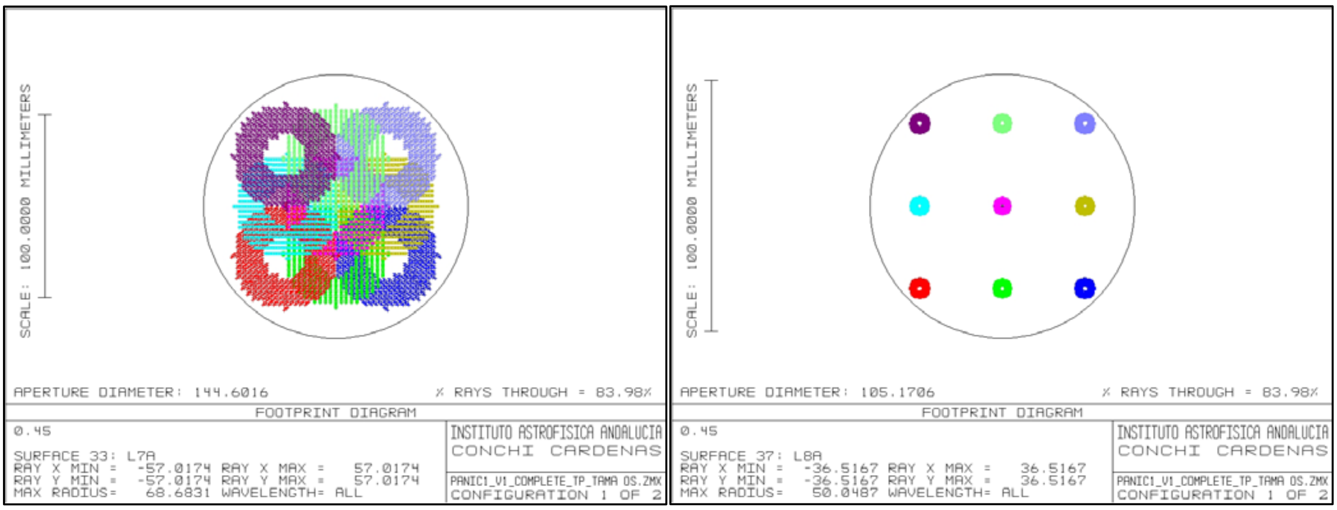

Figure 3.2.6-9 Footprint of the 0.45"/px camera FOV: on the L7A (left), on the L8A (right).

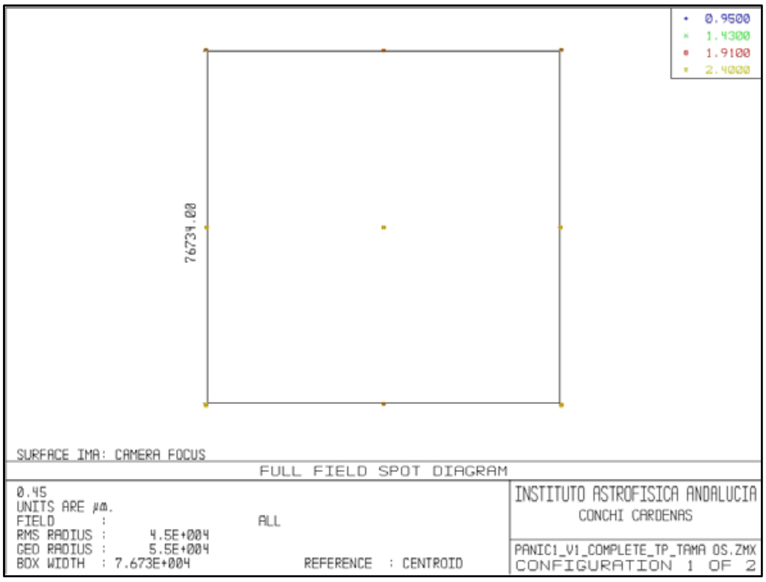

Figure 3.2.6-10 Footprint of the 0.45”/px camera FOV on the detector plane

3.2.6.2.4 0.45”/px optical performance

The Table 3.2-6 lists a summary of the characteristics that describe the performance of PANIC in the 0.45”/px scale. In this table are the figures of merit that provides a rough idea about the design quality.

Parameter	*Requirement (or Goal)*	*Achieved*
FOV	*30’ x 30’*	*31.9’ x 31.9’*
Scale at detector	*0.45 ”/px*	*0.45 ”/px*
Pupil image	*Cold stop available*	*Mechanical available*
Pupil image quality	*< 10% loss in flux for K band*	*< 2% loss in flux all bands*
Wavelength range	*0.95 – 2.5 µm*	*Optimized: 0.95 – 2.5 µm* *Good transmission from 0.8 µm*
Image Quality	*EE80 ≤ 2 pixels (36 µm = 0.90")*	*EE80= 29.8 µm = 0.75" = 1.7 pix., max.*
Distortion, maximum	*< 1.50 % (corner)*	*< 1.32 % max. (corner)*
Transmission	*As much as possible*	*~ 45% (window+9 lenses)*
Gap between detectors	*Minimum*	*167 pixels (minimum)*
Filters	*Broad band: YJHK* *Narrow band ~1%*	*Broad band: zYJHK* *Narrow band ~1%*

Table 3.2-6 Summary of the PANIC performance in the 0.45”/px scale

3.2.6.2.5 0.45"/px Ensquared Energy and Spot diagrams

The FOV has been sampled from the centre to the external field in a radial configuration following the equal area rule. The system has been optimized for the following fields, see Table 3.2-7, to cover the complete detector surface:

Field	X, Y coordinate (º)	X, Y coordinate (mm)
1	(0;0)	(0;0)
2	(0.154, 0.154)	(22.18,22.18)
3	(0.218, 0.218)	(31.39,31.39)
4	(0.266, 0.266)	(38.30,38.30)

Table 3.2-7 Fields used in the 0.45"/px scale

The origin of coordinates is the centre of the detector mosaic. The second column is the fields on the sky, and the third column is the coordinates at the detector plane.

At the detector plane, the image spots analyzed are located in the coloured points that shows the Figure 3.2.6-11. The box indicates the total size of the whole detector (including gap of 167 pixels between detectors).

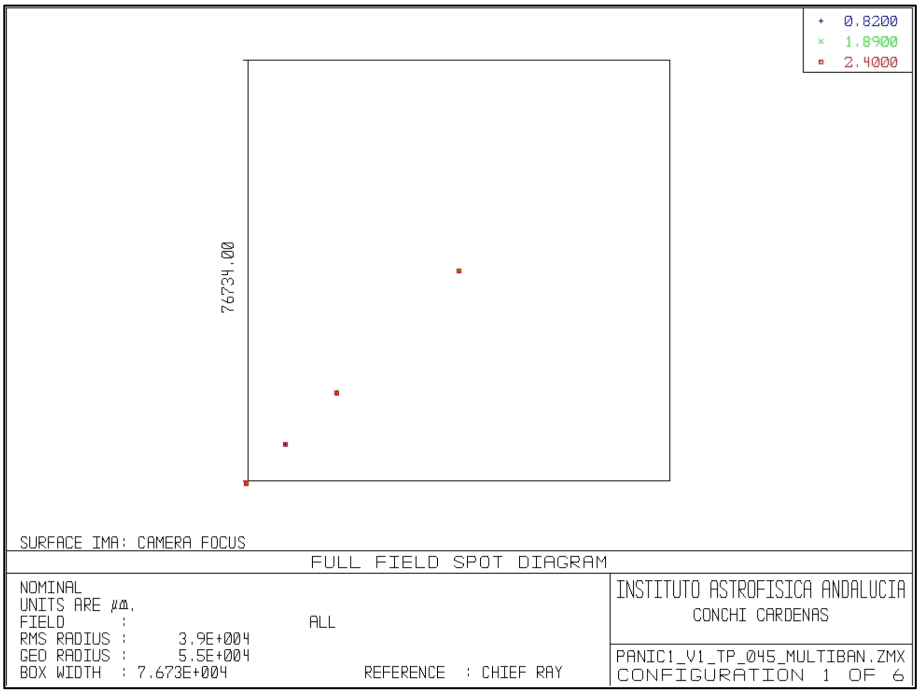

Figure 3.2.6-11 Complete FOV of the 0.45"/px

The performance of the design is evaluated at the wavelength and bandwidths shown in Table 3.2-8. Notice that the design has been optimized to this bands except the z band. The requirement for z band is not optical quality, it is only for transmission in this band. Instead of this, it can be seen that there is optical quality in z band, so the system is able to work in this photometric band.

As the filters will be placed in convergent beam, it has been decided to simulate them by inserting a plate of IR fused silica with a thickness of 12.5 mm between the L7A and L8A. It is possible to refocus the system by a movement of the telescope S2 along the optical axis, so the measurements in defocus are referred to the displacement of the S2 from the nominal position in the polychromatic configuration, and gives the sense (- forward, i. e. sense toward the entrance window, + backward, opposite).

Filter	Wavelength (μm)	EFL (mm)	Focus (mm)
Polychromatic	0.95-2.42	8265.17	0.00
z	0.82-0.99	8257.76	+0.029
Y	0.99-1.08	8259.34	-0.014
J	1.08-1.34	8260.20	-0.025
H	1.50-1.80	8262.49	+0.00
K	1.97-2.42	8265.44	+0.011

Table 3.2-8 Bandwidths of evaluation of the PANIC optical design and their change in focus for the 0.45"/px scale

The image quality of the instrument is specified in terms of the 80 % EE (EE80) for each photometric band, where EE80 is expressed as the square side length which contains the 80% of the image energy. This EE80 is evaluated in Table 3.2-9 using the greater value obtained in the FOV analyzed.

Note that all the bands are in requirements (EE80 ≤ 2 pixels=36μm=0.90").

Filter	EE80 (μm)	EE80 (pix)	EE80 (arcsec)
z	25.00	1.39	0.63
Y	21.52	1.20	0.54
J	20.86	1.16	0.52
H	26.14	1.45	0.65
K	33.58	1.87	0.84
Polychromatic	29.84	1.66	0.75

Table 3.2-9 EE80 in the 0.45"/px scale

For simplicity, it has been presented only the polychromatic EE in Figure 3.2.6-12, the X axis is the half side length square of EE and the Y axis represents the fraction of energy enclosed, where there is indicated with an horizontal line the 80%. In dark it is shown the diffraction limit of the system.

For simplicity, as well, it has been presented only the polychromatic spot diagram in Figure 3.2.6-13. This figures shows the geometrical structure of the image at all points of the field for all the wavelengths considered. Of course, better figures are obtained when the system is refocusing in the photometric bands. The squared boxes indicate the dimension of two pixels in the focal plane (36 μm), and the Airy disk for this configuration is indicated with the dark circle.

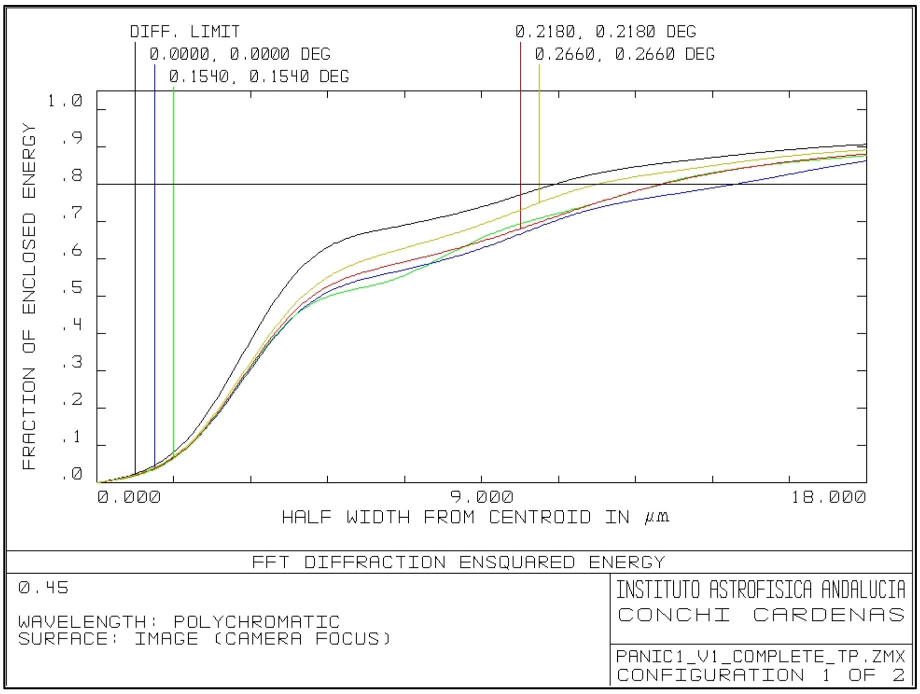

Figure 3.2.6-12 Polychromatic EE of the 0.45"/px camera

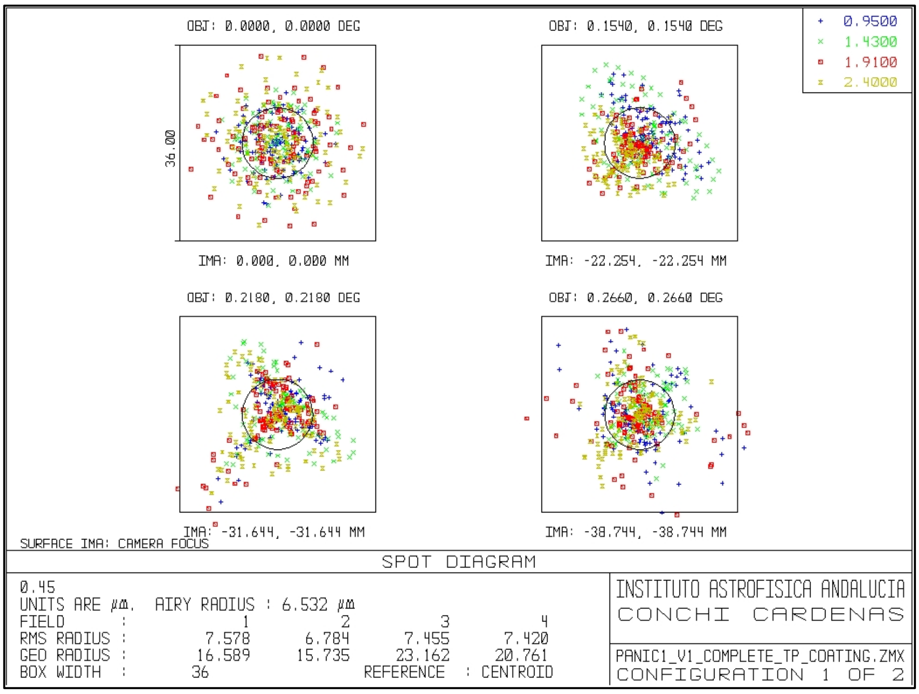

Figure 3.2.6-13 Polychromatic spot diagram of the 0.45"/px camera

3.2.6.2.6 0.45"/px Distortion

The distortion has been calculated in % with respect to the FOV centre which does not have distortion. In Table 3.2-10 we present the values for the central wavelength of the filters. For simplicity we only present in Figure 3.2.6-14 the plot of the maximum distortion obtained in the work photometric band of PANIC. Notice that all the bands are in requirements (D ≤ 1.5 %).

Filter	Wavelength (μm)	Distortion (%)
z	0.82-0.99	1.32
Y	0.99-1.08	1.31
J	1.08-1.34	1.31
H	1.50-1.80	1.30
K	1.97-2.42	1.29

Table 3.2-10 Distortion data in the 0.45"/px scale

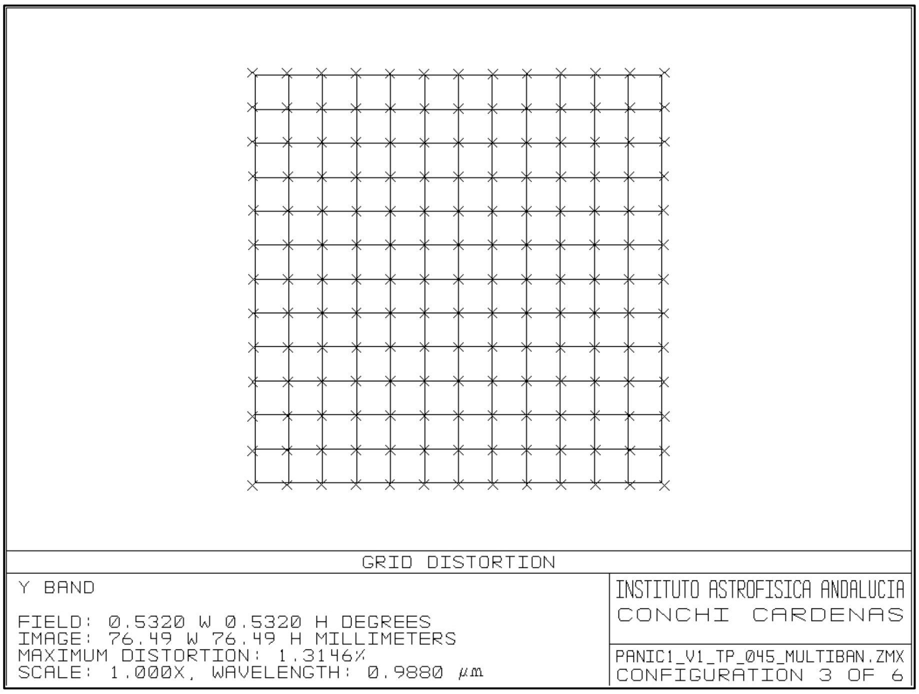

Figure 3.2.6-14 Distortion plot for the 0.45"/px camera

3.2.6.2.7 0.45"/px Transmission

The preliminary estimation for the average throughput in PANIC is done using the transmittances given by the glasses manufacturers (they have been introduced in the glass catalogue of PANIC used in Zemax) for the lenses and the cryostat window. It has been considered AR coating (given by Zemax) both sides and the thickness of any element. We expect better performance in transmission due to the optimization of the AR coating of the lenses with the manufacturers. In Table 3.2-11 and Figure 3.2.6-15 are the values and the plot, respectively, of the expected transmission as function of the wavelength.

In the transmission calculation all the mirrors has been considered, the two telescope mirrors and the three folding mirrors of PANIC. For the telescope mirrors we have modelled an aluminium coating and for the PANIC folding mirrors a gold coating.

λ (μm)	Transmission (%)
0.95	37.7
1.26	52.9
1.57	53.3
1.88	48.5
2.19	41.2
2.5	41.2

Table 3.2-11 Values of the expected transmission for the 0.45"/px scale

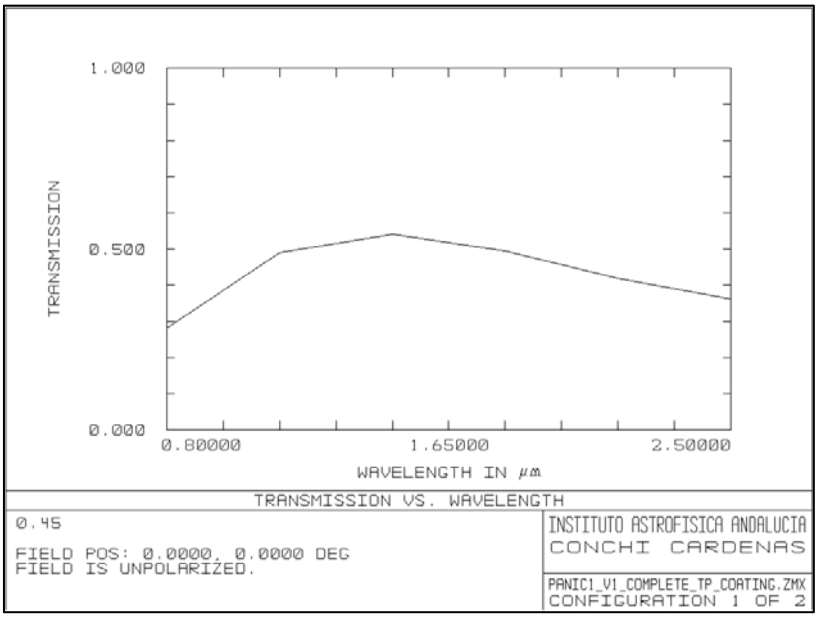

Figure 3.2.6-15 Expected transmission for the 0.45"/px camera

3.2.6.3 0.25"/px camera

3.2.6.3.1 0.25"/px Optics Layout

Figure 3.2.6-16 shows the unfolded optics layout of the 0.25"/px scale of PANIC.

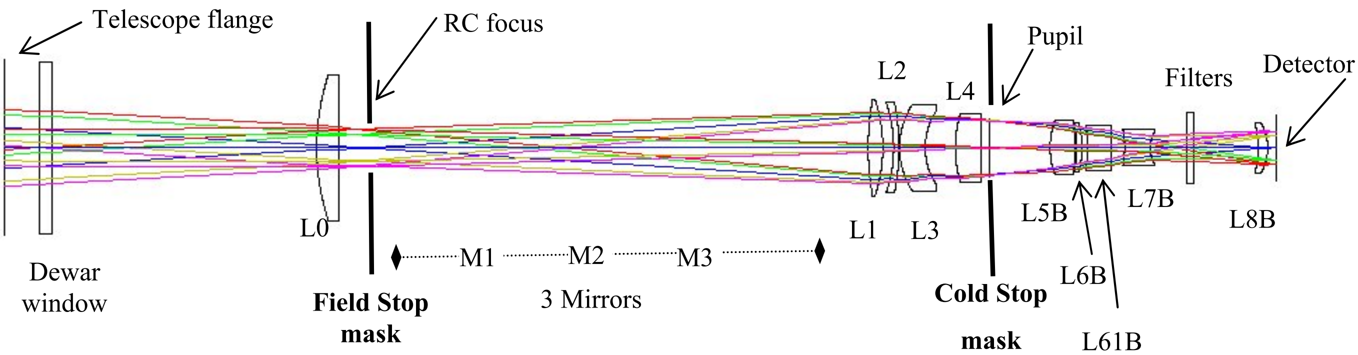

Figure 3.2.6-16 Optics layout of de PANIC the 0.25"/px camera

3.2.6.3.2 0.25"/px optical prescriptions

The prescription of the system is listed in Table 3.2-4 and Table 3.2-12. In Table 3.2-4 are listed all the common elements of the two pixel scales and in Table 3.2-12 there are listed the elements of the scale 0.25"/px that only belong to that pixel scale.

The curvature radius and thicknesses of the lenses are given at 80 K, working temperature of PANIC. For manufacturing and assembly, those parameters have to be replaced by warm parameters, using thermal expansion coefficients defined in ORD4.

Element	*Curvature radius (mm) at 80 K*	*Thickness or Separation (mm) at 80 K*	*Material*	*Aperture ∅ (mm)*
		107.8	*Vacuum*	
L5B	*139.967* *-271.923*	*39.1*	*BaF_2*	*91.3*
		2.6	*Vacuum*	
L6B	*-195.6231* *-180.2618*	*8.0*	*IR Fused Silica*	*83.1*
		8.8	*Vacuum*	
L61B	*-248.5058* *-343.7706*	*37.5*	*E-SF03*	*75.5*
		20.1	*Vacuum*	
L7B	*-173.621* *57.76894*	*40.0*	*BaF_2*	*60.7*
		168.1	*Vacuum*	
L8B	*-160.495* *-90.66532*	*14.6*	*IR Fused Silica*	*81.0*
		13.0	*Vacuum*	
Detector	*FLAT*			

Table 3.2-12 Prescriptions data of the elements that only belong to the 0.25"/px scale

3.2.6.3.3 0.25"/px descriptions

In this section we present all the footprint for the optical components in the 0.25"/px scale configuration from Figure 3.2.6-17 to Figure 3.2.6-23.

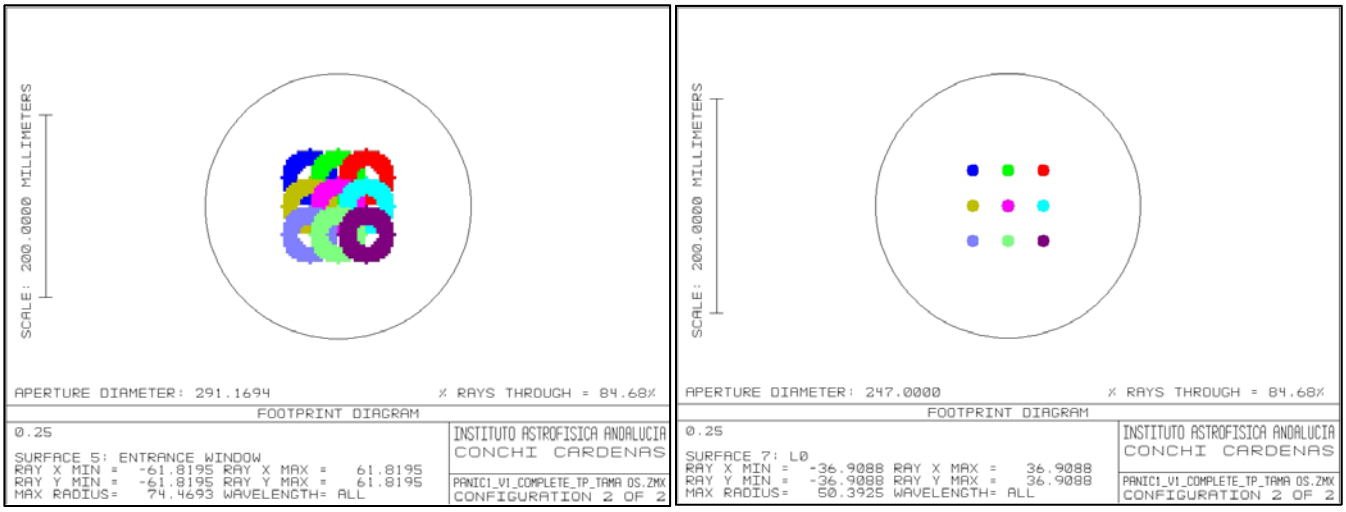

Figure 3.2.6-17 Footprint of the 0.25"/px camera FOV: on the Entrance window (left), on the L0 (right).

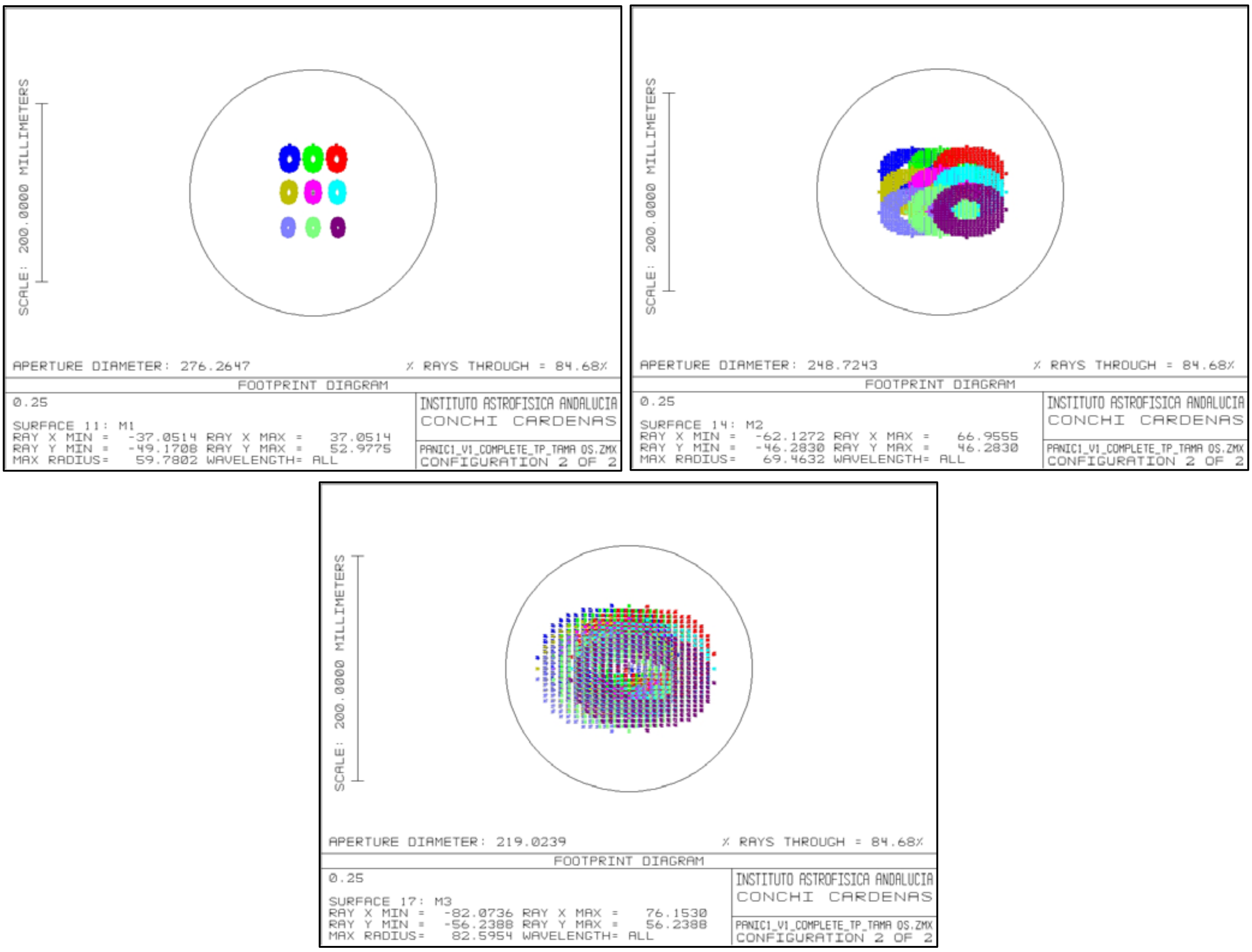

Figure 3.2.6-18 Footprint of the 0.25"/px camera FOV: on the M1 (left up), on the M2 (right up) and on the M3 (bottom).

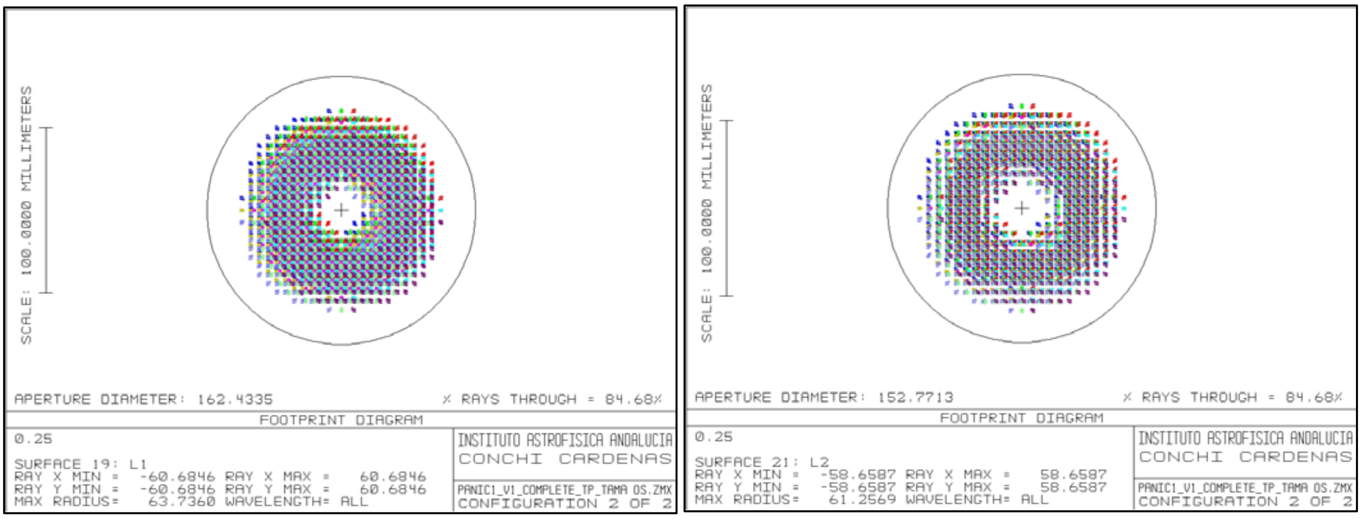

Figure 3.2.6-19 Footprint of the 0.25"/px camera FOV: : on the L1 (left), on the L2 (right).

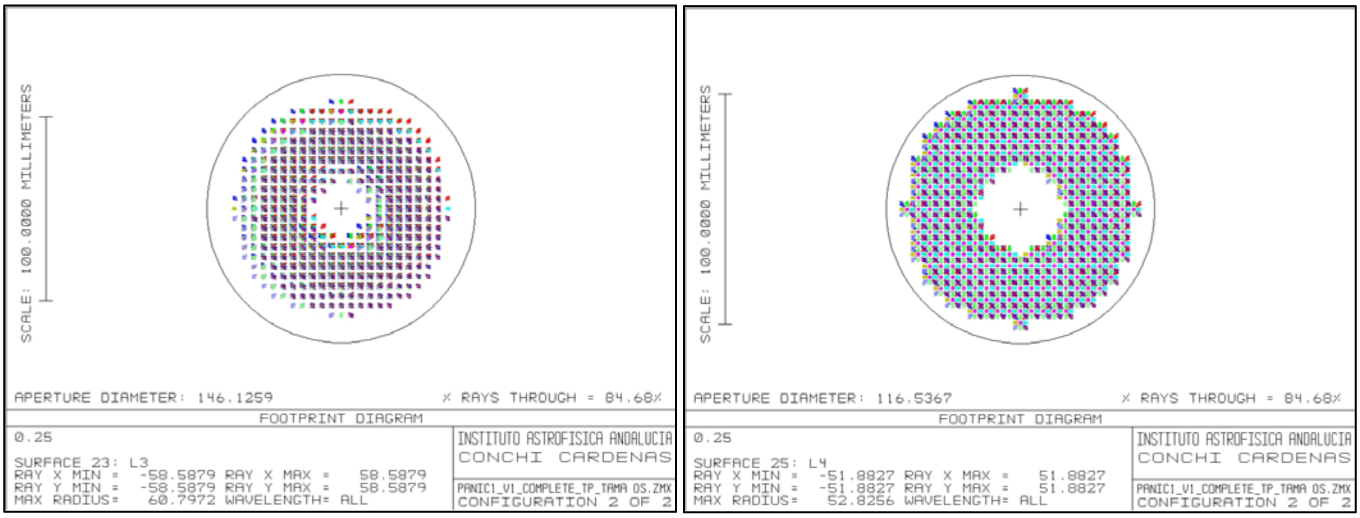

Figure 3.2.6-20 Footprint of the 0.25"/px camera FOV: : on the L3 (left), on the L4 (right).

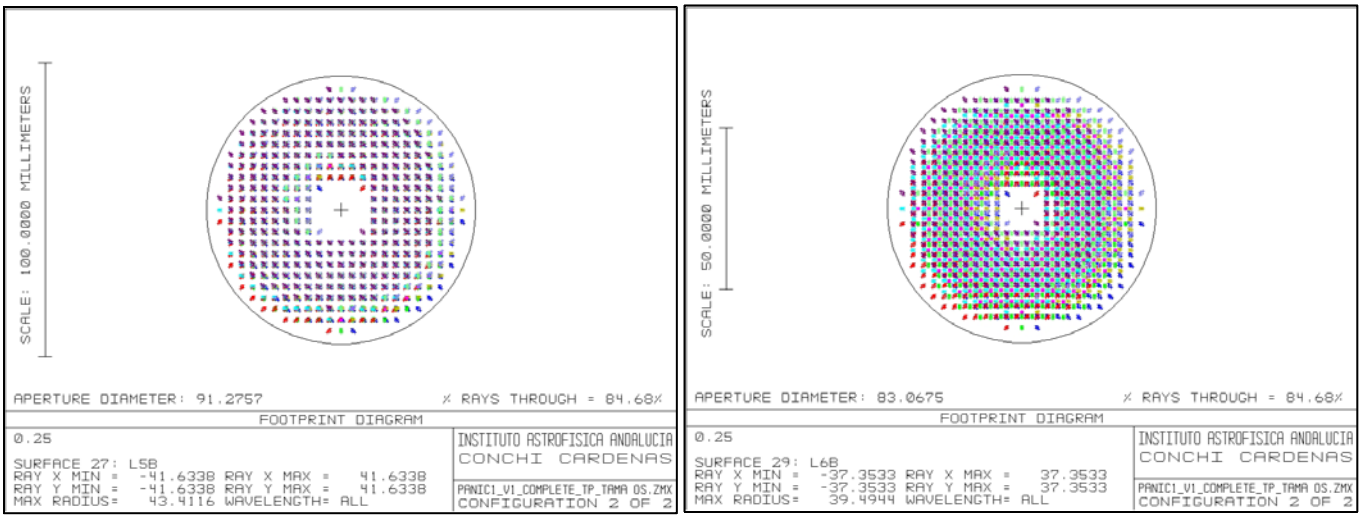

Figure 3.2.6-21 Footprint of the 0.25"/px camera FOV: : on the L5B (left), on the L6B (right).

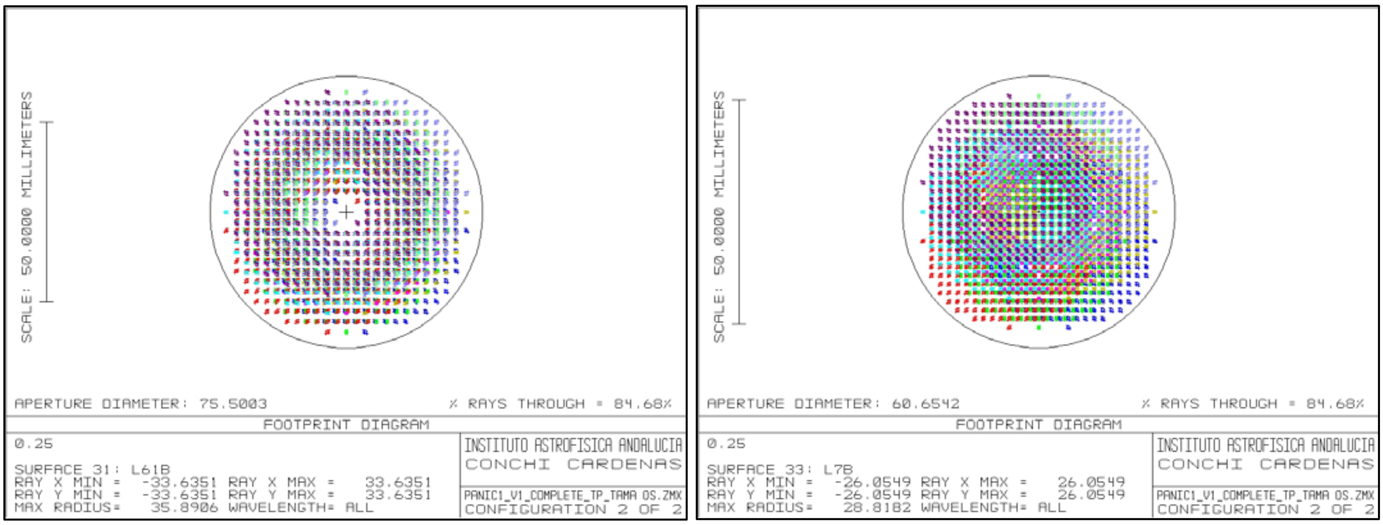

Figure 3.2.6-22 Footprint of the 0.25"/px camera FOV: on the L61B (left), on the L7B (right).

On the detector plane is box indicates the dimension of the detector mosaic and the circle the FOV optimized for the 0.25"/px scale.

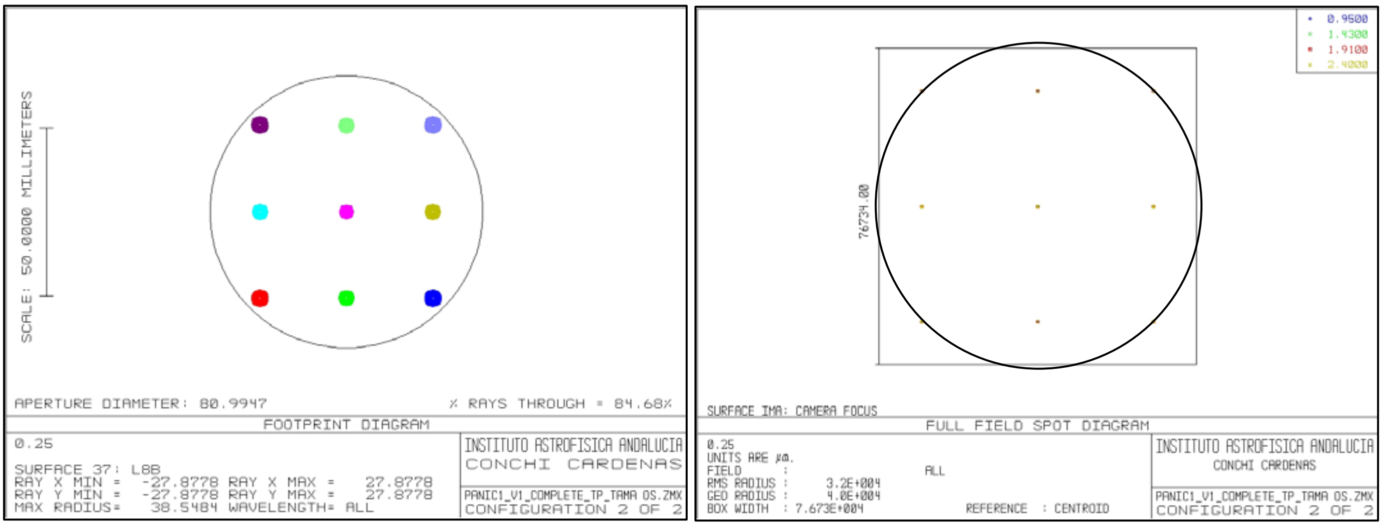

Figure 3.2.6-23 Footprint of the 0.25"/px camera FOV: on the L8B (left), on the detector plane (right).

3.2.6.3.4 0.25"/px optical performance

The Table 3.2-13 lists the characteristics that describe the performance of PANIC in the 0.25"/px scale. In this table are the figures of merit that provides a rough idea about the design quality.

Parameter	*Requirement (or Goal)*	*Achieved*
FOV	*8' (or 17.76') diameter*	*18.32' diameter*
Scale at detector	*0.25 "/px*	*0.25 "/px*
Image Quality	*EE80 ≤3 pixels (54 μm = 0.75")*	*EE80= 41.4 μm = 0.58" = 2.3 pix.,max.*
Distortion, maximum	*< 1.50 % (corner)*	*< 0.22 % max. (corner)*
Transmission	*As much as possible*	*~43% (window+10 lenses)*

Table 3.2-13 Summary of the PANIC performance in the 0.25"/px scale

3.2.6.3.5 0.25"/px Ensquared Energy and Spot diagrams

The FOV has been sampled from the centre to the external field in a radial configuration following the equal area rule. The system has been optimized for the following fields, see Table 3.2-14 to cover the maximum circle inscribed in the detector dimension:

Field	X, Y coordinate (º)	X, Y coordinate (mm)
1	(0;0)	(0;0)
2	(0.062, 0.062)	(16.07, 16.07)
3	(0.088, 0.088)	(22.81,22.81)
4	(0.108, 0.108)	(27.99,27.99)

Table 3.2-14 Fields used in the 0.25"/px scale

The origin of coordinates is the centre of the detector mosaic. The second column is the fields on the sky, and the third column is the coordinates at the detector plane.

At the detector plane, the image spots analyzed are located in the coloured points as it is shown in the Figure 3.2.6-24. The box indicates the total size of the whole detector (including gap of 167 pixels between detectors).

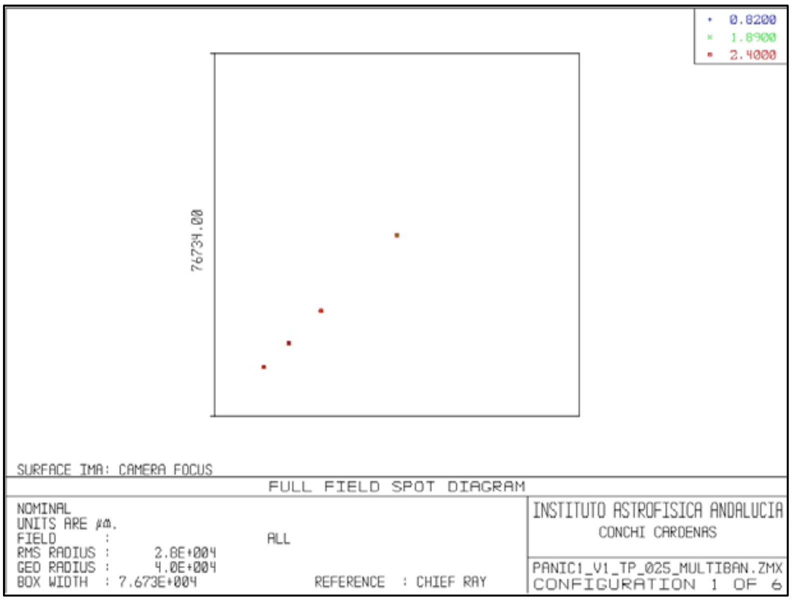

Figure 3.2.6-24 Complete FOV of the 0.25"/px

The performance of the design is evaluated at the wavelength and bandwidths shown in Table 3.2-15. Notice that the design has been optimized to this bands except the z band. The requirement for z band is not optical quality, it is only for transmission in this band. Instead of this, it can be seen that there is optical quality in z band, so the system is able to work in this photometric band.

As the filters will be placed in convergent beam, it has been decided to simulate them by inserting a plate of IR fused silica with a thickness of 12.5 mm between the L7B and L8B. it is possible to refocus the system by a movement of the telescope S2 along the optical axis, so the measurements in defocus is referred to the displacement of the S2 from the nominal position in the polychromatic configuration, and gives the sense (`- forward, i. e. sense toward the entrance window, + backward, opposite).

Filter	Wavelength (μm)	EFL (mm)	Focus (mm)
Polychromatic	0.95-2.42	14840.86	0.00
z	0.82-0.99	14850.25	+0.024
Y	0.99-1.08	14848.67	-0.013
J	1.08-1.34	14845.96	-0.021
H	1.50-1.80	14841.18	+0.002
K	1.97-2.42	14836.37	+0.009

Table 3.2-15 Bandwidths of evaluation of the PANIC optical design and their change in focus for the 0.25"/px scale

The image quality of the instrument is specified in terms of the 80 % EE (EE80) for each photometric band. The EE80 is evaluated in Table 3.2-16 using the greater value given in the FOV analyzed. Note that all the bands are in requirements (EE80 ≤ 3 pixels=54μm=0.75").

Filter	EE80 (μm)	EE80 (pix)	EE80 (arcsec)
z	33.00	1.83	0.46
Y	24.84	1.38	0.35
J	27.78	1.54	0.39
H	37.1	2.06	0.52
K	49.64	2.76	0.69
Polychromatic	41.42	2.30	0.58

Table 3.2-16 EE80 in the 0.25"/px scale

For simplicity, it has been presented only the polychromatic EE in Figure 3.2.6-25, where it is represented the fraction of energy enclosed as a function of the half side length square. It is indicated with an horizontal line the 80% of the EE. In dark it is shown the diffraction limit of the system.

For simplicity, as well, it has been presented only the polychromatic spot diagram in Figure 3.2.6-26. This figures shows the geometrical structure of the image at all points of the field for all the wavelengths considered. Better figures are obtained when the system is refocusing in the photometric bands. The squared boxes indicate the dimension of two pixels in the focal plane (36 μm), and the Airy disk for this configuration is indicated with the dark circle.

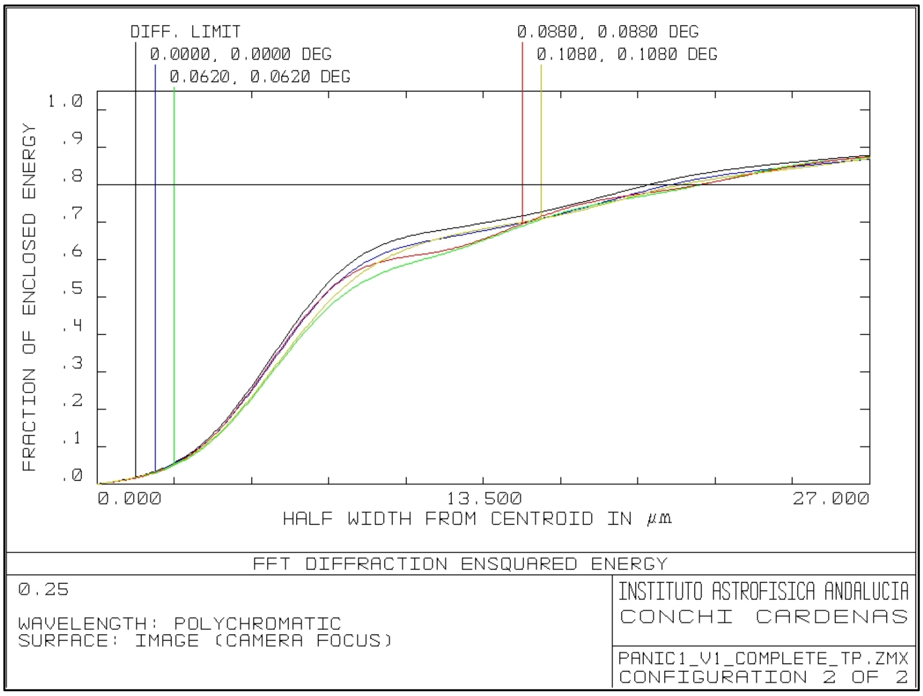

Figure 3.2.6-25 Polychromatic EE of the 0.25"/px camera

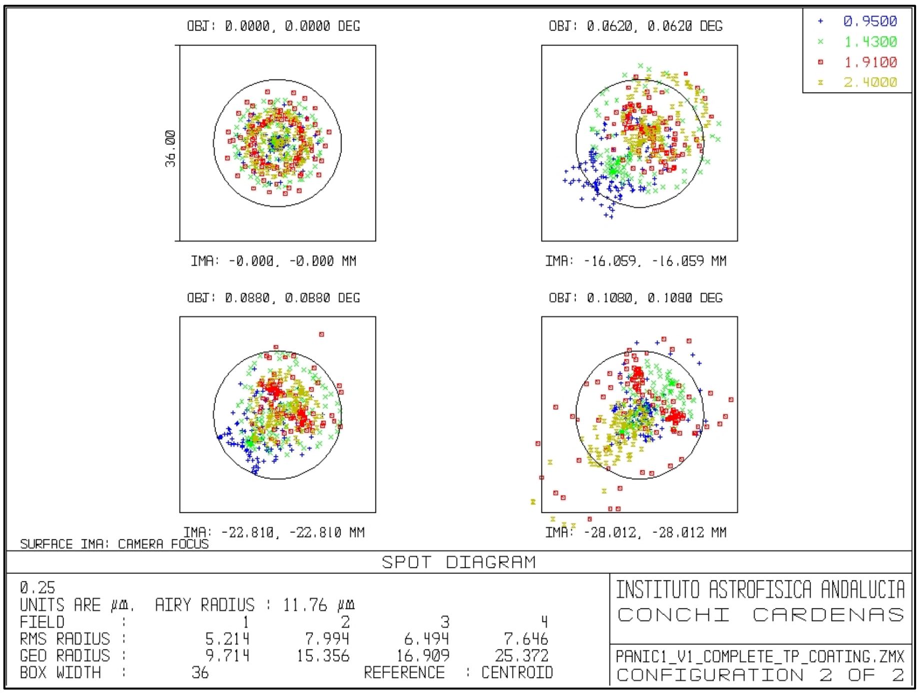

Figure 3.2.6-26 Polychromatic spot diagram of the 0.25"/px camera

3.2.6.3.6 0.25"/px Distortion

The distortion has been calculated in % with respect to the FOV centre which does not have distortion. In Table 3.2-17 we present the values for the central wavelength of the filters. For simplicity we only present in Figure 3.2.6-27 the plot of the maximum distortion obtained in the work photometric band of PANIC. Of course all the bands are in requirements (D ≤ 1.5 %).

Filter	Wavelength (μm)	Distortion (%)
z	0.82-0.99	0.13
Y	0.99-1.08	0.14
J	1.08-1.34	0.15
H	1.50-1.80	0.18
K	1.97-2.42	0.22

Table 3.2-17 Distortion data in the 0.25"/px scale

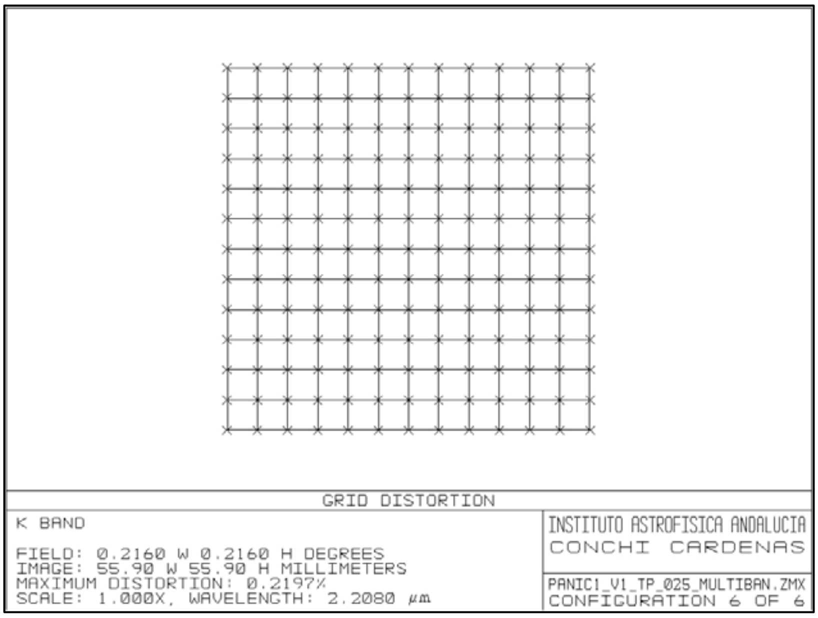

Figure 3.2.6-27 Distortion plot for the 0.25"/px camera

3.2.6.3.7 0.25"/px Transmission

In Table 3.2-18 and Figure 3.2.6-28 are the values and the plot, respectively, of the expected transmission as function of the wavelength, which has been calculated with the same considerations as the 0.45"/px scale.

λ (μm)	Transmission (%)
0.95	36.4
1.26	50.4
1.57	51.0
1.88	47.0
2.19	40.3
2.5	33.8

Table 3.2-18 Values of the expected transmission for the 0.25"/px scale

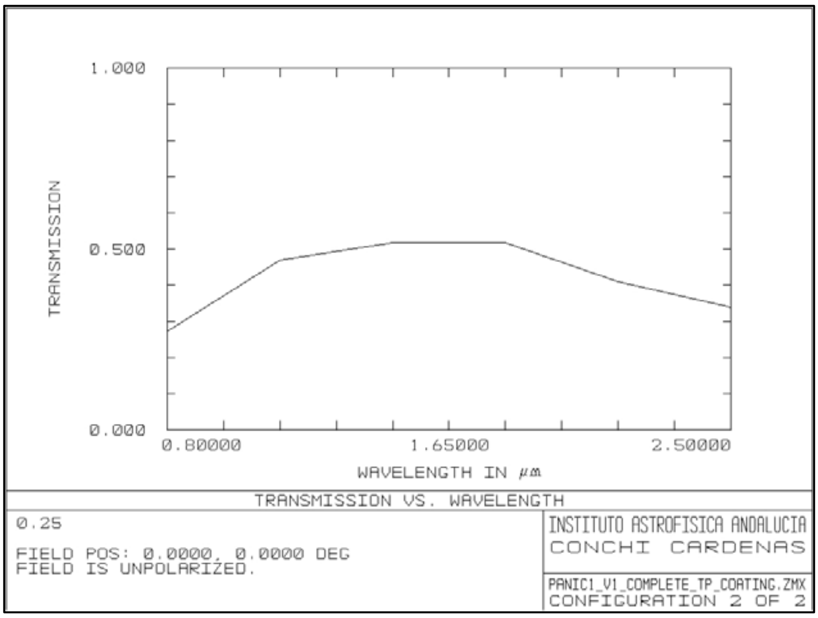

Figure 3.2.6-28 Expected transmission for the 0.25”/px camera

3.2.6.4 Filters

The filters are placed close to the detector (between L7 and L8) in the convergent beam and we have proposed filters with 125 mm of diameter. The thickness is not jet exactly determined because we have found some different criteria and we have not had the confirmation of the manufactures to achieve completely the optical quality requirements that we have asked for the filters depending on the filter thickness. That filters location remove most of the field dependence of any wavelength shift due to the change in incidence angle with field over the filters.

For interference filters, because the focal ratio of the camera and the change in the incidence angle with field over the filters the expected filter performance will suffer a broadening of the apparent band pass, a depression of transmittance values and a shift to shorter wavelengths. For broadband filters the effect is negligible. For narrowband filters we have to calculate carefully this effect and determine the incidence angle which is a flux-weighted mean of the final converging beam to specify to manufacturers the filter to operate at that angle. In Figure 3.2.6-29 and Figure 3.2.6-30 we show the angle over the filters in the position that they are located, the angle on top is the semi cone due to the focal ratio of the camera and on the bottom is the angle variation over the filter due to the field. Due to the constrains imposed during the optical design we do not expect any problem with this, even for %1 narrowband filters.

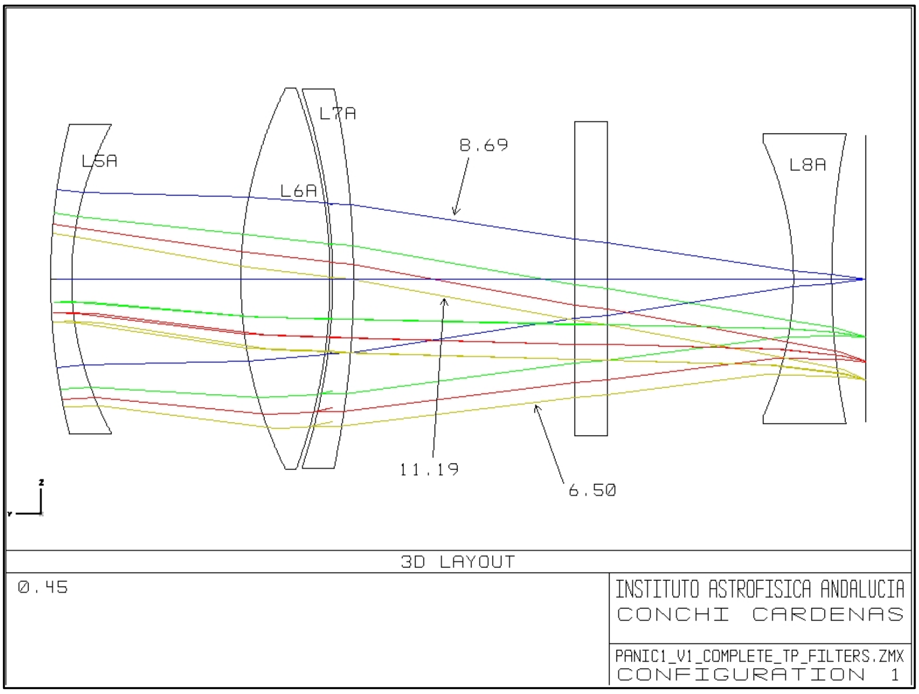

Figure 3.2.6-29 Angle over the filters for the 0.45"/px camera

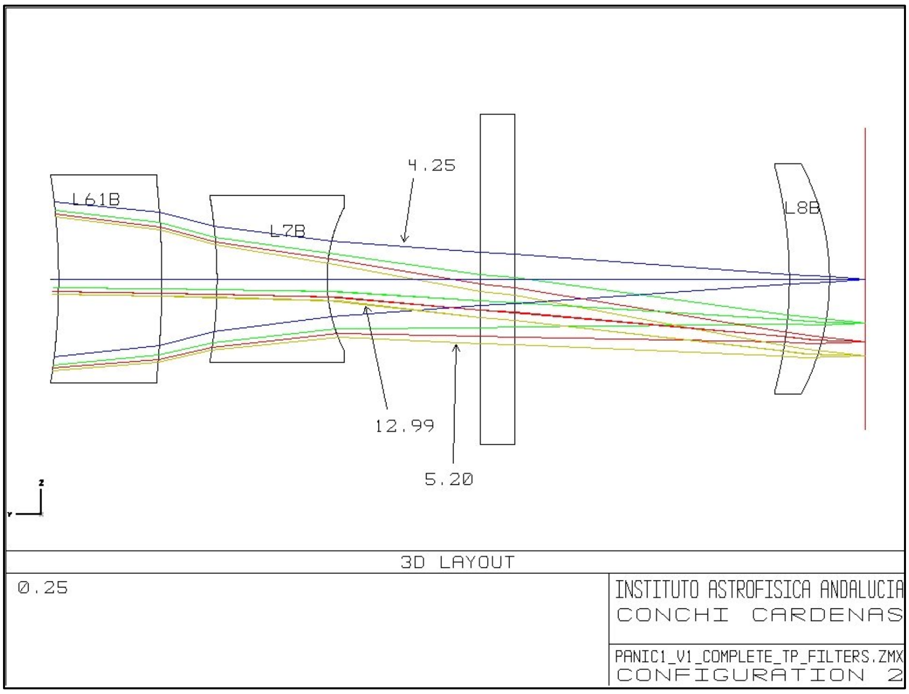

Figure 3.2.6-30 Angle over the filters for the 0.25"/px camera

3.2.6.5 Stray Light

In order to minimize the stray light in PANIC in this stage of the instrument design we have done the following considerations from the point of view of the Optics and Opto-mechanics.

The opto-mechanics design of PANIC has implemented an optical labyrinth in both optical assemblies and all the system is encapsulated to minimize stray light effects and the light interaction between both scales.

The optical design of PANIC:

A) Has been baffled with the two naturally stops: the field stop and the pupil stop. They are explained, respectively, in 3.2.6.5.1 and 3.2.6.5.2 sections.

B) All the lenses have been over dimensioned a 5% over their clear aperture in order to avoid stray light coming from the lens edges.

C) The contribution in the stray light due to the ghost has to be minimizing taking into account the ghost analysis in section 3.2.6.6.

D) The micro-roughness of the lenses and mirrors surfaces will contribute in the total amount of stray light. So, the aim of the design has been not use diamond turned surfaces. In this way, first, there is not any aspheric surface in the optical design of PANIC, and second, we propose to use gold coated glass folding mirrors, to reduce imaging errors and scattered light.

A complete stray light analysis will be done in the following phase of the project.

3.2.6.5.1 Field Stop

In order to achieve a good shielding from off-axis sources of light that would be outside the desired FOV a Field Stop is placed at the position of the RC focal plane, as shown Figure 3.2.6-3, between L0 and M1. This aperture is usually located at an image to limit and define the FOV without adding radiating flux from warm surfaces which is critical in the K band.

In PANIC the Field Stop mask needed has been calculated for the two pixel scales as it is shown in Table 3.2-19. The free opening proposed is square shape with the same orientation as the detector. The optimal positions in axial direction of the Field masks, from the rear surface of L0, are not coincident, there is a space close to 3 mm. This makes possible a mechanical solution which has the 0.45"/px mask fixed and introduces a mobile 0.25"/px mask.

Plate scale	Distance from L0_rear to Field Stop optimal position (mm)	Square length side of the free opening (mm)
0.45"/px	35.16	155.37 ≈ 156
0.25"/px	38.10	62.31 ≈ 63

Table 3.2-19 Position and size of the Field Stop masks

3.2.6.5.2 Cold Stop

A main feature in the optical design of an infrared camera is its cold aperture stop to reduce the thermal background, overall, in the K band. In PANIC the entrance pupil or entrance stop is the telescope primary mirror, S1, which gives the maximum light collecting power, and not the secondary as any Infrared Telescope in which the secondary is undersized.

The cool stop is used to control undesirable light that could reach the detector, it prevents the detector from seeing anything but the optics and the imaged scene, especially the warm interior of the system. In the optical design of PANIC we have generated a good image quality of the S1 in the middle of the optical track, and we have determined the optimal pupil imaging position in function of the photometric bands, as Table 3.2-20 shows.

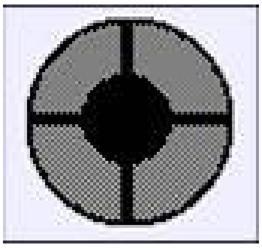

We proposed a mask with an outer hole, which corresponds to the re-imaging S1 diameter, and a inner mask, which corresponds to the S2 obstruction, as the figure shows.

Figure 3.2.6-31 Pupil mask shape

Wavelengths	Distance from L4_rear to Cold Stop optimal position (mm)	Outer hole diameter (mm)	Inner mask diameter (mm)
Polychromatic	13.53	92.18	36.87
Y band	7.72	93.16	37.25
J band	11.37	92.52	36.99
H band	15.40	91.79	36.71
K band	22.30	90.61	36.24

Table 3.2-20 Position and size of the Cold Stop mask

The results are:

a) the pupil mask is the same for the two pixel scales,
b) it shall be positioned between L4 and L5,
c) the position from the L4 (in the optical axis direction) will be 13.53 mm min., and 22. 30 mm max. (see the Figure 3.2.6-3 or Figure 3.2.6-16),
d) the pupil mask is accessible,
e) the outer hole must have a diameter of 92. 18 mm for the minimum in position and 90. 61 mm for the maximum in position,
f) the inner mask, due to the S2 obstruction, must have a diameter of 36. 87 mm for the minimum in position and 36. 24 mm for the maximum in position,
g) it is not necessary the implementation of the obstruction due to the S2 spiders,
h) if we decided to implement the four arms then they can be 1.4 mm of thickness or less.

Notice that the degradation in the pupil re-imaging diameter shall be 3% maximum in K band (as it is required in 3.2.5.1.5). We can calculate the degradation in the diameter for K band due to positioning the pupil at the polychromatic position (13.53 mm) which is 1,73 % < 3%. Also, we have calculated that degradation due to the decentring ± 200 µm (in X or Y axis, perpendicular to the optical axis) and tilt 3 arcmin the pupil is 0.63 %. Adding the three contributions the total degradation is 2.99 %, which is nearly the 3% as maximum permitted. So, we conclude that the pupil fulfils the requirement even in the polychromatic position. A footprint at the polychromatic position of the cold stop for the central and the external fields is shown in Figure 3.2.6-32.

To avoid maximum background suppression losing minimum flux in K band, we propose to place the pupil at the distance of 22.30 mm from the L4, with the dimensions shown in Table 3.2-20. But we can placed it at the polychromatic position being under requirement, because for a degradation of 3 % maximum in the diameter the thermal contribution in the K band is negligible.

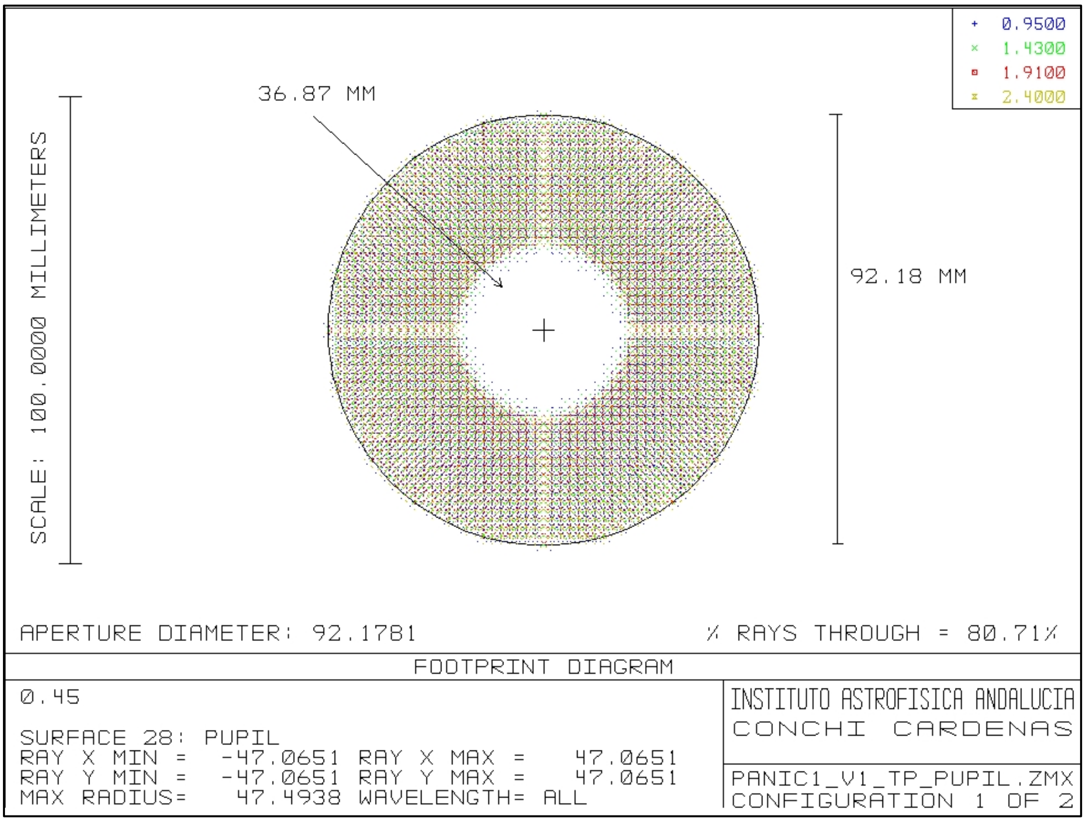

Figure 3.2.6-32 Footprint at the Pupil position

3.2.6.6 Ghost analysis

A preliminary analysis of ghost reflections was performed for PANIC in its two pixel scales. The analysis of ghost images has been made by tracing (first order) all combinations of two reflections within a lens, i. e. a ray from the axial object point is traced to the second surface from which it reflects back to the first surface and then reflecting from it, travels on to the image. This process is iterated for all the possible combinations of two surfaces. The telescope surfaces are not taken into account in this analysis. A 1% reflective coating has been applied to all optical surfaces, including the filter surfaces, this consideration will aid in accurate computation of total ghost energy in Zemax.

We have analyzed the most critical components which produce the ghost images. The Table 3.2-21 and Table 3.2-22 summarize the results obtained for the two pixel scales. A lot of values are not included because they were too far out of focus for the simulation to make sense. The higher results in intensity ratio between a ghost image and its source are the ghost #1 and #3, respectively, the instrument window and the filters, but always is lower than $1{\cdot}10^{-4}$ in all the cases ("in" requirement).

There are three ghosts out of the 10" diameter requirement, they are: #2 (field 1) and #5 (fields 3 and 4). But they do not represent any problem because the requirement of Image/Ghost ratio is completely fulfilled.

In the 0.45"/px scale 10" are equal to 400 µm, so, in principle, the ghost #2 violates this condition but notice that this ghost has a central hole of 60 µm, and both, the source and the ghost are centred in the (0,0) coordinates. The source has a diameter of 29,84 µm, so there will not real superposition.

In the 0.25"/px scale 10" are equal to 720 µm, so, in principle, the ghost #5 (fields 3 and 4) violates this condition. If we calculate the contribution of the ghost in relative energy in the source area, we can notice that it is in the order of 10^{-6} or 10^{-7}.

We can conclude that, in all the cases, the contribution in intensity is insignificant instead of the violation in diameter, so the impact of the ghosts in the total PSF of the system is negligible.

Ghost #	First reflecting surface	Second reflecting surface	Geometrical rms Diameter (µm)	Relative intensity
#1	Window_rear	Window_front	1622 with hole 600 (field 1) 1643 with hole 622 (field 2) 1655 with hole 622 (field 3) 1661 with hole 622 (field 4)	$4.54{\cdot}10^{-5}$ $4.53{\cdot}10^{-5}$ $4.51{\cdot}10^{-5}$ $4.47{\cdot}10^{-5}$
#2	L8A_rear	L0_front	329.8 with hole 60 (field 1)	$2.10{\cdot}10^{-5}$

Table 3.2-21 PANIC ghost analysis for the 0.45"/px scale

Ghost #	First reflecting surface	Second reflecting surface	Geometrical rms Diameter (µm)	Relative intensity
#3	Filter_rear	Filter_front	2596 with hole 1000 (field 1) 2527 with hole 978 (field 2) 2504 with hole 961 (field 3) 2486 with hole 961 (field 4)	$4.34{\cdot}10^{-5}$ $4.35{\cdot}10^{-5}$ $4.36{\cdot}10^{-5}$ $4.36{\cdot}10^{-5}$
#4	Filter_rear	L6B_front	2981.4 (field 1)	$3.25{\cdot}10^{-5}$
#5	L8B_front	L0_rear	1999 with hole 666 (field 1) 1132 (field 2) 477 (field 3) 52 (field 4)	$2.02{\cdot}10^{-5}$ $0.83{\cdot}10^{-5}$ $0.51{\cdot}10^{-5}$ $0.20{\cdot}10^{-5}$

Table 3.2-22 PANIC ghost analysis for the 0.25"/px scale

We also looked to see if any ghost pupil images are formed on the detector, and we did not find anything significant. These could potentially be a problem if the image of the pupil is near the detector, and is smaller than the field of view. But, that does not happen in PANIC.

In conclusion, the effects of the L8A, L8B and L0 dominate this analysis. So, the best way to deal with the ghosts will be put good AR coatings on those lenses and possibly in the filters and in the entrance window. We have estimated that improvement of the AR coating would decrease the intensity ratio about one order of magnitude. If, finally, we would decide to avoid the ghost #2 and/or #5, it is possible to change a little the ROC of the lenses involved in those ghosts.

3.2.7 Tolerance Analysis

A preliminary study of the tolerances for PANIC has been done. In a separate technical note (ORD5) it is described. Tolerances need to be defined for optical manufacturing, position accuracy during assembly and stability during operation.

The nominal criterion to evaluate the acceptance of the degraded system is the half EE80 ≤ 2px=18μm for the 0.45"/px and the half EE80 ≤ 3px=27μm for the 0.25"/px 80 %. The system has been evaluated in terms of the rms spot radius at five fields (FOV centre and 4 external situated at 90% of the FOV corner) and in three wavelengths (to cover the complete spectral range). The tool used to verify the fulfilment of the criterion has been the "Overlay Montecarlo" during the tolerances runs. The tolerances for the elements and sub-systems are done for the following features:

+ For the elements fabrication has been tolerated (the folding mirrors are included):

- the ROC of the two surfaces, front and rear (in the case of flat surfaces it has been tolerated the flatness in fringes),
- the thickness of the element (except for the mirrors),
- and the wedge of the element.

+ And for the barrels and the whole instrument has been tolerated the position in the axial direction, and the decenter and tilt in X and Y (being X and Y contained in the plane perpendicular to the Z axis). The results for the barrels have been presented here in the order of they are nested.

The opto-mechanical arrangement and grouping made for the mechanics for the two pixel scales is shown in Table 3.2-23 and Table 3.2-24.

Optical element	L0	M1	M2	M3	L1	L2	L3	L4	L5A	L6A	L7A	L8A
Groups	barrel 1				lens mount 2				lens mount 3 A			b. A
	optics mount 1								optics wheel			
	complete optics											

Table 3.2-23 PANIC camera groups for the 0.45"/px scale

Optical element	L0	M1	M2	M3	L1	L2	L3	L4	L5B	L6B	L61B	L7B	L8B
Groups									lens mount 3Ba		lens mount 3Bb		
	barrel 1				lens mount 2				lens mount 3 B				b. B
	optics mount 1								optics wheel				
	complete optics												

Table 3.2-24 PANIC camera groups for the 0.25"/px scale

The study has been performed as follows:

+ First, a sensitivity analysis was performed to identify the critical elements in the optical system and define the tolerances in manufacturing and assembly of the lenses and the barrels for the two pixel scales.

At this stage, there are two distances which need compensation due to manufacturing errors:

→ L1-L2 distance,

→ and L6B-L61B distance.

These distances will be done after the factory report of the as-built singlets, such as thicknesses, radii, wedges and lens distances are measured. A new optimization is then carried out and final values of these compensators are evaluated and fixed. Thus this compensator will only compensate for symmetrical aberrations.

+ Second, it has been assigned tolerances to the elements and the barrels and allowing some degradation in the nominal system performance. With the Overlay Montecarlo and with some iteration has been established a limit in degradation for a 97 % of the simulated system being inside the criterion. The results obtained in this stage showed some elements with tight tolerances in the two pixel scales, both in position and tilt. So, we have chosen the following decentring compensators to relax as much as possible the critical values:

→ L2 decenter,

→ L6A decenter,

→ and L5B decenter.

Those elements will be adjusted in decenter while placing an interferometer to cancel the non symmetrical aberrations due to lens wedges and mounting tilts. These compensators have the effect of correcting non-symmetrical aberrations due to

+ Finally, it has been performed a final analysis to determine the tolerances with the compensators implemented, and the ranges needed for the compensators as well. From Table 3.2-25 to Table 3.2-44 we summarize the values for the tolerances after the compensator has been introduced.

3.2.7.1.1 Tolerances for the 0.45"/px scale

In Table 3.2-25 are the values for manufacturing. We have considered a default ranges for the tolerated parameters: for ROC the 0.1% of ROC, for thickness 100 μm, for wedge 3 arc min, and for flatness 1 fringe.

The range obtained for the compensator in L1-L2 distance: ±0.8 mm.

MANUFACTURING ERRORS OF SINGLETS: FIRST STAGE					
ITEM	**R1 (mm)**	**R2 (mm)**	**Thickness (μm)**	**Wedge (arc min)**	**Flatness (fringes @ 632.8 nm)**
WINDOW	-	-	± 100	± 2.95'	1-1
L0	± 0.420	-	± 100	± 3.00'	-1
M1	-	-	-	-	1
M2	-	-	-	-	1
M3	-	-	-	-	1
L1	± 0.470	± 0.300	± 100	± 3.00'	-
L2	+ 0.130; - 0.260	+ 0.430; - 0.409	± 100	± 1.16'	-
L3	+ 0.032; - 0.123	+ 0.094; -0.025	+ 100; - 87	± 2.83'	-
L4	+ 0.145; - 0.210	± 3.000	± 100	± 3.00'	-
L5A	± 0.250	+ 0.064; - 0.072	± 100	± 3.00'	-
L6A	+ 0.128; - 0.082	+ 0.146; - 0.172	± 100	± 3.00'	-
L7A	+ 0.144; - 0.130	± 0.350	± 100	± 3.00'	-
FILTER	-	-	± 100	± 3.00'	1-1
L8A	± 0.120	± 0.280	± 100	± 3.00'	-

Table 3.2-25 Manufacturing tolerances for individual elements for the 0.45"/px scale

Next tables show the integration tolerances for the different barrel which contain the singlets: Barrel 1 is in Table 3.2-26, Lens mount 2 is in Table 3.2-27, Lens mount 3A is in Table 3.2-28 and Barrel 4A is in Table 3.2-29. Note that Barrel 1 and Lens mount 2 are common for the two pixel scales. We have considered a default ranges for the tolerated parameters: for Tilt 3 arc min, for decenter 100 μm and for position 200 μm.

The range obtained for the compensator in dectenter for L2 and L6A are shown in the tables.

Barrel 1 (L0-M1-M2-M3)					
SINGLET	**TILT X (arc min)**	**TILT Y (arc min)**	**DECENTER X (μm)**	**DECENTER Y (μm)**	**POSITION Z (μm)**
L0	± 3.00'	± 3.00'	± 100	± 100	± 200
M1	± 2.91'	± 3.00'	± 100	± 100	± 200
M2	± 3.00'	± 2.65'	± 100	± 100	± 200
M3	± 3.00'	± 2.24'	± 100	± 100	± 200

Table 3.2-26 Integration tolerances within the barrel 1 for the 0.45"/px scale

Lens mount 2 (L1-L2-L3-L4-Cold Stop)					
SINGLET	**TILT X (arc min)**	**TILT Y (arc min)**	**DECENTER X (μm)**	**DECENTER Y (μm)**	**POSITION Z (μm)**
L1	± 3.00'	± 3.00'	± 100	± 100	± 200
L2	± 3.00'	± 3.00'	Compensator ± 400	Compensator ± 400	± 200
L3	± 3.00'	± 3.00'	± 100	± 100	± 200
L4	± 3.00'	± 3.00'	± 100	± 100	+ 200; - 160

Table 3.2-27 Integration tolerances within the lens mount 2 for the 0.45"/px scale

Lens mount 3A (L5A-L6A-L7A)					
SINGLET	**TILT X (arc min)**	**TILT Y (arc min)**	**DECENTER X (μm)**	**DECENTER Y (μm)**	**POSITION Z (μm)**
L5A	± 3.00'	± 3.00'	± 100	± 100	+ 109; - 163
L6A	± 3.00'	± 3.00'	Compensator ± 300	Compensator ± 350	+ 152; - 150
L7A	± 3.00'	± 3.00'	± 100	± 100	± 200

Table 3.2-28 Integration tolerances within the lens mount 3A

Barrel 4A (L8A)					
SINGLET	**TILT X (arc min)**	**TILT Y (arc min)**	**DECENTER X (μm)**	**DECENTER Y (μm)**	**POSITION Z (μm)**
L8A	± 3.00'	± 3.00'	± 100	± 100	± 200

Table 3.2-29 Integration tolerances within the barrel 4A

Next tables show the integration tolerances for the sub-barrels and finally the instrument. We show them as they are nested. First there are the Optics mount 1 (Table 3.2-30) and the Optics wheel (Table 3.2-31), them the whole instrument assembly (Table 3.2-32) and finally the alignment of the instrument with the telescope (Table 3.2-33). Note that Optics mount 1 is common for the two pixel scales. We have considered a default ranges for the tolerated parameters: for Tilt 3 arc min, for decenter 100 µm and for position 200 µm, also.

The only available adjust, once the system is cooled, will be the telescope refocusing (using the S2) although for integration a detector adjustment in position and tilt is possible. The tilt in the detector will be required to compensate for the angle introduced when the decentering compensator are used.

Sub-barrels integration (Optics mount 1)					
BARREL	**TILT X (arc min)**	**TILT Y (arc min)**	**DECENTER X (µm)**	**DECENTER Y (µm)**	**POSITION Z (µm)**
Barrel 1	± 2.61'	± 2.61'	± 100	± 100	± 200
Lens mount 2	± 3.00'	± 3.00'	± 100	± 100	± 200

Table 3.2-30 Integration tolerances within the Optics mount 1

Sub-barrels integration (Optics wheel)					
BARREL	**TILT X (arc min)**	**TILT Y (arc min)**	**DECENTER X (µm)**	**DECENTER Y (µm)**	**POSITION Z (µm)**
Lens mount 3A	± 3.00'	± 3.00'	± 100	± 100	± 200
Barrel 4A	± 3.00'	± 3.00'	± 100	± 100	± 200

Table 3.2-31 Integration tolerances within the Optics wheel in the 0.45"/px scale

Assembly errors (whole instrument)					
BARREL	**TILT X (arc min)**	**TILT Y (arc min)**	**DECENTER X (µm)**	**DECENTER Y (µm)**	**POSITION Z (µm)**
Cryostat window	± 3.00'	± 3.00'	± 100	± 100	± 200
Optics mount 1	± 3.00'	± 3.00'	± 100	± 100	± 200
Optics wheel	± 3.00'	± 3.00'	± 200	± 200	± 200
Detector	± 3.00'	± 3.00'	-	-	± 200

Table 3.2-32 Assembly tolerances for the different units in the 0.45"/px scale

Alignment (telescope-whole instrument)					
BARREL	**TILT X (arc min)**	**TILT Y (arc min)**	**DECENTER X (mm)**	**DECENTER Y (mm)**	**POSITION Z (µm)**
Whole instrument	± 6.00'	± 6.00'	1.00	1.00	± 200

Table 3.2-33 Tolerances for whole instrument to the telescope in the 0.45"/px scale

Figure 3.2.7-1 shows the overlay EE for the montecarlo systems generated with the values of tolerances that we have summarized. More than 97% of the systems are inside the criterion half EE80 ≤ 18 µm as required.

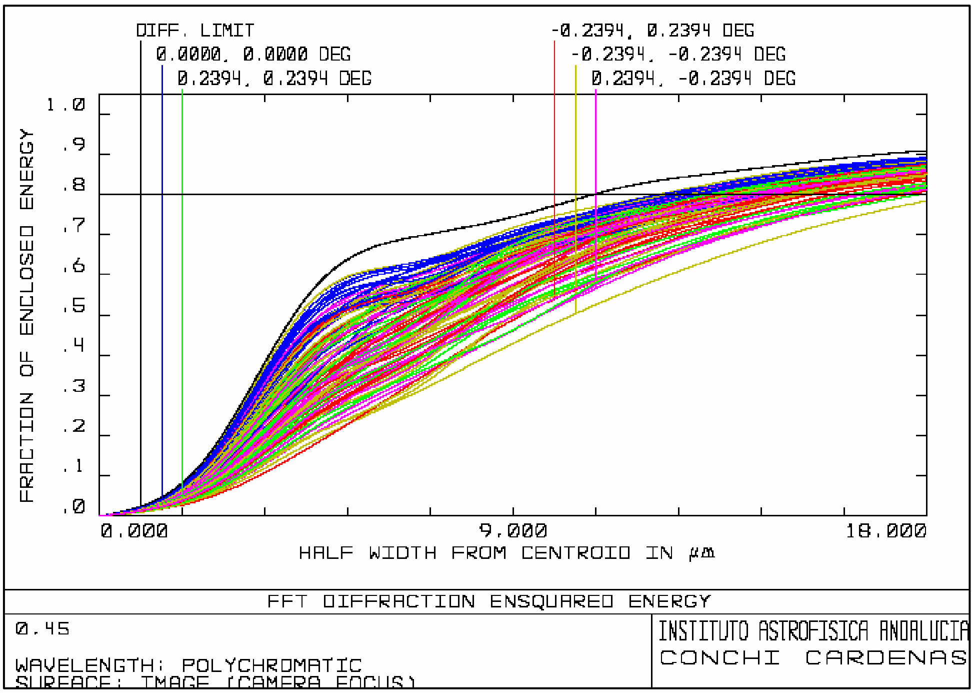

Figure 3.2.7-1 Montecarlo overlay of the EE80 for the tolerances in the 0.45"/px

3.2.7.1.2 Tolerances for the 0.25"/px scale

In Table 3.2-34 are the values for manufacturing considering the 0.25"/px scale. We have considered the same ranges as in the 0.45"/px analysis in the tolerated parameters. We can conclude that this scale impose the value in wedge of L0 and L2, since result lower values in this scale, although the difference is not to much. There not limitation to the rest of values obtained. The values in blue emphases result as the values more restrictive and they must be the limit in that cases.

The range obtained for the compensator in L6B-L61B distance: ±0.3 mm.

MANUFACTURING ERRORS OF SINGLETS: FIRST STAGE					
ITEM	**R1 (mm)**	**R2 (mm)**	**Thickness (µm)**	**Wedge (arc min)**	**Flatness (fringes @ 632.8 nm)**
WINDOW	-	-	± 100	± 2.82'	1-1
L0	± 0.420	-	± 100	± 3.00'	-1
M1	-	-	-	-	1
M2	-	-	-	-	1
M3	-	-	-	-	1
L1	± 0.470	± 0.300	± 100	± 3.00'	-
L2	± 0.260	± 0.430	± 100	± 1.05'	-
L3	± 0.150	± 0.120	± 100	± 3.00'	-
L4	± 0.210	± 3.000	± 100	± 3.00'	-
L5B	± 0.140	± 0.280	± 100	± 3.00'	-
L6B	± 0.200	± 0.180	± 100	± 3.00'	-
L61B	± 0.250	± 0.350	± 100	± 3.00'	
L7B	± 0.170	± 0.060	± 100	± 3.00'	-
FILTER	-	-	± 100	± 3.00'	1-1
L8B	± 0.160	± 0.090	± 100	± 3.00'	-

Table 3.2-34 Manufacturing tolerances for individual elements for the 0.25"/px scale

Next tables show the integration tolerances for the different barrel which contain the singlets: Barrel 1 is in Table 3.2-35, Lens mount 2 is in Table 3.2-36, Lens mount 3Ba is in Table 3.2-37, Lens mount 3Bb is in Table 3.2-38 and Barrel 4B is in Table 3.2-39. Note that Barrel 1 and Lens mount 2 are common for the two pixel scales. For Barrel 1, the 0.25"/px scale do not violates the values given for them in the 0.45"/px scale. In the case of the Lens mount 2, the L2 values are imposed by the 0.25"/px scale, but do not represent tight values. The others barrel have values quite relaxed.

The range obtained for the compensator in dectenter for L2 and L5B are shown in the tables.

Barrel 1 (L0-M1-M2-M3)					
SINGLET	**TILT X (arc min)**	**TILT Y (arc min)**	**DECENTER X (μm)**	**DECENTER Y (μm)**	**POSITION Z (μm)**
L0	± 3.00'	± 3.00'	± 100	± 100	± 200
M1	± 3.00'	± 3.00'	± 100	± 100	± 200
M2	± 3.00'	± 3.00'	± 100	± 100	± 200
M3	± 3.00'	± 3.00'	± 100	± 100	± 200

Table 3.2-35 Integration tolerances within the barrel 1 for the 0.25"/px scale

Lens mount 2 (L1-L2-L3-L4-Cold Stop)					
SINGLET	**TILT X (arc min)**	**TILT Y (arc min)**	**DECENTER X (μm)**	**DECENTER Y (μm)**	**POSITION Z (μm)**
L1	± 3.00'	± 3.00'	± 100	± 100	± 200
L2	± 2.73'	± 2.73'	Compensator ± 400	Compensator ± 600	± 200
L3	± 3.00'	± 3.00'	± 100	± 100	± 200
L4	± 3.00'	± 3.00'	± 100	± 100	± 200

Table 3.2-36 Integration tolerances within the lens mount 2 for the 0.25"/px scale

Lens mount 3Ba (L5B-L6B)					
SINGLET	**TILT X (arc min)**	**TILT Y (arc min)**	**DECENTER X (μm)**	**DECENTER Y (μm)**	**POSITION Z (μm)**
L5B	± 2.35'	± 2.35'	Compensator ± 500	Compensator ± 400	± 200
L6B	± 3.00'	± 3.00'	± 100	± 100	± 200

Table 3.2-37 Integration tolerances within the lens mount 3Ba

Lens mount 3Bb (L61B-L7B)					
SINGLET	**TILT X (arc min)**	**TILT Y (arc min)**	**DECENTER X (μm)**	**DECENTER Y (μm)**	**POSITION Z (μm)**
L61B	± 3.00'	± 3.00'	± 100	± 100	± 200
L7B	± 3.00'	± 3.00'	± 100	± 100	± 200

Table 3.2-38 Integration tolerances within the lens mount 3Bb

Barrel 4B (L8B)					
SINGLET	**TILT X (arc min)**	**TILT Y (arc min)**	**DECENTER X (μm)**	**DECENTER Y (μm)**	**POSITION Z (μm)**
L8B	± 3.00'	± 3.00'	± 100	± 100	± 200

Table 3.2-39 Integration tolerances within the barrel 4B

Next tables show the integration tolerances for the sub-barrels and finally the instrument. We show them as they are nested. First there are the Optics mount 1 (Table 3.2-40), second, the Lens mount 3B (Table 3.2-41) and the Optics wheel (Table 3.2-42), them the whole instrument assembly (Table 3.2-43) and finally the alignment of the instrument with the telescope (Table 3.2-44). Note that Optics mount 1 is common for the two pixel scales but this scale do not impose values to the other scale. The same happens with the alignment to the telescope. The alignment for Barrel 3B can be completely relaxed if we verify this barrel with its sub-barrels completely attached. The others barrel have values quite relaxed.

In this scale the only available adjust, once the system is cooled, will be the telescope refocusing (using the S2) too. So the same consideration is done with respect to the detector adjustment in position and tilt to compensate for the angle introduced when the decentering compensator are used.

Sub-barrels integration (Optics mount 1)					
BARREL	**TILT X (arc min)**	**TILT Y (arc min)**	**DECENTER X (μm)**	**DECENTER Y (μm)**	**POSITION Z (μm)**
Barrel 1	± 3.00'	± 3.00'	± 100	± 100	± 200
Lens mount 2	± 3.00'	± 3.00'	± 100	± 100	± 200

Table 3.2-40 Integration tolerances within the Optics mount 1 for 0.25"/px scale

Sub-barrels integration (Lens mount 3B)					
BARREL	**TILT X (arc min)**	**TILT Y (arc min)**	**DECENTER X (μm)**	**DECENTER Y (μm)**	**POSITION Z (μm)**
Lens mount 3Ba	± 2.36'	± 2.36'	± 100	± 100	± 200
Lens mount 3Bb	± 2.46'	± 2.46'	± 100	± 100	± 200

Table 3.2-41 Integration tolerances within the Lens mount 3B

Sub-barrels integration (Optics wheel)					
BARREL	**TILT X (arc min)**	**TILT Y (arc min)**	**DECENTER X (μm)**	**DECENTER Y (μm)**	**POSITION Z (μm)**
Lens mount 3B	± 3.00'	± 3.00'	± 100	± 100	± 200
Barrel 4B	± 3.00'	± 3.00'	± 100	± 100	± 200

Table 3.2-42 Integration tolerances within the Optics wheel in the 0.25"/px scale

Assembly errors (whole instrument)					
BARREL	**TILT X (arc min)**	**TILT Y (arc min)**	**DECENTER X (µm)**	**DECENTER Y (µm)**	**POSITION Z (µm)**
Cryostat window	± 3.00'	± 3.00'	± 100	± 100	± 200
Optics mount 1	± 3.00'	± 3.00'	± 100	± 100	± 200
Optics wheel	± 3.00'	± 3.00'	± 200	± 200	± 200
Detector	± 3.00'	± 3.00'	-	-	± 200

Table 3.2-43 Assembly tolerances for the different units in the 0.25"/px scale

Alignment (telescope-whole instrument)					
BARREL	**TILT X (arc min)**	**TILT Y (arc min)**	**DECENTER X (mm)**	**DECENTER Y (mm)**	**POSITION Z (µm)**
Whole instrument	± 6.00'	± 6.00'	1.00	1.00	± 200

Table 3.2-44 Tolerances for whole instrument to the telescope in the 0.25"/px scale

Figure 3.2.7-2 shows the overlay EE for the montecarlo systems generated with the values of tolerances that we have summarized. More than 97% of the systems are inside the criterion half EE80 ≤ 27 µm as required.

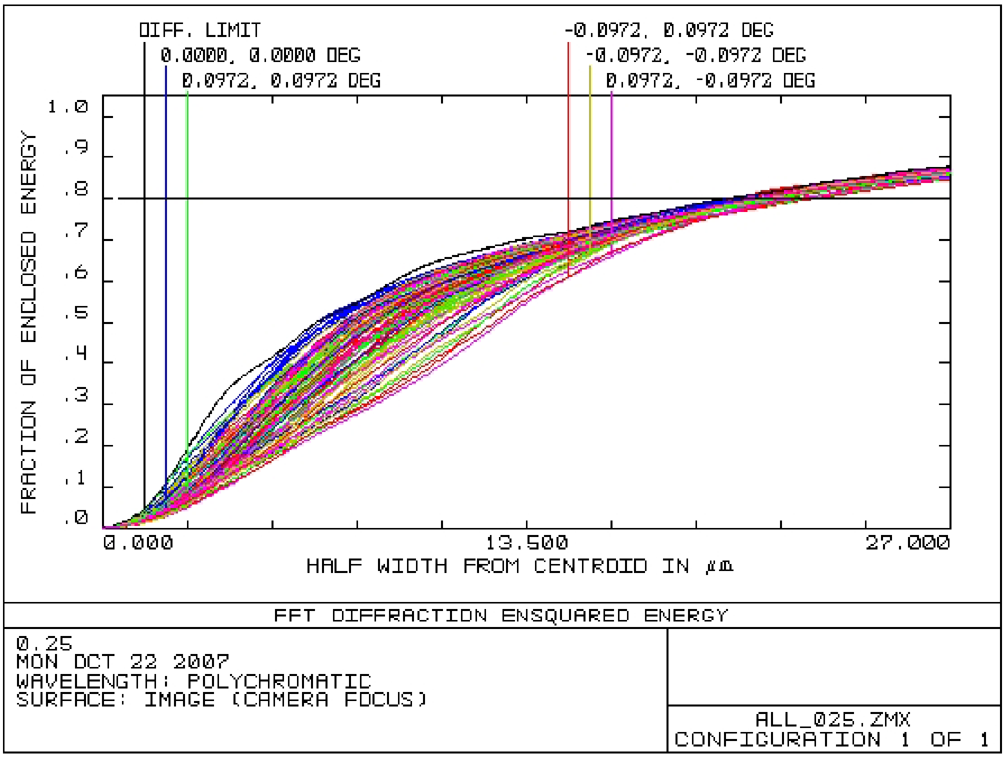

Figure 3.2.7-2 Montecarlo overlay of the EE80 for the tolerances in the 0.25"/px

It has been presented the tolerances for image quality up to date, which shows values that are not too tight if we use the compensator proposed. The results are detailed in the ORD5 and feed the opto-mechanical and alignment strategy of the instrument. In the following phase of PANIC a complete image quality error budget will be develop, to include thermal errors, glass parameters (index melt, glass homogeneity and surface irregularity) and image stability as well and its effect on tolerances.

3.2.8 AIV

A preliminary optical AIV plan has been made for PANIC. A separate technical note (ORD6) describes in detail this complete AIV plan for the instrument and only covers engineering tests regarding the optics. We hardly recommend to read it. The aim of that document is to determine the procedures and equipment required for integration of the instrument and verification tests. These tools will have to be available for the PANIC team, as the integration in subsystem and system level will be an in-house tasks.

It has been divided in three main categories related to the optical integration process from components manufacture and tests, barrel integration (subassemblies) and tests, and system integration and final engineering tests. To design this plan it has been necessary the identification of the adjustments and compensators which come from the tolerance analysis given in section 3.2.7. The different tasks and tests regarding each integration stage are described at each level (components, subsystem or system).

The optical elements of PANIC are grouped in five main units as shown in Figure 3.2.8-1:

- Barrel 1 (L0-M1-M2-M3),
- Barrel 2 (L1-L2-L3-L4-cold stop),
- Barrel 3A and 3B (L5A-L6A-L7A and L5B-L6B-L61B-L7B, respectively),
- and Barrel 4A and 4B (L8A and L8B, respectively).
- The fifth unit is the Optics Wheel (Barrel 3A-Barrel 4A and Barrel 3B-Barrel 4B, respectively) which place the optics according to the desired plate scale.

The optical AIV process will have two independent responsibilities. The optical elements manufacture will be accepted at the optical shop as individual elements and the integration of these lenses in the barrels and in the full instrument will be done by the PANIC team. The rationale behind the integration process is to test the functionality of the different pieces at each integrating step as these are being integrated. In that sense the system integration and verification should not display any fault at the subsystem or component level allowing a quick engineering and science verification. The barrels with decentering compensator will be assembled with an interferometric adjustment, and during the integration the compensator in distance will be adjusted. For Barrel 1, which does not have adjustments proposed, the alignment will be verify. All the sub-barrels will be cryogenically verified. Finally, the whole instrument will be assembled and tested, as we do not expect to need further adjustments than the mounting tolerances, the only adjustment to be done is the one for the detector, in position and tilt. A more detail explanation has been done in the technical note referenced about the AIV.

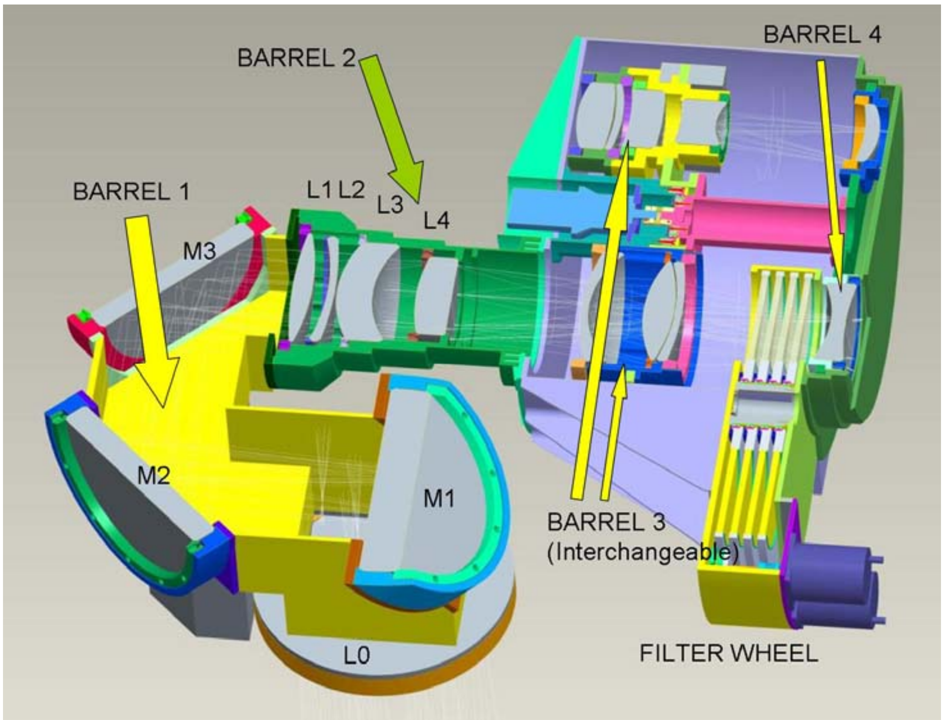

Figure 3.2.8-1 Opto-mechanical layout showing the main assemblies regarding the optical elements

3.2.9 Conclusions

The nominal optical design meets desired performance criteria, and contains margin to be applied to fabrication and alignment tolerances. To achieve this, an specific control plan during integration phases should be considered. In the following phase a deeper study of the tolerances and quality compensators, environmental change, and stray light will be done.

The design contains only spherical surfaces (i.e. no conic or aspheric surfaces) and special care has been taken in the selection of lens materials not using high index refraction materials in order to include all the photometric bands, even the z band, in the system, avoiding some critical materials. The correction of off-axis aberrations due to the wide-field available, the correction of chromatic aberration due to the wide spectral coverage, the introduction of narrow band filters (~1%) in the system minimizing the degradation in the filter pass-band have been achieved with this optical design. An important point is the production of the internal cold stop with good optical quality which reduces the background in K band considerably.

It has been presented the feasibility of the two pixel scales, 0.45"/px and 0.25"/px in the FOV required, being the two systems independent each other. Notice that the optical design of the 0.45"/px scale will not be affected if the other scale is suppressed.

3.3 Cryostat and Mechanisms

3.3.1 Cryostat

3.3.1.1 Requirements

3.3.1.1.1 Temperature

Due to background radiation the local temperature inside the shield should not exceed 100 K. This is also valid for local spots like cable feed-throughs or motors. Temperature changes should be in a range that the tolerances of the optics are met. The detector has a working temperature of about 77 to 80 K which has to be investigated. The required stability is ±0.1 K. Warm up and cool down of the detector has to be slower than 0.5 K/min.

3.3.1.1.2 Cooling system

The cooling system should be convenient to use on Calar Alto. This means that it should run at least one observing night without any maintenance, service or any other interrupt. Refilling should be necessary only once a day.

3.3.1.1.3 Flexure

The flexure of the cryostat due to the movement of the telescope has to meet the requirements defined by the optics.

3.3.1.2 Design Report

The cryostat is a nitrogen bath cryostat with a large vessel to cool the complete structure. To reduce LN_2 consumption and thermal gradients we use 30 layers of multilayer insulation (MLI) on the cold surface. This should reduce the heat load from radiation to about 5 W/m^2. For a constant detector temperature we use a second small LN_2 vessel exclusively to cool the detector. For weight reduction we will use dished ends on the vacuum can instead of flat thick walled plates.

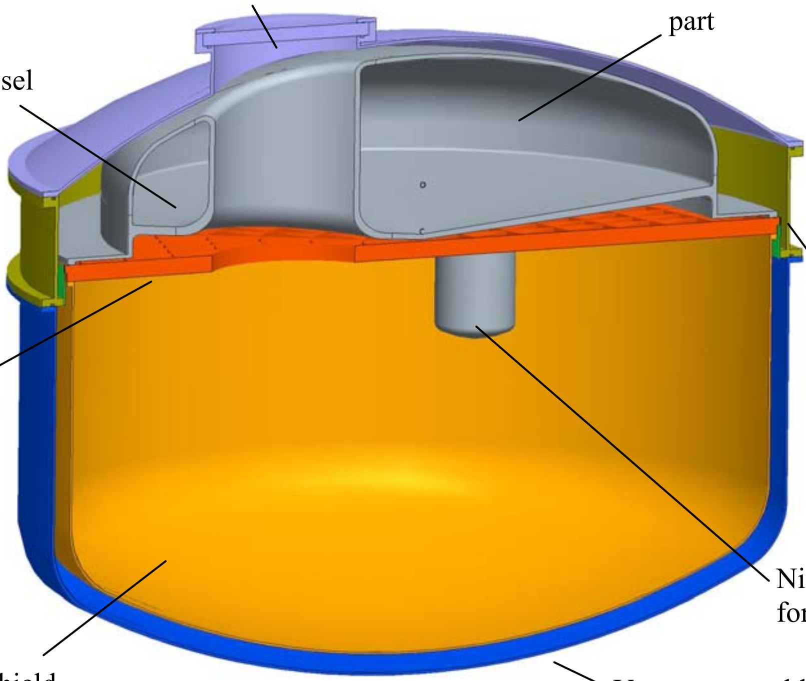

Figure 3.3.1-1: PANIC cryostat setup

3.3.1.2.1 Vacuum can

The vacuum can consists out of 3 parts. There is a central ring where we have the cold warm connections to the optical bench with spacers from glass-fiber reinforced plastics (GRP). Also mounted to this ring there are all connections like electrical feedthroughs, LN_2 feedthroughs, vacuum pumping flange, safety valve and vacuum gauge.

To the telescope side there will be a dished flange with the entrance window here called "Vacuum upper part".

At the opposite side there will be a dome flanged to the central ring called "lower part". The dome uses a dished boiler end.

All parts of the vacuum can are made from aluminium for weight reduction. All flanges and walls are weight optimized to meet the weight limitations of the telescope.

For the handling of the cryostat we have to add a mounting structure and feet to handle the instrument with a cart.

3.3.1.2.2 Nitrogen vessel for cold bench cooling

To cool the cold bench we use a Nitrogen vessel. The upper part of the vessel is a dished boiler end. The light path goes right through the vessel which makes a vertical tube welded into the vessel necessary. The vessel will have a geometrical volume of about 107 litres. Due to the movement of the telescope it is only possible to fill it half. The usable volume has to take into account that the vertical tube could be completely in the liquid. The resulting max filling will be about 46 l. We will have a filling and an exhaust gas tube. Besides there will be an additional third tube for the safety valve. The vessel will be filled from the side through the central ring. Filling will be done by pointing the telescope to zenith. The filling tube from the side goes to the bottom of the LN_2 vessel. The exhaust gas line ends in the centre of the vessel. It will be filled until LN2 is spilled out of the exhaust gas line. The third tube will end about in the centre of the LN_2 vessel. When the vessel is full, the filling line will be closed and the exhaust gas line opened. If it is necessary to drain the vessel the filling line is opened and the exhaust gas line is closed. The pressure of the evaporating gas will press the LN_2 out of the filling line when pointing to zenith.

The thermal contact area to the cold bench is ring shaped on the rim of the bottom flange. This is due to the deformation of the nitrogen vessel from pressure inside which should not have any influence on the optical bench.

The extremely weight reduced LN_2 vessel for the cold bench could not be calculated in a standard way. So we had to use FEM. Due to the risk of this calculations we are going to have a crosscheck of the results from an external company.

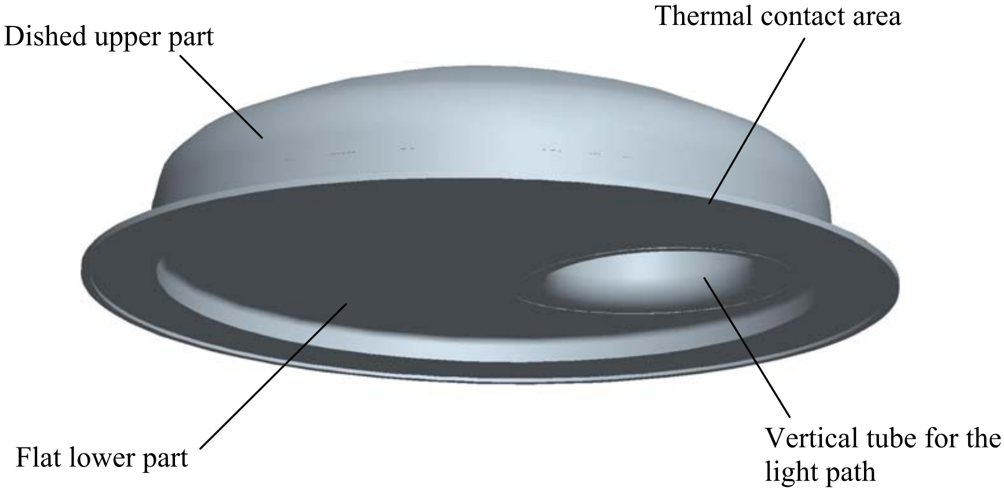

Figure 3.3.1-2: Nitrogen vessel for cold plate

3.3.1.2.3 Nitrogen vessel for detector cooling

The detector will be cooled by a separate nitrogen reservoir. This is necessary in order to have a constant temperature which in other case would change with the filling level and the orientation. Also this vessel will be filled from the side through the central ring. There are three tubes with functionality similar to the tubes of the large vessel.

3.3.1.2.4 Spacers

The spacers connect the cold and the warm parts of the cryostat. They have to be stiff to fulfill the requirements on flexure and they have to have a very low heat conductivity. Furthermore they have to compensate the thermal shrinking of the cold structure. We therefore use GRP (glass-fibre reinforced plastic). With a ring of 12 sheets which are flexible in radial direction and stiff in all other directions we solved this problem.

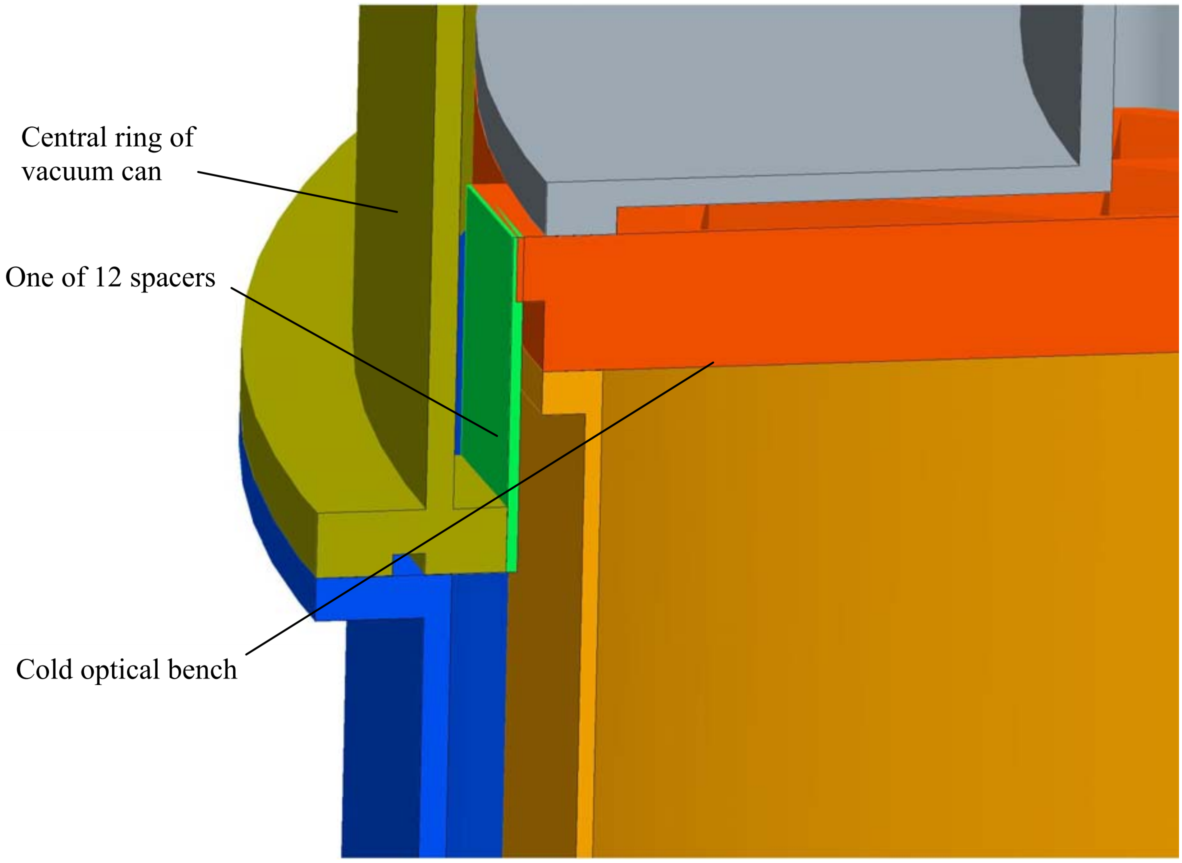

Figure 3.3.1-3: Cold-warm spacers from the central ring to the optical bench

3.3.1.2.5 Thermal connection of the detector

The detector package will be connected to a separate small nitrogen vessel. This will bring a temperature stability which is almost independent from the ambient conditions. The expected stability is better than ±0.2 K. The required stability of ±0.1 K makes a controller necessary. This controller will also be used to control the warm up and cool down of the detector.

The heat dissipation of the detector will be compensated by the Nitrogen inside the small vessel. The heat dissipation of the preamplifier has to be cooled by the large Nitrogen vessel.

3.3.1.2.6 Thermal investigations

3.3.1.2.6.1 Nitrogen vessel for cold bench

1	Radiation on surface, 4.3 m^2, with multilayer insulation (5 W/m^2)	21.5 W
2	Radiation through the window	22 W
3	Conductivity through spacers	5 W
4	Conductivity through filling tubes	0.1 W
5	Conductivity through cables	3 W
6	Power consumption detector preamplifier and electronics	5 W
	Complete heat input	57 W
	Evaporation rate	1.3 l/h
	Hold time with 45 l LN2	35.5 h

3.3.1.2.6.2 Nitrogen vessel for detector cooling

1	Radiation on surface, 0,09 m^2	0.03 W
2	Conductivity through spacers	0.05 W
3	Conductivity through filling tubes	0.05 W
4	Power consumption detector	0.05 W
	Complete heat input	0.18 W
	Evaporation rate	4*10-3 l/h
	Hold time with 1 l LN2	250 h

3.3.1.2.6.3 Thermal gradient

Because we want to save weight we use only one Nitrogen vessel to cool the cold bench. In other instruments we enclosed the inner vessel with a second outer actively cooled shield. The use of only one Nitrogen vessel results in a thermal gradient and temperature changes over the cold bench due to the filling level and the orientation of the cryostat. To keep the Nitrogen consumption small and to reduce the gradient we will use multilayer insulation (MLI). Nevertheless there is still a small resulting temperature change.

To get an idea of what we have to expect we made some finite element (FE) calculations. We calculated the temperature distribution with maximum filling when pointing to horizon and with an almost empty vessel in the same orientation. These are extreme positions which almost never will be used for observation.

With the full vessel we have a gradient of about 1.5 K, the almost empty vessel has a gradient of about 5.5 K. A temperature change of 1 K at 80 K results in a change in dimension of about 10 μm on 1 m. The temperature changes are very slow so that a large effect only happens if the instrument does not move.

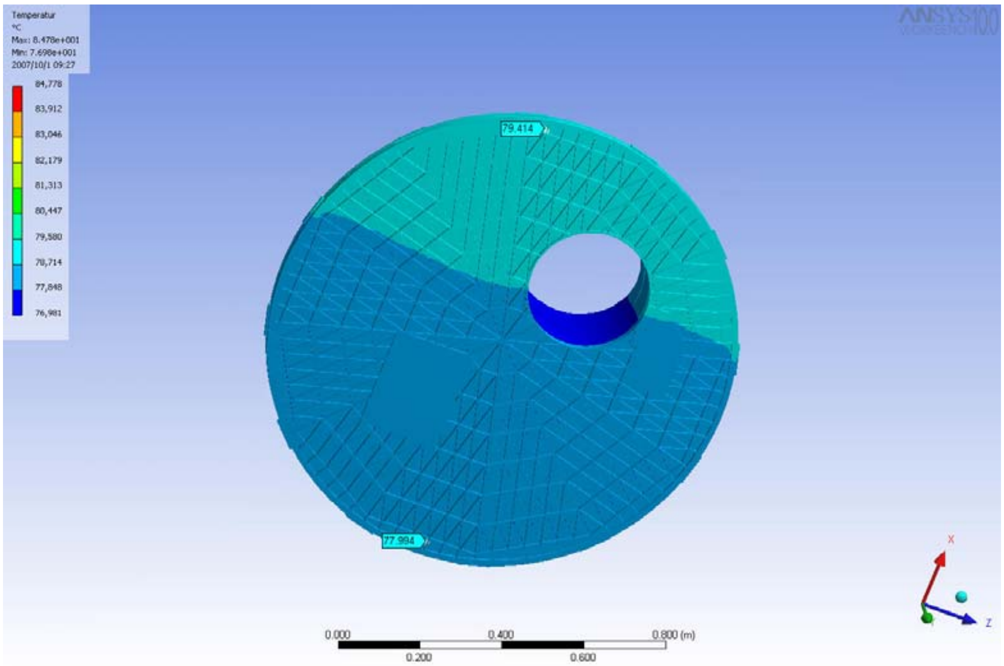

Figure 3.3.1-4: Temperature distribution with half filled vessel (maximum filling), pointing to horizon

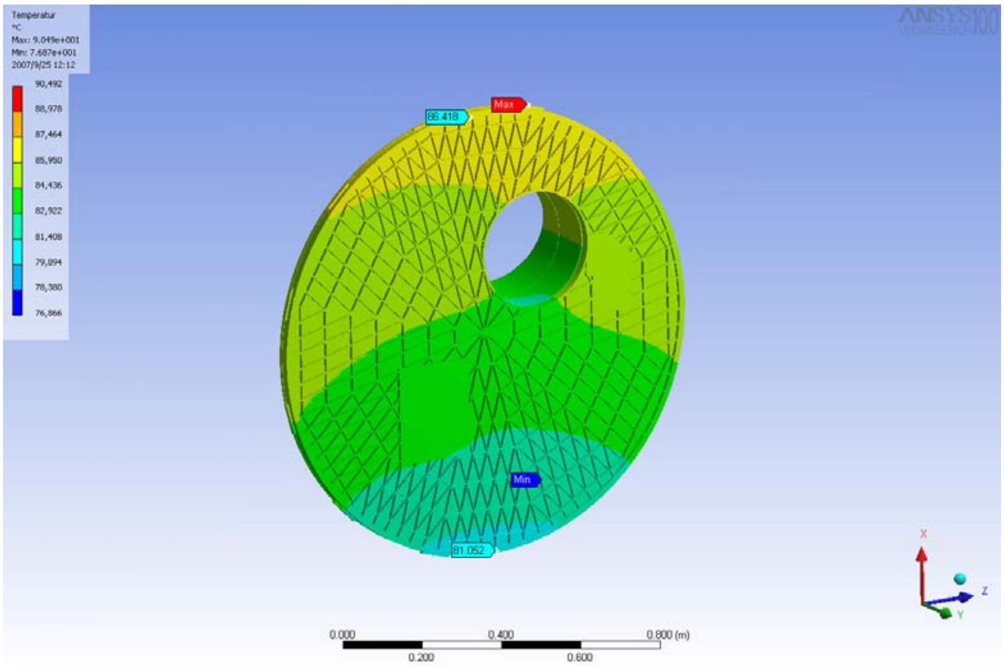

Figure 3.3.1-5: Temperature distribution with almost empty vessel, pointing to horizon

3.3.1.2.7 Telescope adapter

The cryostat is mounted to the telescope mirror cell by an adapter shown in Figure 3.3.1-6. It is made from steel and it has two flanges with diameters of 720 mm and 1240 mm, which are eccentric by 245 mm. The off-straight sheet metal cone in-between the flanges has a wall thickness of only 1 mm. The stiffness of the cone is increased by 24 gusset plates. The total mass of this structure is 33 kg.

The results of various FEM simulations including this telescope adapter are shown in section 3.3.2.2.7.

Figure 3.3.1-6: PANIC telescope adapter.

3.3.2 Mechanisms

3.3.2.1 Requirements

All mechanical and optical components inside the cryostat have to be designed for a temperature of 77 K. Their position and the position tolerances are defined in section 3.2.

For test purposes all mechanisms have to work at room temperature also. However there are no requirements for the position tolerances at this temperature.

The mechanics should be stiff enough to work for all telescope orientations with the required precision.

3.3.2.2 Design Report

The optical elements of PANIC are arranged in two groups. These groups are mounted directly to the cold bench. The first assembly (optics group 1) consists of the mirrors M1 to M3, the lenses L0 to L4 and the cold stop. The lenses L5 to L8 are different for each of the two pixel scales and therefore mounted onto an optics wheel. This wheel has two positions and is driven by a geared stepper motor. The filter unit has four filter wheels with 6 positions each. So in total 20 filters (or 19 filters and a dark) can be installed. The opto-mechanics is completely encapsulated to minimize stray light effects from the bench and the cold shields. Both optics assemblies do not touch each other. An optical labyrinth ensures light tightness between them. The arrangement scheme of all optical elements of PANIC is shown in Table 3.3-1 and Table 3.3-2. The detector array is mounted directly to the optics wheel unit.

Optical element	L0	M1	M2	M3	L1	L2	L3	L4	L5A	L6A	L7A	L8A
Groups					lens mount 2				lens mount 3			
	optics group 1								optics wheel			
	complete optics											

Table 3.3-1: Grouping of the optical elements of PANIC for the 0.45 arcsec/pixel scale.

Optical element	L0	M1	M2	M3	L1	L2	L3	L4	L5B	L6B	L61B	L7B	L8B
Groups									lens mount 3a		lens mount 3b		
					lens mount 2				lens mount 3				
	optics group 1								optics wheel				
	complete optics												

Table 3.3-2: Grouping of the optical elements of PANIC for the 0.25 arcsec/pixel scale.

Element	Mass
Lenses	14 kg
Mirrors	9 kg
Lens and mirror mounts incl. lenses and mirrors	51 kg
Filter wheel unit incl. filters	20 kg
Optics wheel unit incl. mount	38 kg
Field stop wheel	6 kg

Table 3.3-3: Mass estimation of the cryogenic opto-mechanics.

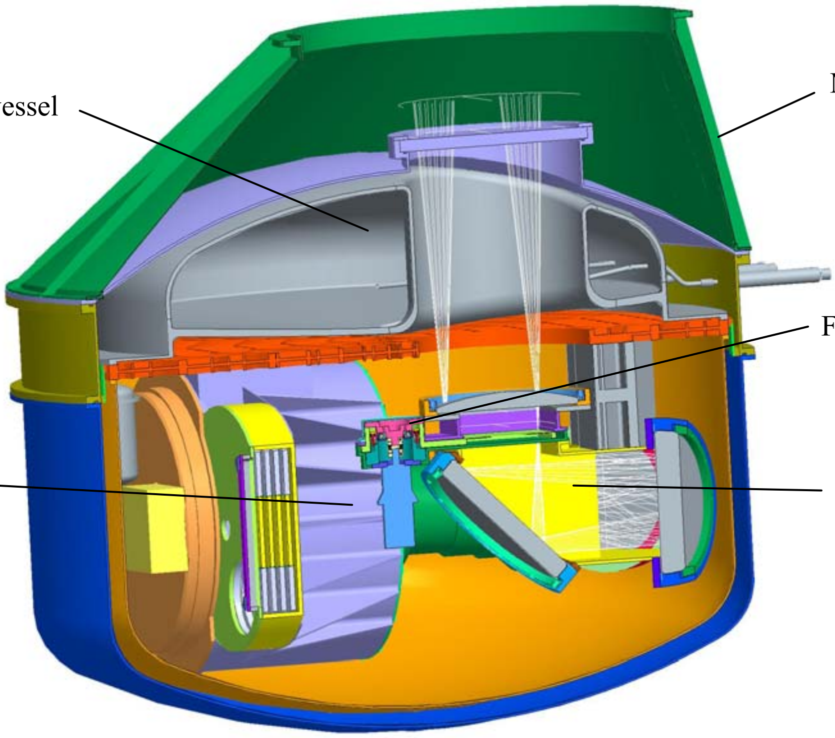

Figure 3.3.2-1: Section through PANIC (the vacuum window and the detector unit are not shown).

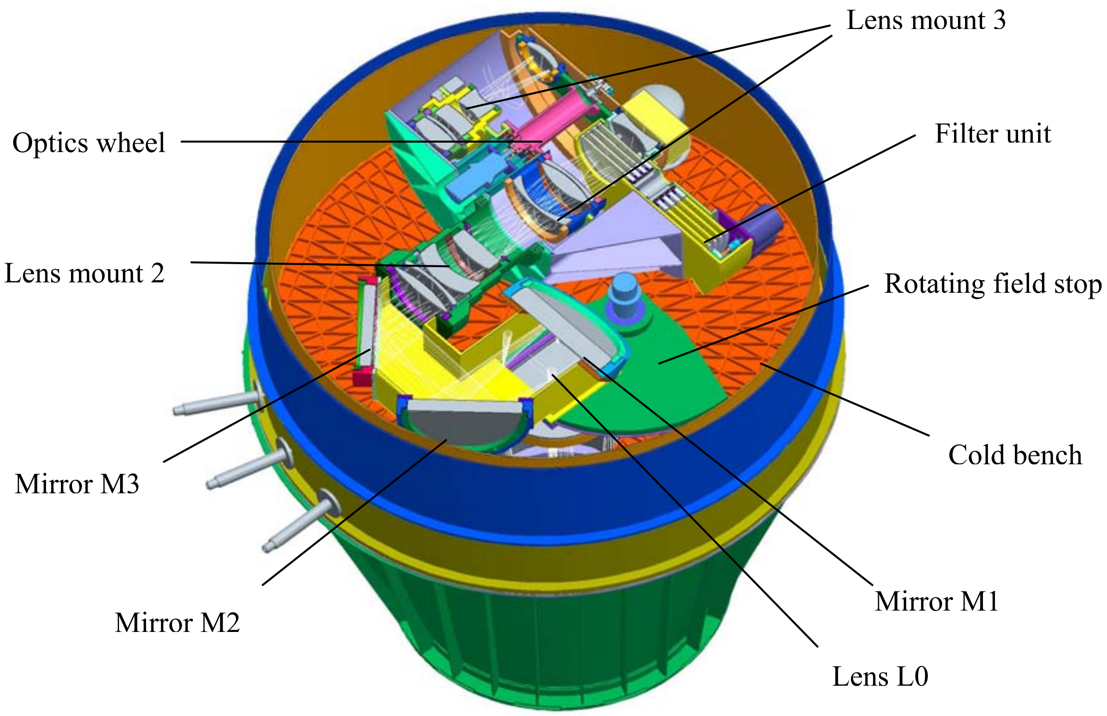

Figure 3.3.2-2: Cold bench and optics

3.3.2.2.1 Entrance window

The entrance from Infrasil has a diameter of 330 mm and a thickness of 20 mm. As shown in Figure 3.3.2-3, it is mounted to a cylindrical flange of the vacuum vessel by a retainer ring. It is sealed by an o-ring. The FEM results of the window deformation due to atmospheric pressure are shown in section 3.3.2.2.7.3.

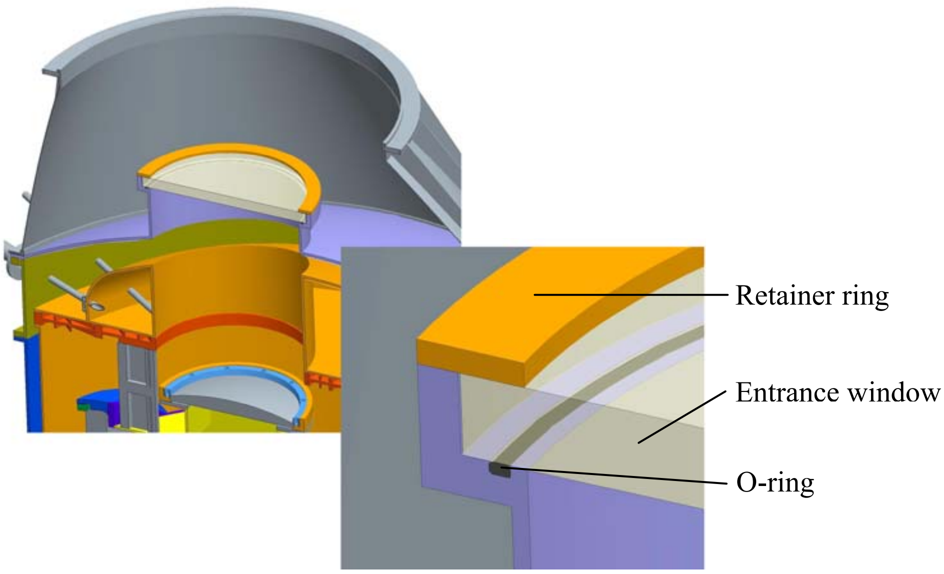

Figure 3.3.2-3: Entrance window

3.3.2.2.2 Mounting of cryogenic lenses and mirrors

The most difficult task of the lens mount design is to make sure that the lenses survive cooling and at the same time achieve the tight tolerances required by the optical design. If the lenses/mirrors were mounted in a conventional way, e.g. with a threaded retainer ring, the different thermal expansion properties of the materials used might lead to severe damage during cooling. Therefore, a mounting method is employed that uses chamfers at both the lenses/mirrors and the mount parts. In this case, a chamfer angle of 40° is chosen for both outer edges of each lens/mirror, the lens mount and the retainer ring. Figure 3.3.2-4 shows how this principle was used for the cold optics of OMEGA2000. The lenses sit in the conical surfaces of the mount. The retainer rings keep the lenses in this position by the forces of eight disk spring packages each. Temperature changes result in diameter changes of the parts. These changes lead to an axial displacement of the lenses and retainer rings because the parts can slide on the chamfer surfaces relatively to each other, assuming that the chamfers are manufactured very precisely and that friction can be neglected. This mounting method has been successfully used in both OMEGA2000 (for lenses with diameters between 106 mm and 155 mm) and in PYRAMIR (for lenses with diameters of about 20 mm).

Lens/mirror	Material	Thermal expansion between T=293K and 77 K [%]	Diameter [mm]	Mass [kg]
L0	fused silica (FS)	0.001	250	2.05
M1	FS	0.001	270	4.00
M2	FS	0.001	240	2.97
M3	FS	0.001	215	1.98
L1	CaF_2	-0.284	162	0.87
L2	E-SF03	?	156	0.68
L3	FS	0.001	145	1.50
L4	BaF_2	-0.306	114	1.80
L5A	FS	0.001	162	0.73
L6A	S-FPL51	?	148	1.17
L7A	E-SF03	?	147	0.60
L8A	S-FTM16	?	114	0.70
L5B	BaF_2	-0.306	98	1.21
L6B	FS	0.001	98	1.28
L61B	E-SF03	?	85	0.74
L7B	BaF2	-0.306	65	0.74
Filter	B270	?	125	0.22
L8B	FS	0.001	90	1.95
Mounts	AlMg4.5Mn	-0,378	-	-

Table 3.3-4: Material list of cryogenic optical elements and their mounts

The cold optics parts are made of at least nine different materials, each material having different thermal expansion properties: eight optical materials for the lenses and mirrors and aluminium AlMg4.5Mn for the mount parts. Table 3.3-4 shows that the fused silica (FS) lens actually becomes slightly larger when cooled down to 80 K, whereas the BaF_2 lens shrinks by about 0.3 %. This behaviour is nonlinear for all the materials used, which means that e.g. the fused silica lens shrinks and expands again while temperature changes from 300 K to 80 K.

Of course, cooling of the mount parts and the lenses does not start simultaneously, because the lenses are cooled by the mount, and the retainer rings are cooled by the corresponding lenses and by the screws in the spring packages. To understand the movements of the lens mount parts while being cooled from 300 K to 77 K, Figure 3.3.2-5 shows a sequence of snapshots of thermal conditions. In Figure 3.3.2-5a the lens mount, the lens and the retainer ring are at room temperature (300 K). When the cryostat is filled and the cold plate and the filter unit are cooling, the mount starts cooling only after a certain delay. This means that the lens mount shrinks, as shown in Figure 3.3.2-5b. The lens and the retainer ring are shifted upwards because the lens can slide on the 40° chamfer relatively to the mount. In the next phase (see Figure 3.3.2-5c), the lens changes its diameter and thickness since its cooling via the chamfer contact surface to the mount. Therefore, lens and retainer ring move downwards. Finally, in Figure 3.3.2-5d, the retainer ring cools down and shrinks, causing an upward movement relative to the lens.

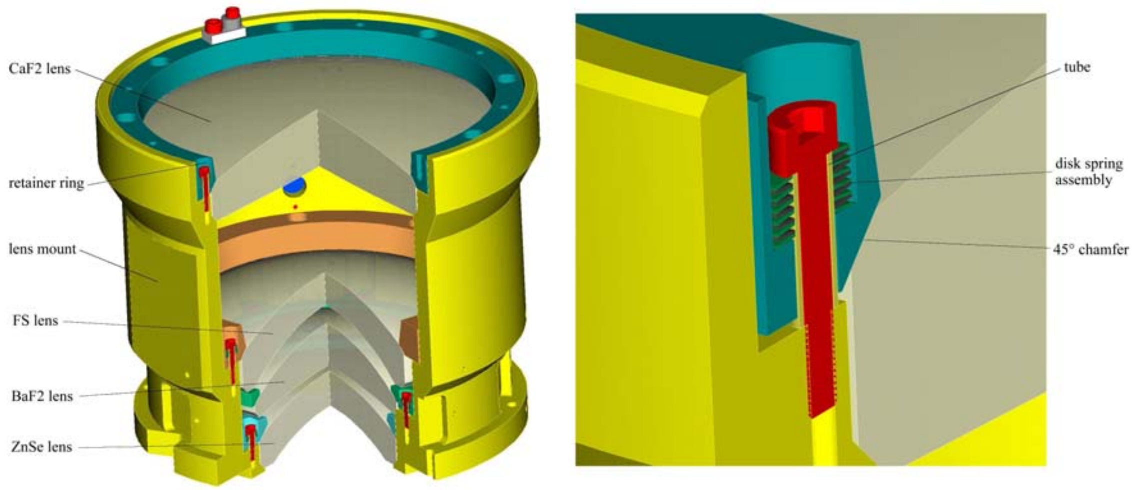

Figure 3.3.2-4: **Cold optics of OMEGA2000 with spring loaded cryogenic lens mount**

This cooling model is of course very schematic. The real process is much more complicated because the parts change their dimensions simultaneously after a certain time. The delay depends very much on material properties like thermal conductivity (which is a function of the temperature itself) and thermal expansion as well as on the size and quality of contact surfaces. A rough surface will slide less easily and give poorer thermal contact to another part than a smooth one. For this reason, the chamfers are diamond turned. Note that low thermal conductivity will lead to an inhomogeneous temperature distribution inside one part.

Measurements during the development of OMEGA2000 have shown that in the case of the CaF_2 lens the maximum temperature difference between the lens and the mount during the whole cooling period is about 40 K. In the case of fused silica this difference is about 60 K. The maximum temperature gradient in the lens from its centre to its edge is 5 K and 12 K respectively. This does not cause much thermal stress. The larger temperature difference in the case of a fused silica test plate is mainly due to the fact that the surface quality and angle of its chamfer, being hand-polished, are less accurate than the surface and angles of the diamond-turned CaF_2 test plate.

Although the chamfers of all parts were machined with the highest possible accuracy (both shape and surface quality), it is not possible to simply put the parts together to meet the optical specification for lens alignment. Radial holes in the lens mount allow the measurement and adjustment by fine-pitch threaded screws of each lens. In principle, the lens adjustment can also be done by cooling down and warming up again. However, this self-centering only works for radial misalignments of more than about 0.1 mm. For values smaller than that, the centering forces seem to be too low to overcome friction. In the case of OMEGA2000, the manufacturing tolerances for the chamfer angle were ± 3 arcmin for the mount parts and ± 2 arcmin for the lenses. The tolerances of the chamfer position were ± 0.01 mm.

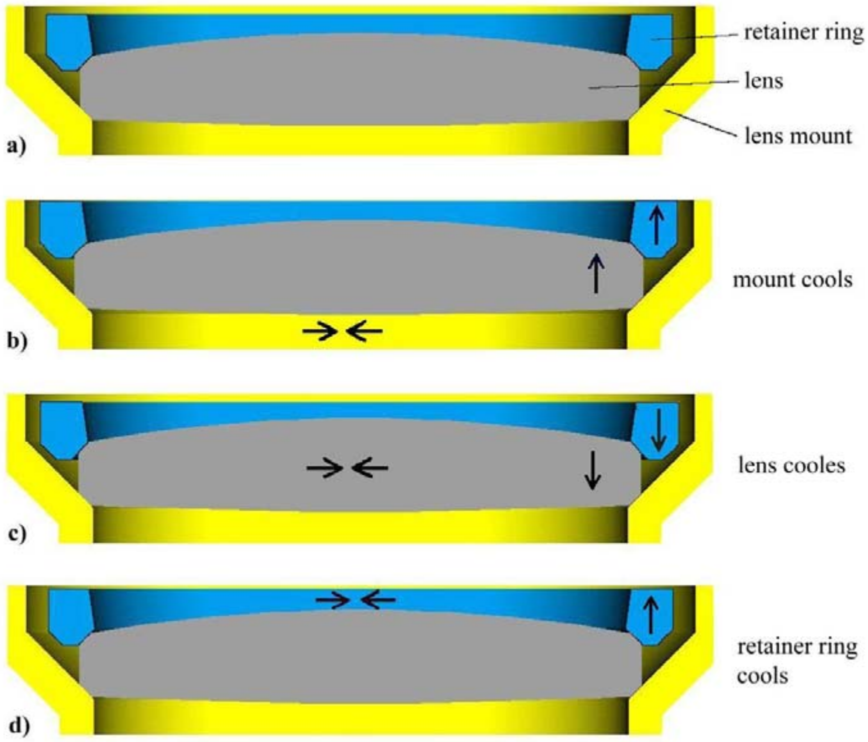

Figure 3.3.2-5: Displacements of lens and retainer ring due to thermal shrinkage during cooling from room temperature to 77 K. The arrows in axial direction show movements relative to the lens mount supporting surface. a) All parts at room temperature, b) Lens mount cooling, lens and ring still much warmer, c) Cold lens mount, lens cooling, retainer ring still much warmer, d) Cold lens and lens mount, retainer ring cooling

The radial force component F_R of the spring force F_F which centres the lens can be calculated as

$$F_R = F_F \cdot \sin\alpha \cdot \cos\alpha$$

with α being the chamfer angle relative to the optical axis, assuming that friction can be neglected.

Tests with the focal reducer of OMEGA2000 have shown that once the lenses were aligned as accurately as possible, e.g. to ± 0.01 mm, changes in the lens position introduced by multiple cooling cycles and changes in cryostat orientation could not be measured. The accuracy of the measuring device was ± 0.005 mm.

3.3.2.2.3 Optics wheel unit

Since PANIC offers two different pixel scales, the optics wheel carries two sets of lenses (one set of four and one set of five lenses). These are the lenses L5A to L8A and L5B to L8B (see Figure 3.3.2-6).

The optics wheel is driven by a cryogenic stepper motor Phytron VSS 52 and a modified Harmonic Drive gear PMG-14A with a ratio of 100:1. The distance between the optical axis and the rotation axis is 140 mm. The motor needs 200 steps to do a full turn. This means, that one motor step rotates the optics wheel by 1.08 arcmin which corresponds to a lateral lens shift of 44 µm, which is the positioning accuracy.

At the beginning the wheel has to be initialized by a mechanical reference switch from Saia. After that, both positions of the optics wheel are reached by turning the motor by a certain number of full steps. A feedback of the actual position is given by a resolver RE-15 from LTN Servotechnik.

The wheel has a preloaded double row ball bearing WAD933ZZ from ADR (outer diameter ~ 66.7 mm). The bearing is very stiff and since the wheel is very well balanced, there will be very little moment around both axes, which are perpendicular to the rotation axis. All metal parts of this unit are made of AlMg4.5Mn except the ball bearing, the bearing support rings, the motor and the screws. For a true run tolerance of the wheel a very tight fit between the ball bearing and its surrounding parts has to be achieved. This is hard to achieve with the surrounding parts made from an aluminium alloy and the bearing made from steel. A slightly too tight fit e.g. between the bearing outer ring and the wheel mount (see Figure 3.3.2-7) will lead to a damage of the bearing because the steel has a shrinkage from ambient to liquid nitrogen temperature of about 0.3 % whereas AlMg4.5Mn shrinks by 0.39%. This problem is solved by two stainless steel bearing support rings, both inside and outside the ball bearing (see Figure 3.3.2-8). These rings are solid enough to keep the stress away from the bearing, which the shrinking wheel mount tries to introduce. So a high true run accuracy of the wheel can be realized by tight bearing fits over the whole temperature range.

In most cryogenic wheels the ball bearings are the thermal bottle neck for the cooling-down or warming-up process. This is because the bearings are made from stainless steel, which has a rather poor heat conductivity and because there are only point contacts between the bearing rings and the balls.

From experiments which were made during the development of the cryogenic wheels of LINC-NIRVANA we can estimate that the whole unit will be cooled down from ambient temperature to 77 K after about 30-35 hours.

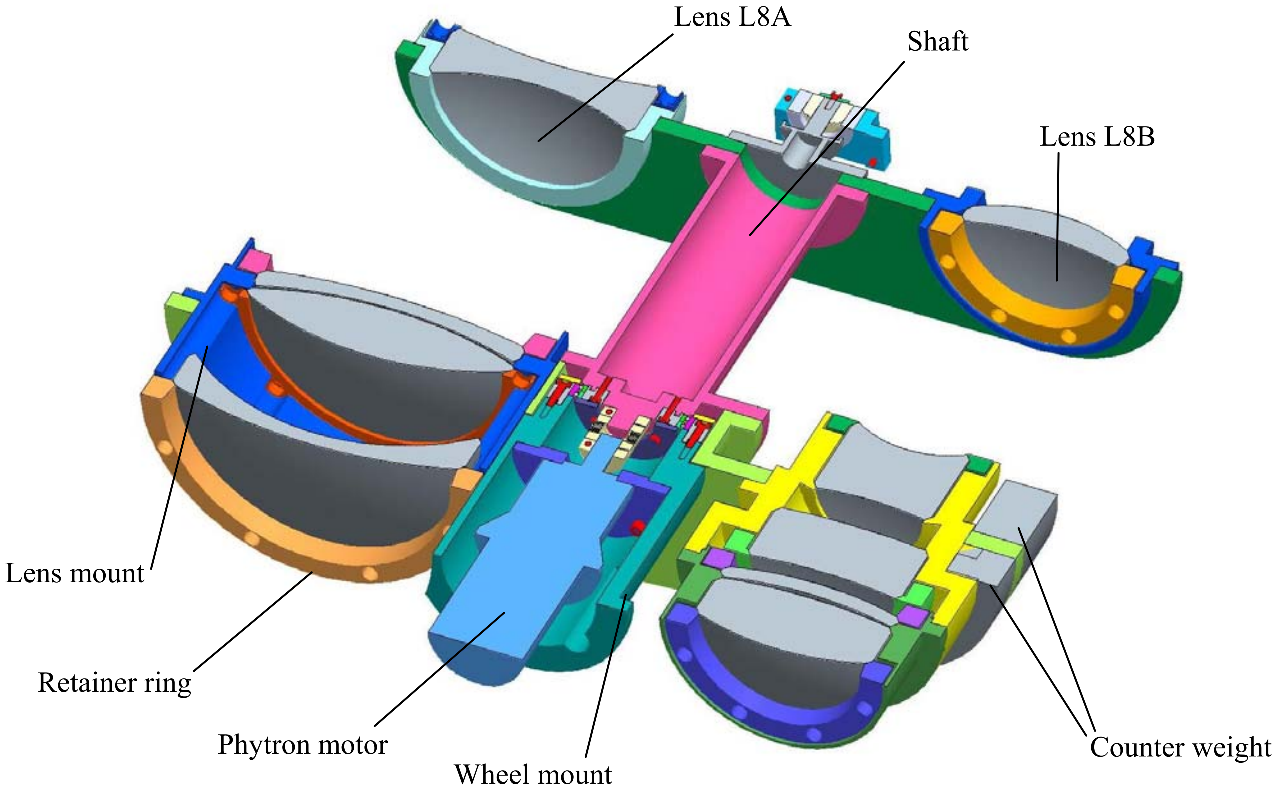

Figure 3.3.2-6: Optics wheel without housing

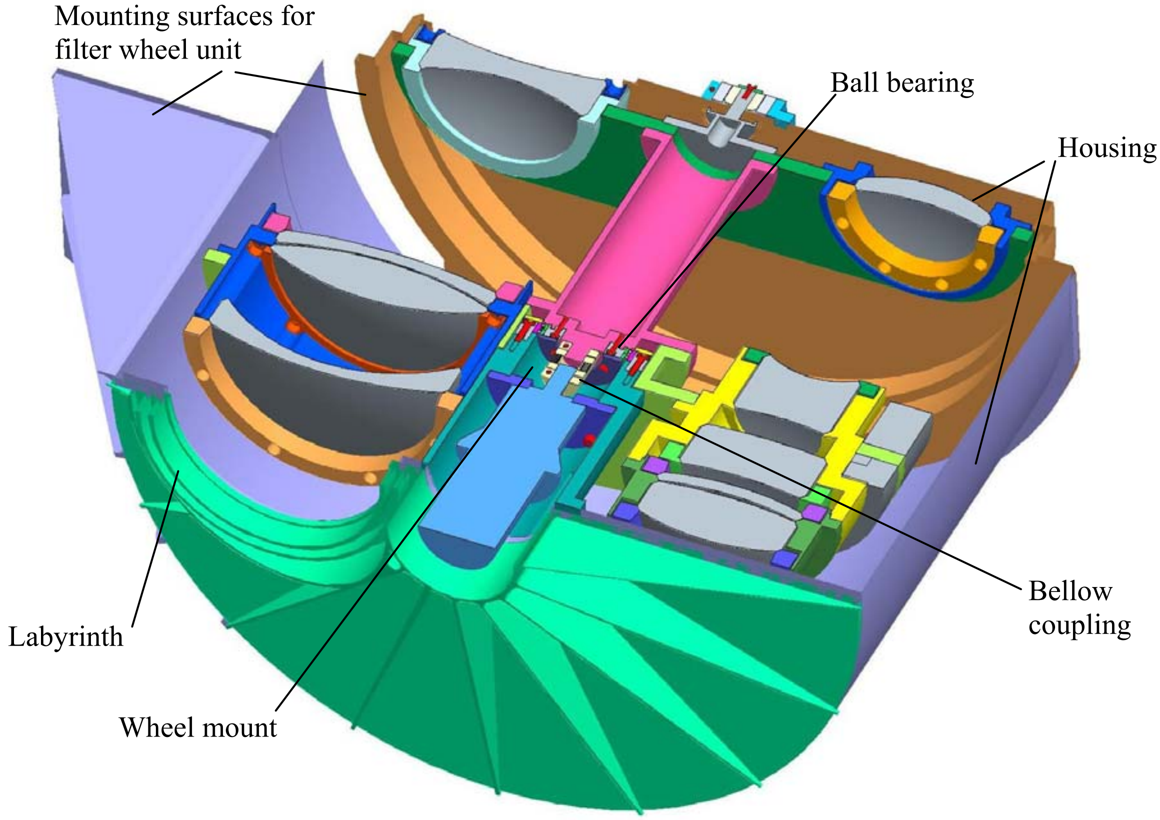

Figure 3.3.2-7: Section view of optics wheel unit

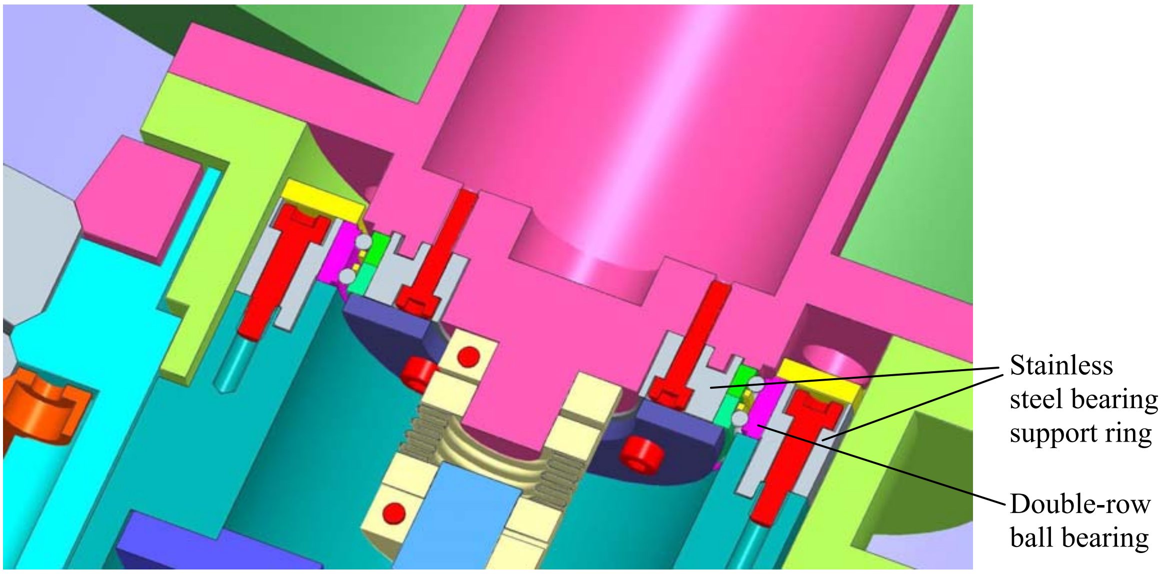

Figure 3.3.2-8: Optics wheel ball bearing (detail view of Figure 3.3.2-7)

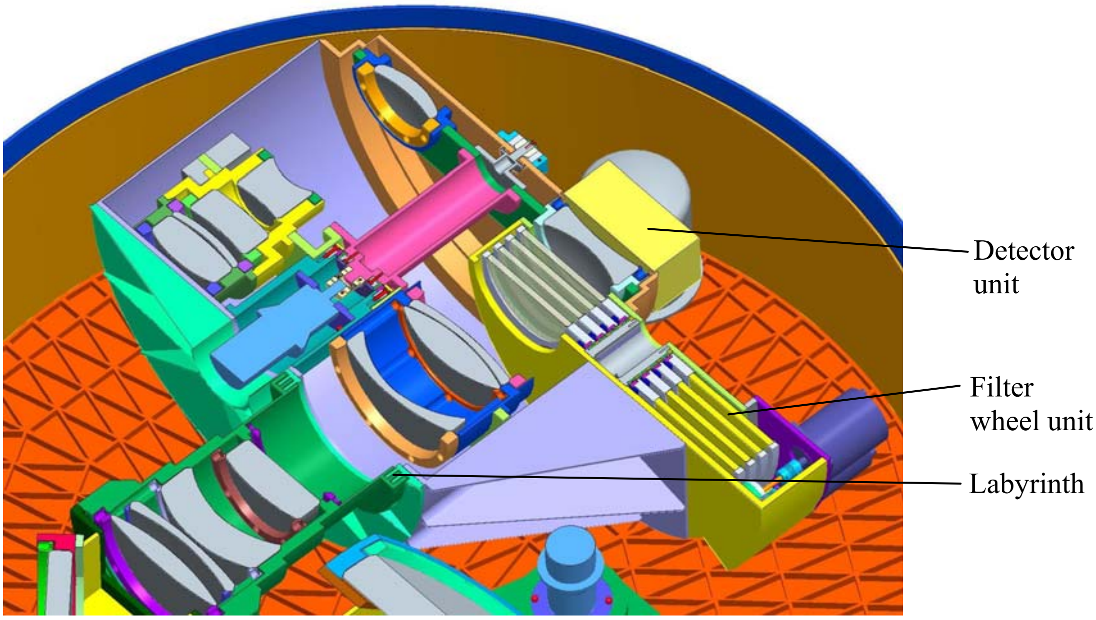

Figure 3.3.2-9: Detail view of optics wheel and filter unit

3.3.2.2.4 Filter wheel unit

Each of the four filter wheels has an external toothing and is driven by a Phytron VSS 65 stepper motor and a backlash-free gear. The transmission ratio is 12.8:1. Therefore, the positioning accuracy of the wheel is 360°/(200 steps/turn*12.8) = 8 arcmin, which corresponds to 0.32 mm in the centre of a filter.

The filter wheels have preloaded double row ball bearings WAD937ZZ from ADR (outer diameter ~73 mm), which are very similar to the bearings of the optics wheel (see section 3.3.2.2.3).

The wheels are very well balanced by counter weights, so there will be very little moment around both axes, which are perpendicular to the rotation axis.

Figure 3.3.2-11 shows that there are six positions in each filter wheel, five of them can hold filters and one remains empty. This hole is bigger than the others to access the filters in the wheels below through an opening in the housing. This opening is normally covered and light tight.

A set of three spring clips hold the filters in their position. To avoid scratching of the filters, there are thin protection rings between the filters and the spring clips.

For feeding back the wheel position resolvers (RE-15 from LTN Servotechnik) are mounted on the back side of the motors (not shown in Figure 16).

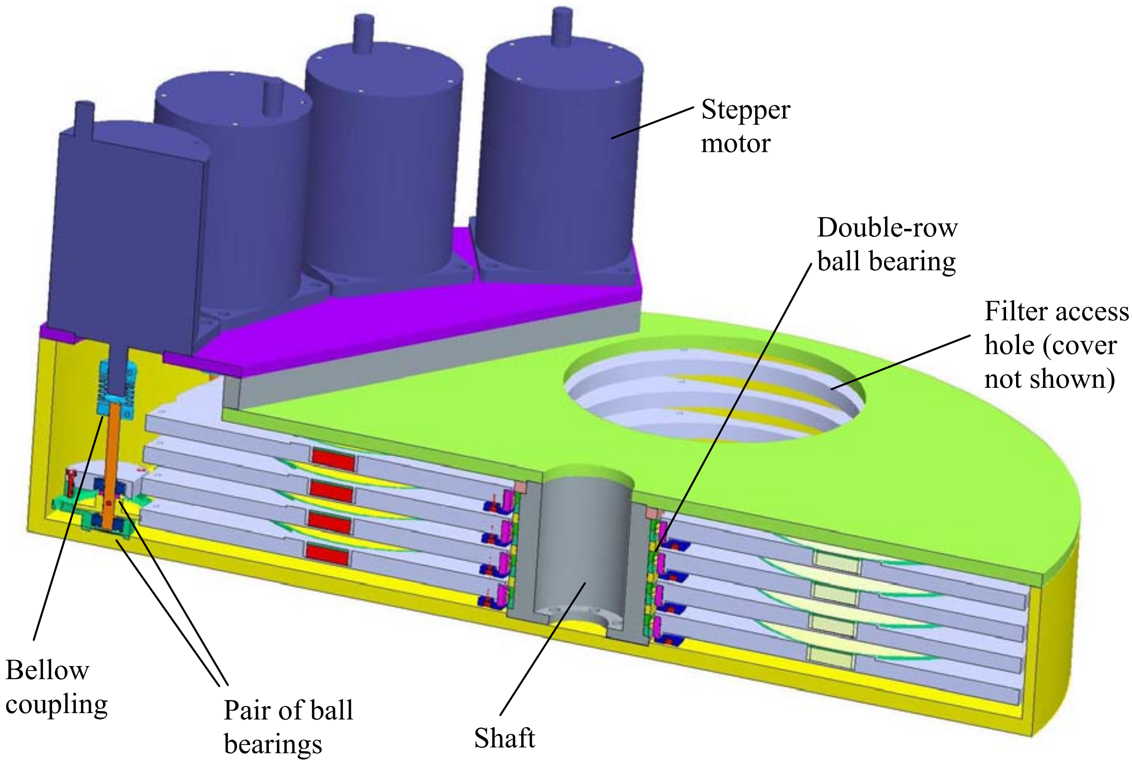

Figure 3.3.2-10: Filter wheel unit with four filter wheels.

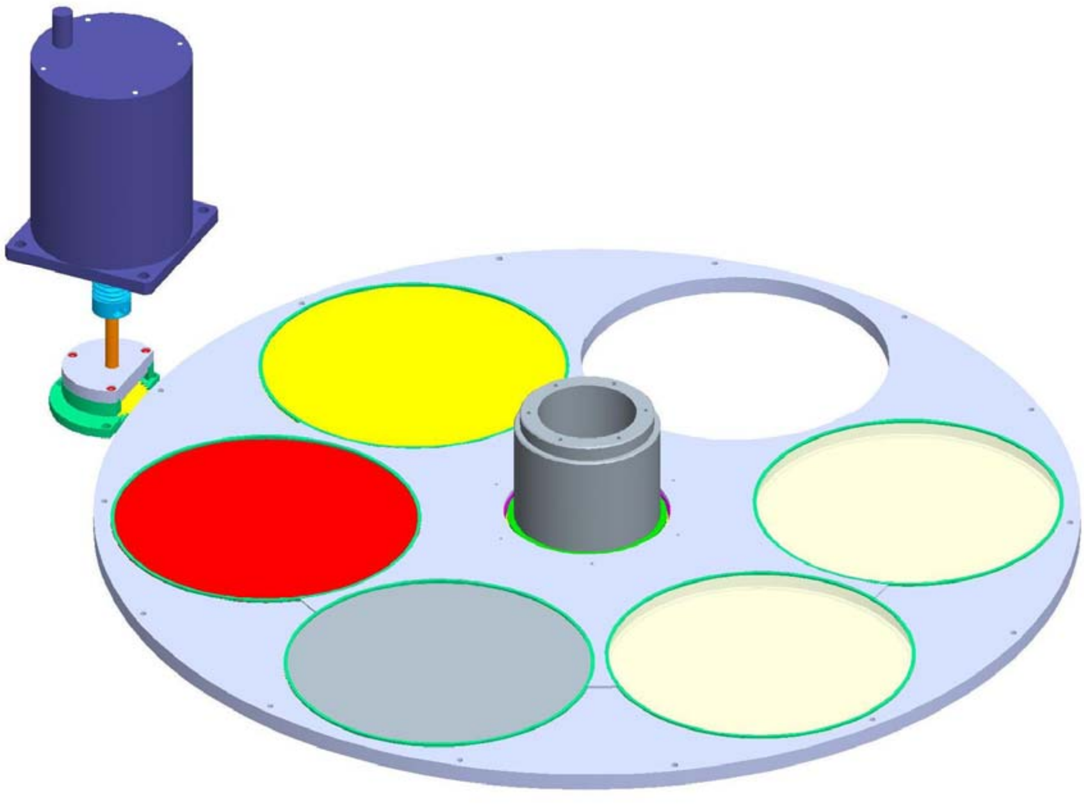

Figure 3.3.2-11: Filter wheel with drive unit.

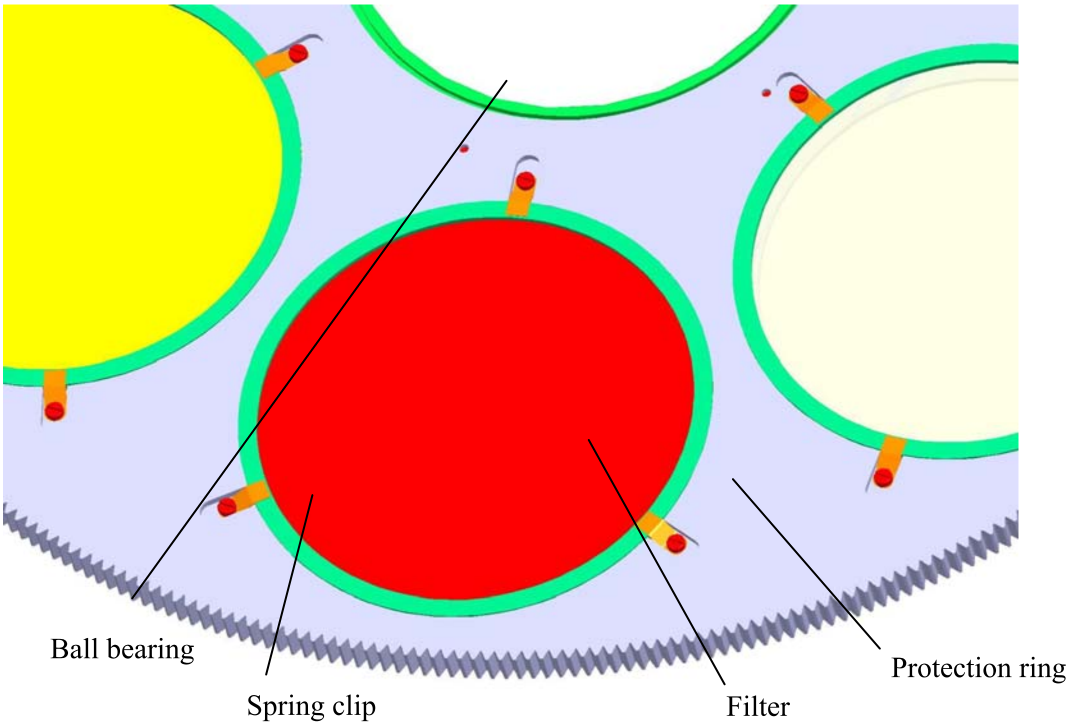

Figure 3.3.2-12: Detail view of filter wheel.

3.3.2.2.5 Rotating field stop

The field stop is located between L0 and M1. The field stop mask for the 0.45 arcsec/pixel scale has a free opening of 156 x 156 mm. It is machined into the housing of the field stop wheel. When PANIC is used with the 0.25 arcsec/pixel scale, a field stop mask of 63 x 63 mm is turned into the optical beam. It rotates by 75° and it has two positions, which are defined by mechanical limit switches from Saia. For simplicity the same motor, Harmonic Drive gear and ball bearing is used as for the optics wheel. So identical spare parts can be used for both units. The distance between both field stops axial direction is 2 mm.

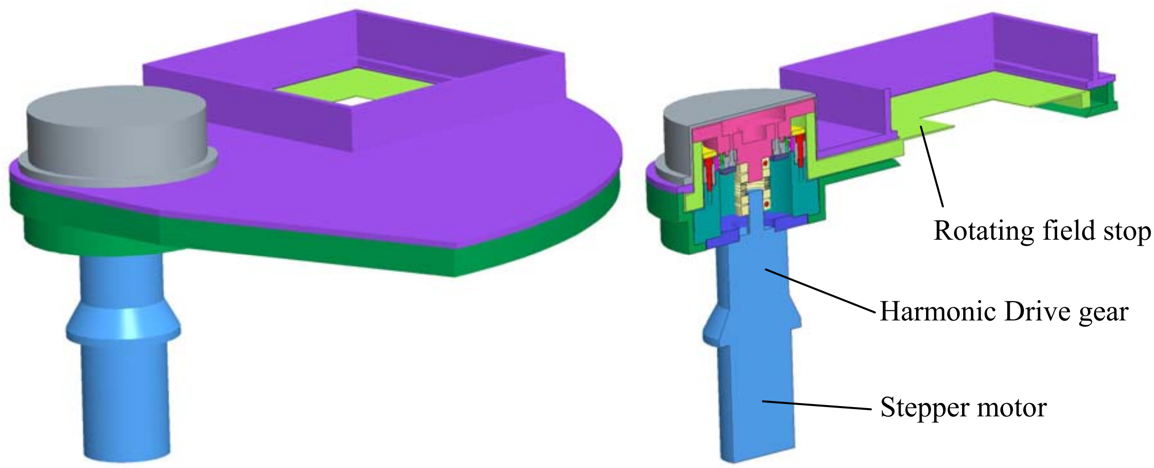

Figure 3.3.2-13: Rotating field stop, total view and section.

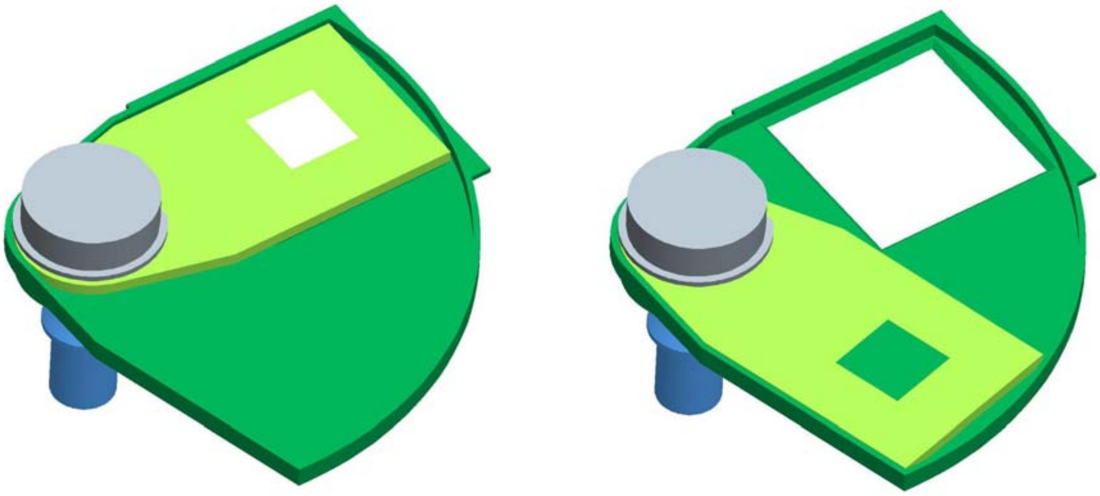

Figure 3.3.2-14: Rotating field stop in two positions with the housing upper part hidden (left: field stop for 0.25 arcsec/pixel in use, right: field stop for 0.45 arcsec/pixel in use)

3.3.2.2.6 Detector mount

The detector unit is mounted directly to the housing of the optics wheel unit. Tip, Tilt and focus position is adjusted once by shimming or machining without additional actuators. However, details about the detector assembly are not yet available.

3.3.2.2.7 FEM simulation results

3.3.2.2.7.1 Simulation of cryostat with optics replaced by point masses

For the first FEM simulation the whole opto-mechanics was replaced by two point masses, representing one optics assembly each (Figure 3.3.2-15). The point masses are located in the corresponding centre of gravity. In the following the deformation of the instrument by gravitational forces is shown for both horizontal and vertical telescope pointing (horizon and zenith).

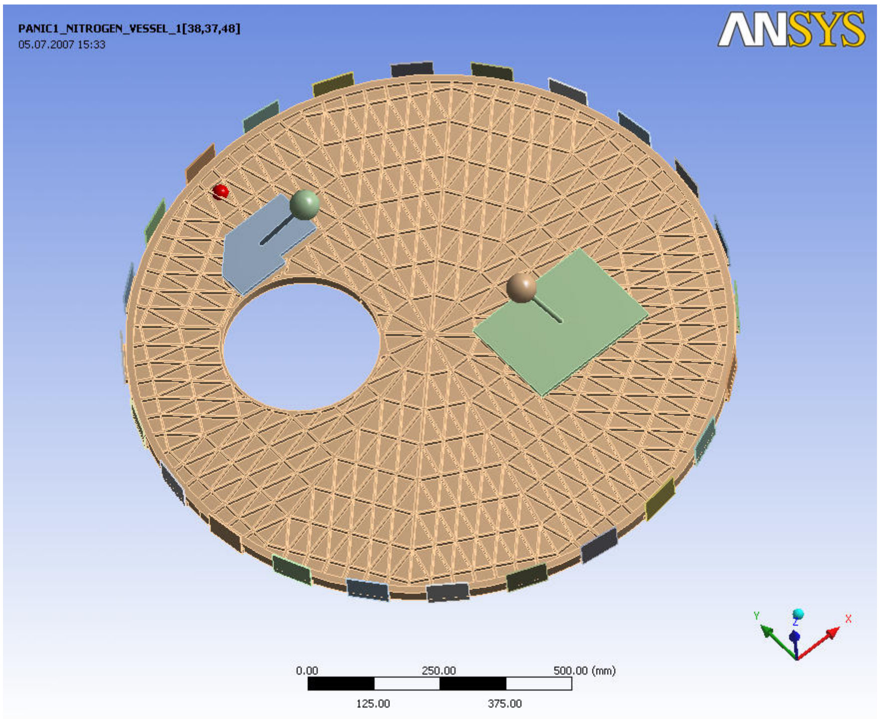

Figure 3.3.2-15: Both optics assemblies have been replaced by point masses (the rest of the cryostat is not shown).

3.3.2.2.7.1.1 Telescope pointing to zenith

The maximum deformation of the optical bench due to bending is 0.094 mm. The effect on the optical components has to be further investigated. Figure 3.3.2-16 and Figure 3.3.2-17 show both the same results, although in Figure 3.3.2-16 the cryostat is not shown.

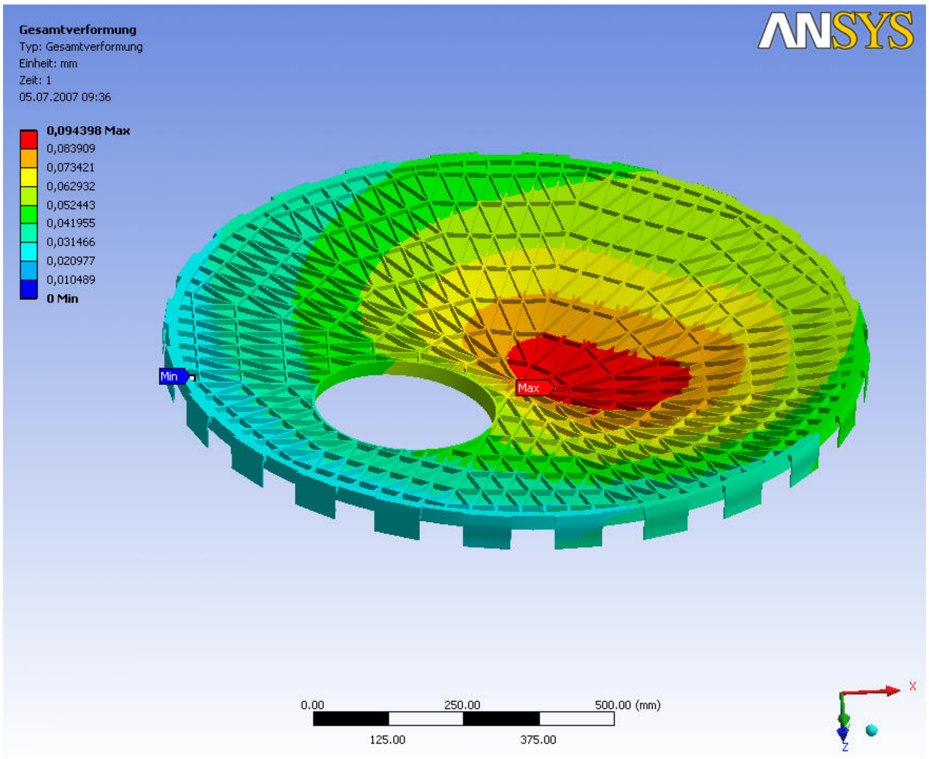

Figure 3.3.2-16: Displacement of cold bench with the telescope pointing to zenith (gravity vector in z-direction)

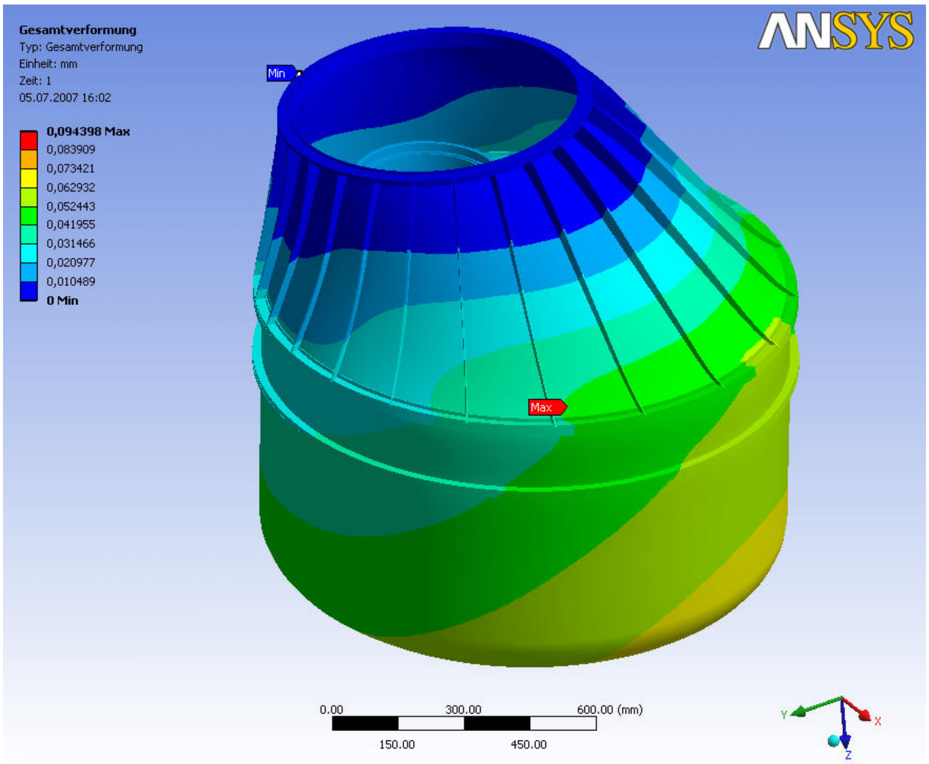

Figure 3.3.2-17: Cryostat displacement with the telescope pointing to zenith (gravity vector in z-direction)

3.3.2.2.7.1.2 Telescope pointing to horizon

The maximum absolute displacement of the bench (with respect to the telescope) with the telescope pointing to horizon is 0.120 mm. This can be split into a radial displacement of about 0.070 mm and a tilt of about 4.8 arcsec.

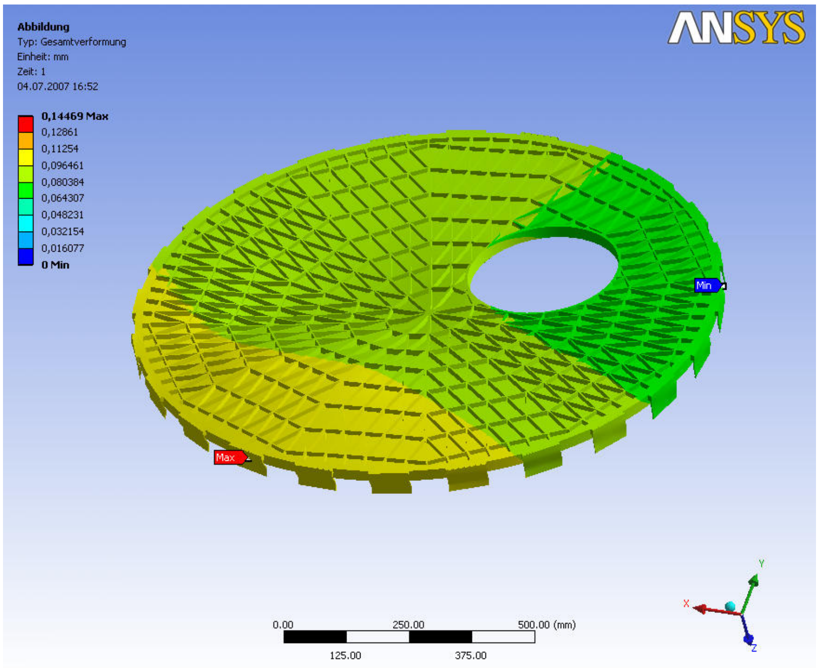

Figure 3.3.2-18: Displacement of cold bench with the telescope pointing to horizon (gravity vector in -y-direction)

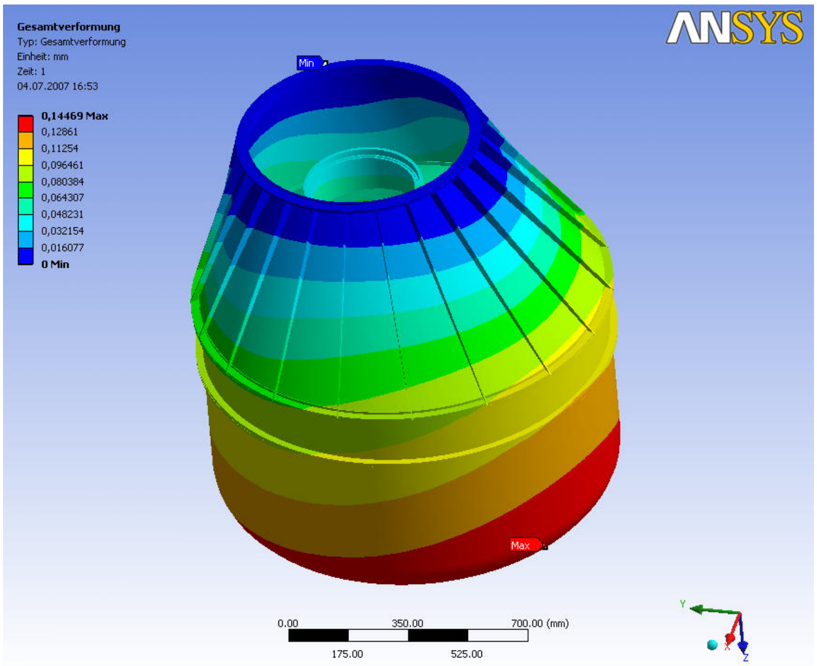

Figure 3.3.2-19: Cryostat displacement with the telescope pointing to horizon (gravity vector in -y-direction)

3.3.2.2.7.2 FEM simulation of a detailed model

In this simulation the point masses of chapter 3.3.2.2.7.1 were replaced by detailed models which use the optics mounts, lenses mirrors and wheels. By this, the displacement and tilt of each individual optical element and optical group due to gravity can be investigated.

Table 3.3-5 summarizes the simulation results. All values are absolute values with respect to the telescope flange. The tilt and shift values for individual lenses and mirrors as well as the lens mounts (as described in Table 3.3-1) in respect to their corresponding units are very small and can be neglected.

Pos.	Gravity vector	Remark	Optical bench tilt	Optical bench shift (direction)	Optics group 1	Optics wheel
1	-y	Telescope pointing to horizon	5.3 arcsec	77 µm (-y)	25 arcsec	22 arcsec
2	-x	Telescope pointing to horizon	4.9 arcsec	80 µm (-x)	22 arcsec	25 arcsec
3	+z	Telescope pointing to zenith	3.9 arcsec	30 µm (*)	5 arcsec	5 arcsec

Table 3.3-5: Tilts and displacements of optical bench and optical groups.

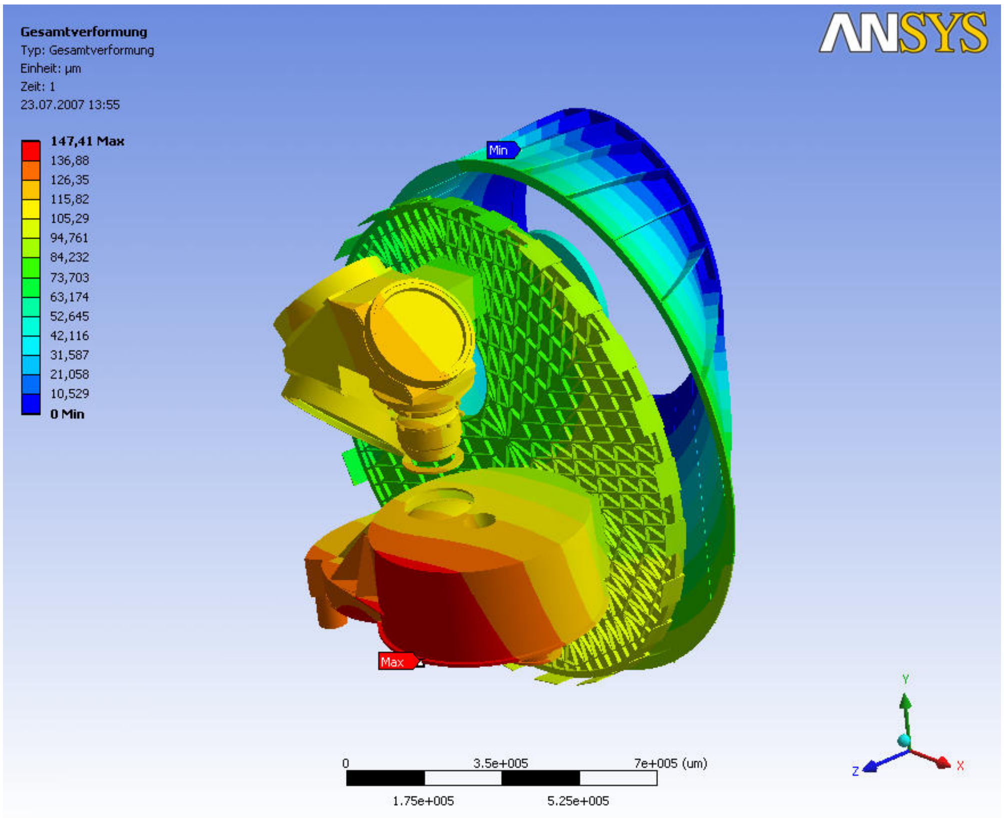

Figure 3.3.2-20: Displacement of cold bench and optics with the telescope pointing to horizon (gravity vector in -y-direction)

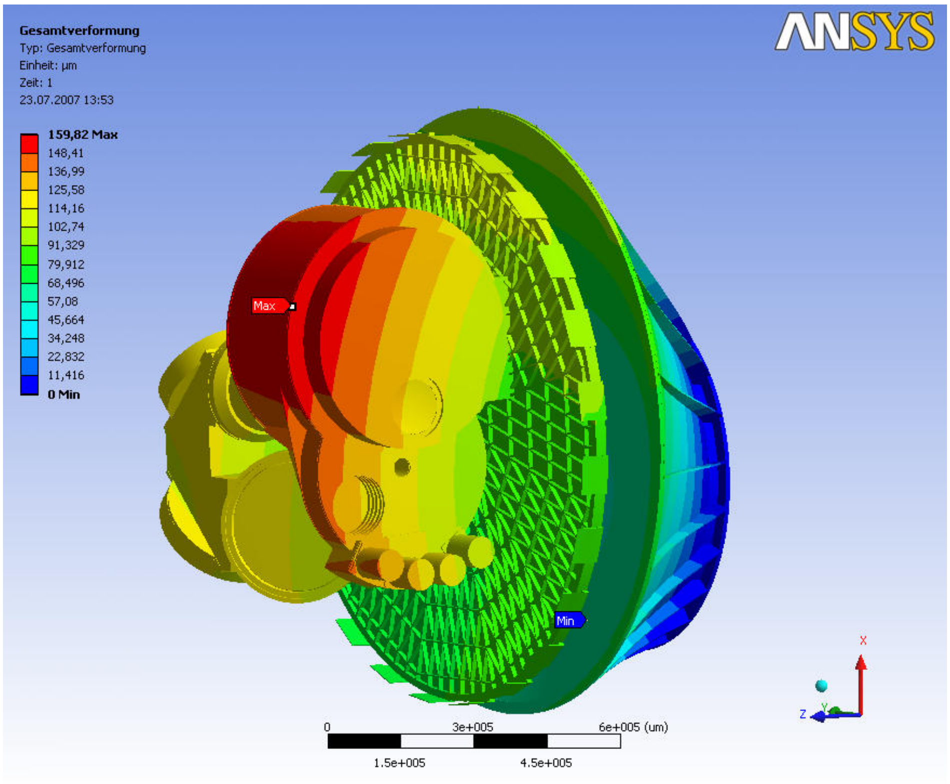

Figure 3.3.2-21: Displacement of cold bench and optics with the telescope pointing to horizon (gravity vector in -x-direction)

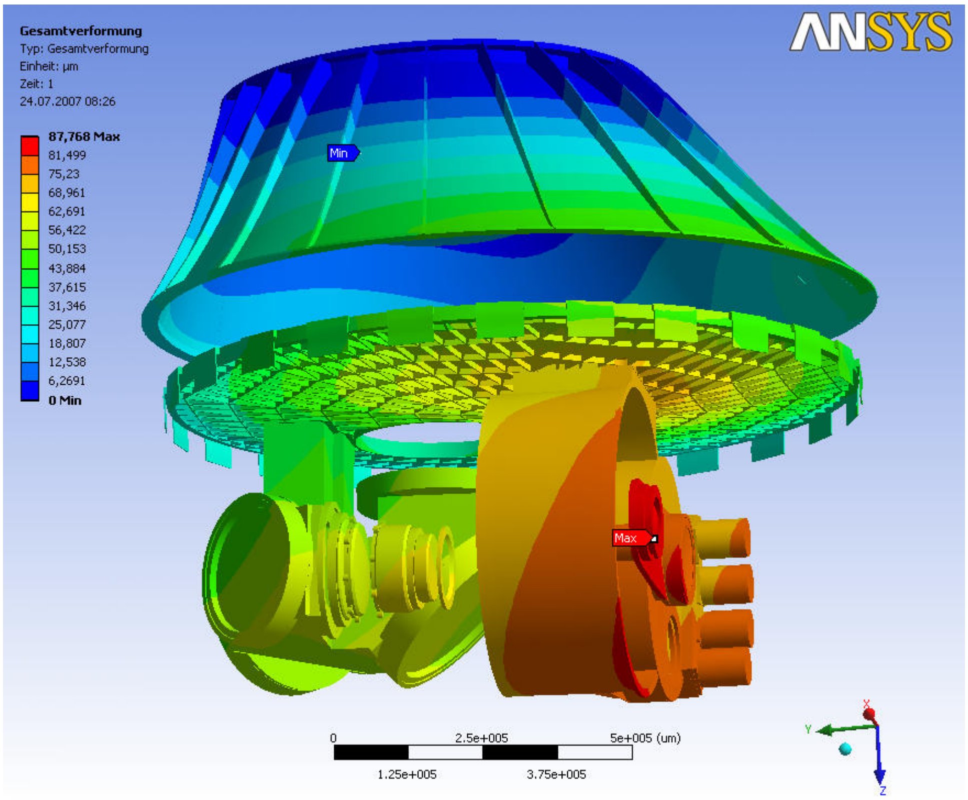

Figure 3.3.2-22: Displacement of cold bench and optics with the telescope pointing to zenith (gravity vector in +z-direction)

3.3.2.2.7.3 Bending of entrance window

The entrance window from Fused Silica has a diameter of 330 mm and a thickness of 20 mm.

The FEM analysis shows a maximum displacement of 33.2 µm due to a differential pressure of 1 bar and a maximum stress of about 4.3 N/mm2, which is about 1/11 of the rupture modulus of fused silica.

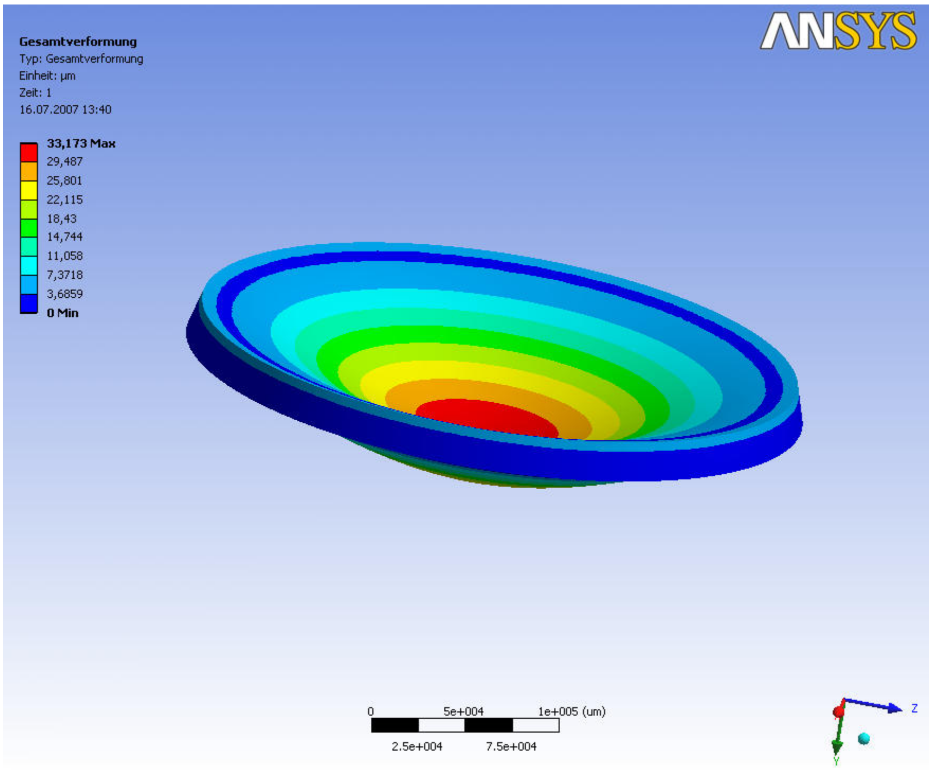

Figure 3.3.2-23: Simulation of entrance window deformation due to a differential pressure of 1 bar.

The following equation from [1] gives a max. deformation of 63 µm:

$$\text{max. deformation} = (0.696 * p * r^4) / (E * t^3)$$

with p… differential pressure (10^5 Pa)

r… effective radius (in this case 150 mm)

E… Young's modulus (70000 N/mm^2)

t… window thickness (20 mm)

The reason for the difference between the FEM and the calculated results is unclear. Only measurements can show, which of both values is closer to reality.

To calculate the minimum thickness, various equations can be found in the web (see [2], [3] and [4]).

Using the following equation from [2], the minimum window thickness is 14.3 mm:

$$T_{min} = \text{sqrt}\,(1.1 * p * r^2 * S / M)\ \ [\text{psi}]$$

with S… safety factor (in this case 4)

M…rupture modulus (for fused silica 7000 psi)

r… effective radius (in inches)

p… differential pressure (in psi)

The equations from [3] and [4] give similar results. So, a window thickness of 20 mm seems to be sufficient.

3.3.2.2.7.4 Bending of mirror M1 due to gravity

For the biggest of the three cryogenic mirrors, the bending due to gravity has been simulated using ANSYS. The mirror was placed horizontally with the gravity vector in –y direction (see Figure 3.3.2-24). The maximum value in the center is 47 nm peak-to-valley (PTV). This corresponds to a RMS value of 13.3 nm when the following worst case relationship for defocus (e.g. from [5]) is used:

$$PTV = 2 * \text{sqrt}3 * RMS$$

The wavelength range of PANIC is 0.8 - 2.5 microns. Thus, if we specify the maximum deflection (RMS) of the reflecting surfaces to be lambda/20, the upper limit for the RMS deflection would be:

$$\text{max. RMS deflection} = 0.8\ \mu m / 20 = 40\ nm$$

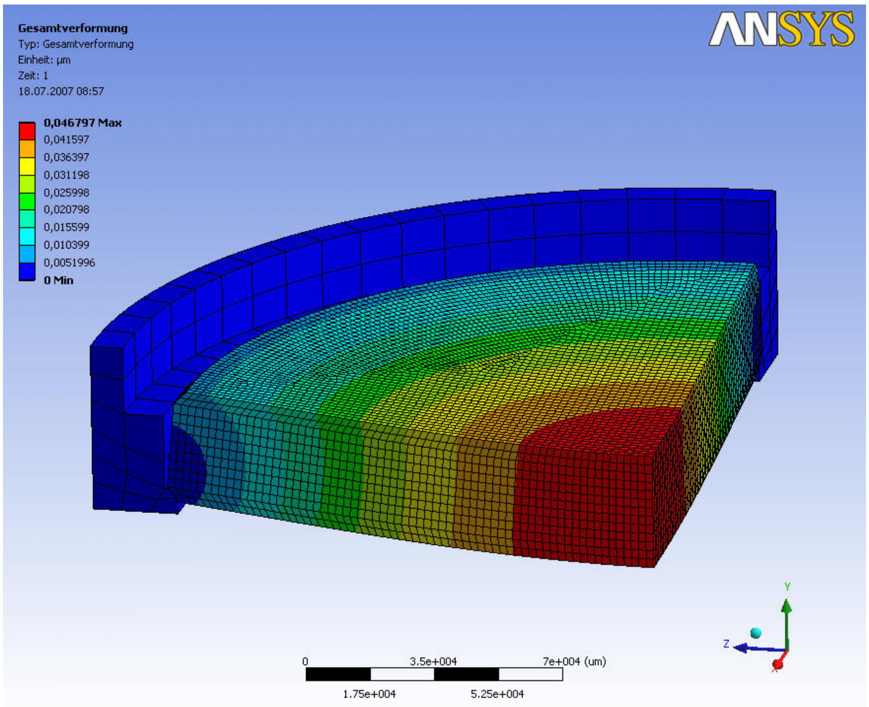

Figure 3.3.2-24: Deformation of mirror M1 due to gravity in -z direction.

3.3.2.2.8 Error budget

The error budget calculation for the optical elements and groups (see section 3.2) shows critical decentre values for the lenses L5 and L6 (0.45 arcsec/px) and for the tilt of lenses L1, L2, L4 L5 and L7. Realistic values from a manufacturing point of view are 25 µm for decentre and roughly 60 arcsec for tilt (for a 100 mm diameter lens)

The most difficult requirement however is the decentre value of the optics wheel: The decentre of the lens group L5A to L8A (0,45 arcsec/pixel) must not exceed 39 µm. The following list shows several potential decentre effects of this group and their expected values:

a) Positioning accuracy of the wheel due to gear transmission errors:

The transmission accuracy of the Harmonic Drive gear HD14, 100:1 is less than 2 arcmin. With a distance between the optical axis and the axis of rotation of 140 mm, the positioning accuracy of the optics is 80 µm.

b) Positioning accuracy of the motor:

The Phytron stepper motor needs 200 steps for a full turn. With a gear transmission ratio of 100:1, one step of the motor gives a rotation of the wheel of 1.08 arcmin or a optics decentre of 44 µm.

c) Ball bearing true run tolerance:

The true run tolerance of the ball bearing WAD933ZZ from ADR is 12 µm.

d) Optics shift due to thermal gradient:

As shown in section 3.3.1.2.6.3., the cold bench can have a thermal gradient under certain conditions. This means that the optics wheel and the optics group 1 can move with respect to each other by up to 15 µm.

e) Deformation of the cold structure due to varying gravitation vectors:

The Finite Element Analysis shows deformations, which can result in decentre of the optics wheel of up to 20 µm.

f) Positioning accuracy of the optics wheel on the bench:

The manufacturing accuracy on a conventional CNC milling machine is about ± 10 µm. This means that the positioning accuracy of the wheel on the cold bench is about 20 µm in each direction.

For the current mechanical design, it seems to be unrealistic to meet the specifications since the expected decentre values of a) and b) are already higher than what is acceptable for the optical quality. Only f) could by compensated by adjustment.

A mechanical design which allows to position the optics with the required precision in a cryogenic environment would be much more complex.

However optical tolerance calculations show, that if certain compensators are introduced in the optical design, most tolerances can be relaxed significantly. This means that certain optics groups have to be measured interferometrically and corrected before they are mounted to the complete optics assembly.

These compensators are:

- Axial distance between L1 and L2
- Decentre in x and y of L2
- Decentre in x and y of L6A

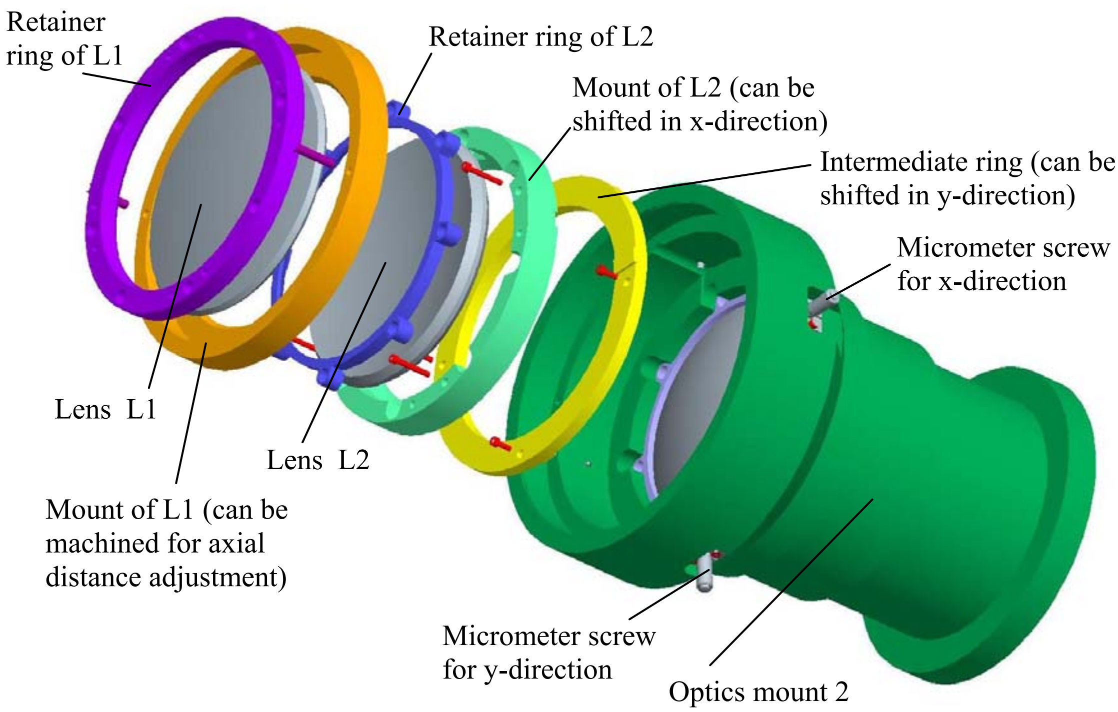

Figure 3.3.2-25: Optics mount 2 with mechanical decenter adjustment of lens L2 with micrometer screws (exploded view).

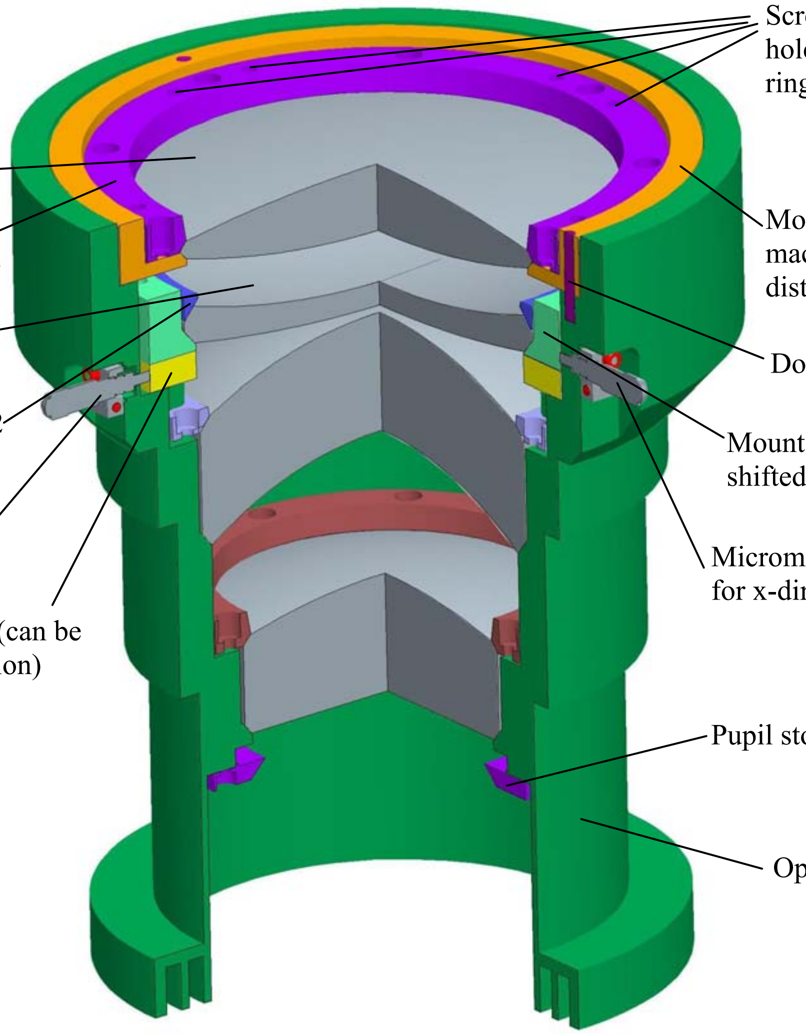

Figure 3.3.2-26: Section of optics mount 2

The axial distance between L1 and L2 can be adjusted by machining one of the mount parts. The centricity adjustment of L2 and L6A requires some additional mount parts, which can be moved by micrometer screws. Figure 3.3.2-25 shows how this could look like for L2. Lens L2 is mounted to a ring, which can by moved along a groove in x-direction by a pair of micrometer screws (e.g. Mitutoyo 148-207). An intermediate ring can slide in a groove of lens mount 2 in x-direction, controlled by another pair of micrometer screws. This design allows to adjust the lens decenter in both directions independently. Once the correct position is found both rings can be fixed by M3 screws through access holes in the ring in front of them.

3.3.2.2.9 Total weight limit and possible solutions

An overall mass estimation of PANIC is given in Table 3.3-6. The total mass is 463 kg. With the centre of gravity located about 630 mm away from the telescope interface flange, the instrument adds a moment of about 2530 Nm to the telescope (assuming that most of the electronics is mounted close to the mirror cell of the telescope).

Part or unit	***mass [kg]***	
Cryostat		
Vacuum can	66	Calculated from CAD model
Cold structure with shield and MLI	122	Calculated from CAD model
LN_2 (half filling 45 l)	36	
Optics and Opto-Mechanics		
Filter wheel unit, incl. filters	20	Calculated from CAD model
Lens and mirror mounts incl. lenses and mirrors	51	Calculated from CAD model
Optics wheel incl. housing and mount (w/o lenses)	23	Calculated from CAD model
Telescope Adapter	33	Calculated from CAD model
Detector Package		
Detector	1	Estimated
Detector stage	3	Estimated
Electronics		
Read-out electronics	7	Estimated
Control unit (motors, temperature ...)	24	Estimated
Cabling, rack	22	Estimated
Miscellaneous (screws, cables, etc.)	15	Estimated
Contingency	30	Estimated
Sum	453	

Table 3.3-6: Overall mass estimation of PANIC with two pixel scales

So both the weight and the moment limit of the 2.2m telescope are well exceeded by the current two-pixel scale design. Since we do not see a way to reduce weight or to reduce the distance between the centre-of-gravity and the telescope flange while keeping the same instrument performance, the only possibility seems to be to have only one pixel scale. In this case the optics wheel and the rotating field stop mask would not be necessary anymore and the cryostat could by significantly smaller. Figure 3.3.2-27 and Figure 3.3.2-28 show the design of the instrument with one pixel scale, Table 3.3-7 shows a mass estimate for this option.

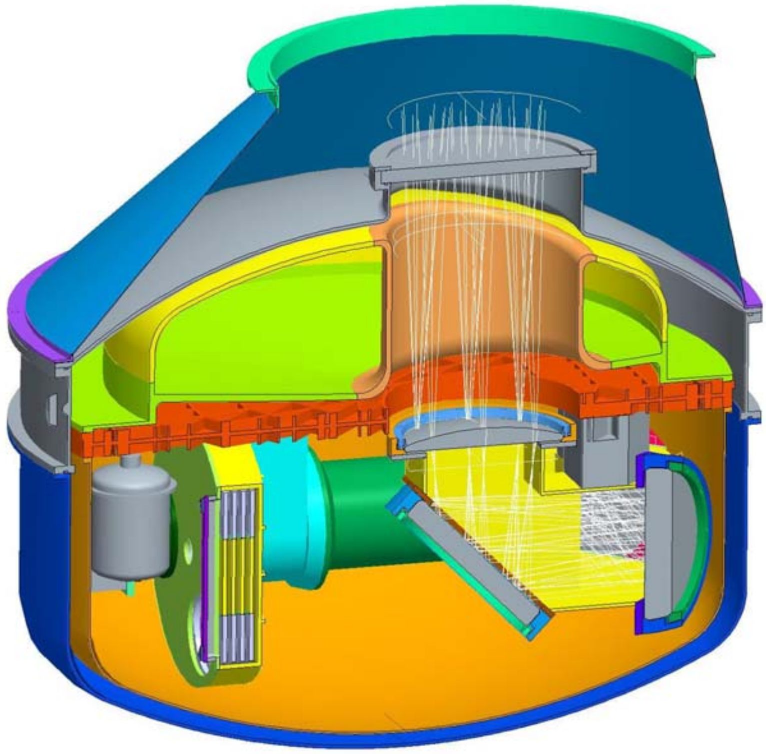

Figure 3.3.2-27: Section of the one-pixel scale design (similar to Figure 3.3.2-1)

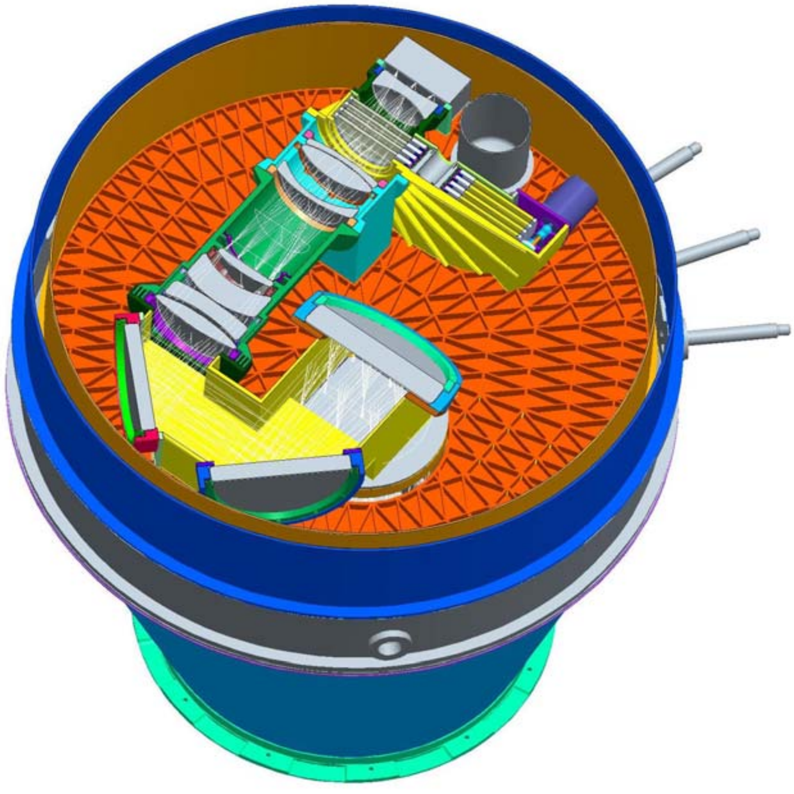

Figure 3.3.2-28: Cold bench and optics of the one-pixel scale design (similar to Figure 3.3.2-2)

Part or unit	*mass [kg]*	
Cryostat		
Vacuum can	64	Calculated from CAD model
Cold structure with shield and MLI	92	Calculated from CAD model
LN_2 (half filling 35 l)	28	
Optics and Opto-Mechanics		
Filter wheel unit, incl. filters	20	Calculated from CAD model
Lens and mirror mounts incl. lenses and mirrors	53	Calculated from CAD model
Telescope Adapter	26	Calculated from CAD model
Detector Package		
Detector	1	Estimated
Detector stage	3	Estimated
Electronics		
Read-out electronics	7	Estimated
Control unit (motors, temperature ...)	24	Estimated
Cabling, rack	22	Estimated
Miscellaneous (screws, cables, etc.)	15	Estimated
Contingency	30	Estimated
Sum	385	

Table 3.3-7: Overall mass estimation of PANIC with only one pixel scale

It is obvious that even with a one pixel scale design the original ZEISS limit is exceeded. The weight is less than the CAFOS limit, the moment of 2000 Nm is slightly over the CAFOS value (1860Nm) but this will not cause problems.

Details of the mechanical design (general layout, lens holders, filter wheels) and the mechanical tolerances are similar and/or identical to the two pixel scale design. Since the most critical part of the two pixel scale design - the optics wheel - is not needed, the mechanics can meet the requirements set by the optics.

3.4 Electronics

3.4.1 ROE

3.4.1.1 Scope

This document describes the design of PANIC's readout electronics.

3.4.1.2 Requirements

- the ROE shall operate four HAWAII2-RG detectors
- a possibility to read an area of 15″x 15″ (33 x 33 pixels at 0.45″/pixel) of the detector at an minimal rate of 8 ms/frame; in this mode PANIC could be used for fast photometry. Final goal is 1ms/frame. This mode will also be used for guiding, but at much lower frame rates.
- the ROE noise shall be small compared with the ReadOut noise of the detector
- the ROE shall be low power
- all voltages on detector shall be in allowed range during power on/off

3.4.1.3 General Information

The ROE used with Omega2000 could operate 40 channels in total. Since PANIC uses four HAWAII2-RG detectors with a total of 128 channels, a new design of the standard MPIA ReadOut Electronics is required. The new ROE uses new parts which are smaller and cheaper. So the old ROE was housed in a 19 inch 7 height units case, whereas the new ROE is housed in a 13 inch 3 height units case.

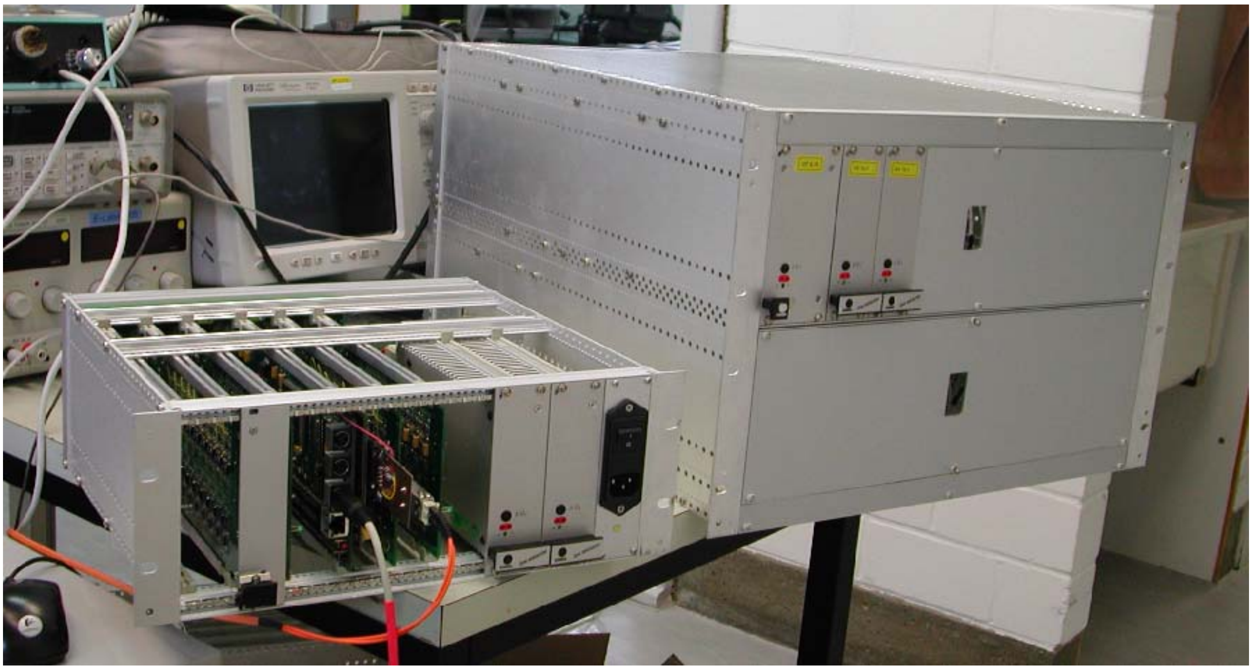

Figure 3.4.1-1 new ROE (left) versus old ROE (right)

The left side in Figure 3.4.1-1 shows the new ReadOut Electronics, the right side the former one.

The new development was started in summer 2006. The complete ReadOut Electronics consists of the following electronic boards:

- ROCon - ReadOutController
- AD36 - 36 channel analog to digital converter
- H2RG_CB - HAWAII2RG Clock/Bias board
- BP6 - 6 slot backplane connecting the above three boards
- OPTPCI - feeds the data from the fiberlink to the PCI bus
- CA36 – 36 channel cryogenic preamplifier

All boxes, boards and cables are specifically designed and built according to the EMC criterion (for more information refer to IEC/EN 61000-4).

The central board of the new ROE is the ReadOutController ROCon. It generates the pattern needed for clocking the detector and has circuitry for data transmission via fibers. The Clock/Bias board transforms the clocks from the ROCon board to the levels required by the detectors and generates programmable detector supply voltages. The AD36 board has 36 analog to digital converters with 16 bit resolution and a sampling rate of 1 million samples per second. The AD36 boards are connected to the detectors via CA36 cryogenic preamplifier boards. The complete ROE thus consists of 4 AD36, 1 ROCon and 1 Clock/bias board; these are connected by a 6 slot backplane BP6. The OPTPCI is installed in the PC/workstation and receives the data via fiber link.

3.4.1.3.1 ROCon – ReadOutController

The ReadOutController board controls the activities of the whole ROE. The ROCon is populated with two FPGAs, two fiber transmitters and a microcontroller module. One FPGA together with 8 MegaByte SRAM forms the pattern generator. The second FPGA together with the two fiber modules do the data gathering and transmission to the PANIC workstation. The microcontroller module handles the commands from the serial line or ethernet.

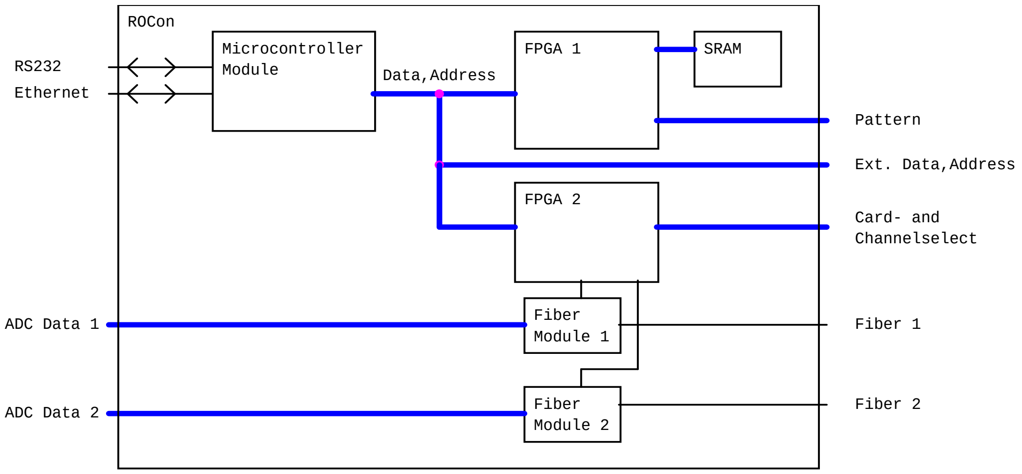

Figure 3.4.1-2 ROCon block diagramm

To run the pattern generator you first have to send commands containing the different chunks of the pattern. The pattern also contains the trigger for the AD36 boards. Next you have to send a program table. The program table contains the sequence of the patterns and the number of repetitions of each pattern.

If the pattern generator is running the AD36 boards are triggered periodically. This trigger arms a sequencer in FPGA 2 which starts at the completion of conversion of the AD36 boards. This sequencer is programmable via commands. It reads the conversion results of the AD36 boards in the desired order and transmits them to the PANIC workstation via Fiber 1 and 2.

Fiber 1 and 2 can transmit 132 Mbyte/sec each.

3.4.1.3.2 AD36 - 36 channel analog to digital converter

The AD36 board houses 36 ADCs with suitable differential drivers and a FPGA. The synchronous serial outputs of the ADCs are connected to the FPGA. When conversion is completed all 36 conversion results are present in FPGA internal registers and can be read from the ROCon.

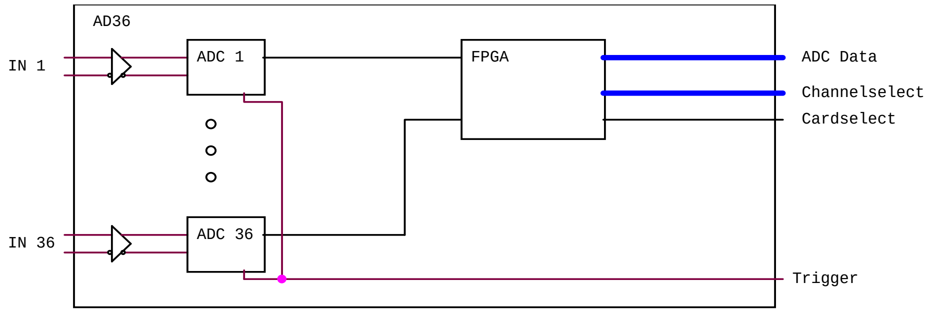

Figure 3.4.1-3 AD36 block diagram

The ADCs have 16 bits resolution and a throughput of 1 MSPS. For more information refer to the data sheet of the AD7677.

With a scale of 0.45″/pixel an area of 15″x 15″ of the detector can be read in about 1.1 ms.

On the prototype the noise performance for a single correlated read with shorted inputs of the AD36 board results in a standard deviation of 0.8 counts. Adding the noise of the cryogenic preamplifiers will result in about 1.0. Assuming a charge storage capacity of 100,000 electrons this would be a noise of approximately 2.1 electrons for a double correlated read. This value is small compared with the read noise of 15 electrons for the detector.

3.4.1.3.3 H2RG_CB - HAWAII2RG Clock/Bias board

The H2RG_CB board generates all supply- and bias voltages needed by the 4 HAWAII2RG detectors. The bias voltages are generated with a DAC and can be adjusted remotely. Further the H2RG_CB board does a level translation of the pattern coming from the ROCon to appropriate levels. At last this board houses a FPGA. The FPGA provides 4 synchronous serial interfaces to set up the HAWAII2RG internal registers. Some of the pattern lines are routed to the FPGA in order to trigger the change of detector internal register values via a serial write.

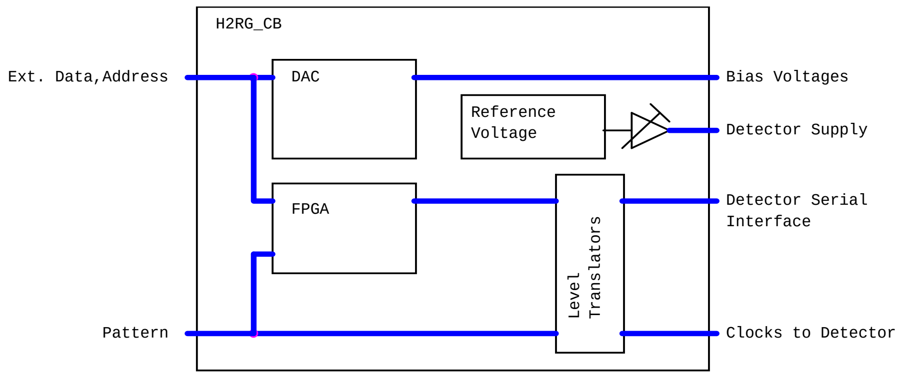

Figure 3.4.1-4 H2RG_CB block diagram

3.4.1.3.4 BP6 - 6 slot backplane

The BP6 connects the above three boards. There are 4 slots for AD36 boards, 1 slot for 1 ROCon and 1 for the H2RG_CB board. The backplane also connects to the power supplies and delivers the power to the different boards.

The BP6 is layouted impedance controlled and has termination circuitry onboard. This provides optimum signal integrity for high speed signals.

3.4.1.3.5 OPTPCI - fiberlink interface

The OPTPCI board receives the data sent by the ROCon. Receiver 1 and 2 parallelizes the data stream and writes it to the corresponding FIFOs. If an adjustable threshold is reached a DMA request is produced and the data is written to the memory of the PANIC workstation.

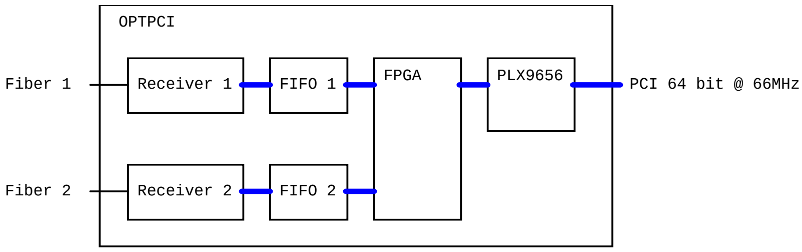

Figure 3.4.1-5 OPTPCI block diagram

The OPTPCI should be installed in a PCI slot with 64 bits @ 66MHz to reach the maximum data rate of approximately 250 Mbytes per second. However the OPTPCI can be run in a PCI slot with 32 bits @ 33 MHz. This will reduce the achievable data rate to approximately 100 Mbytes per second.

3.4.1.3.6 CA36 – 36 channel cryogenic preamplifier

The CA36 board translates the detectors single ended output signal to a differential signal:

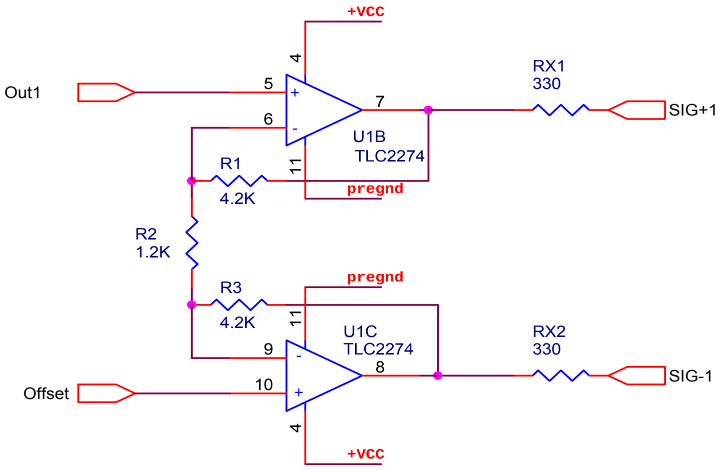

Figure 3.4.1-6 single channel of the CA36 board

There are four preamplifier boards in the cryostat located close to the detectors. The schematics for the CA36 are done but due to missing information from Teledyne (formerly known as Rockwell) and missing information of the mechanical details the cryogenic preamplifier board cannot be layouted at the moment.

3.4.1.3.7 Power Supply

The ROE in this configuration needs two supplies of 5 volts. One supplies the digital circuits of the ROE, the second supplies the analog circuits. At the moment there are two 5 volts / 8 Amps switching supplies in use. We estimate a maximum power consumption of about 50 watts.

3.4.1.3.8 Detector protection circuitry

Since the used detectors are not inexpensive, protection circuitry is included in the ROE to avoid damage. The first part is located on the Clock/Bias board, the second part on the 36 channel cryogenic preamplifier.

All biases and clocks needed by the detectors are generated by the Clock/Bias board. In Figure 3.4.1-7 the zener rectifier limits the detector supply voltage to 4,7 volts in case of a circuit failure. All other supplies and clocks are clamped via a Schottky rectifier to that voltage. This ensures that no detector input voltage can be greater than VDD + 0.2 volts and prevents latchup of detector input pins. The remote controlled DAC has a power on reset input. This guarantees that all biases are at 0 volts after power on.

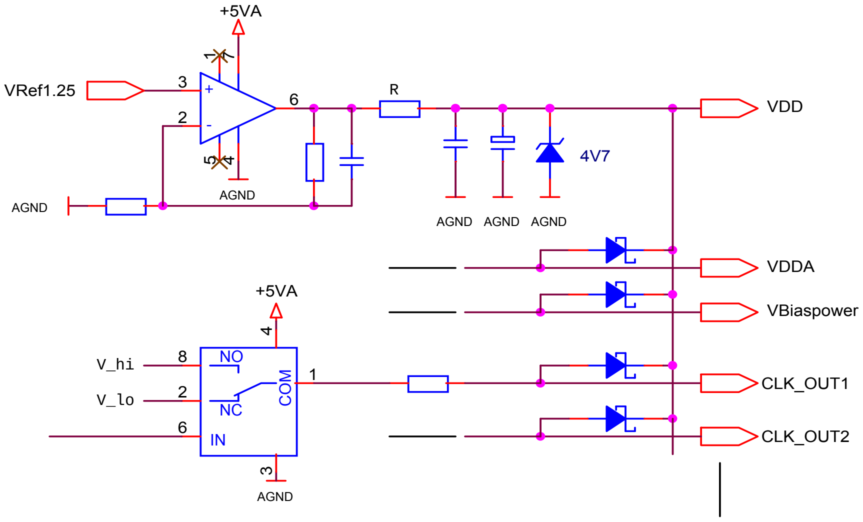

Figure 3.4.1-7 Protection circuitry on Clock/Bias board

More protection circuitry is integrated to the 36 channel cryogenic preamplifier. Each detector input pin is protected with the circuit in Figure 3.4.1-8. This circuit prevents damages caused by electrostatic discharge and ensures that no voltage greater than 4.7 volts is applied to any detector pin.

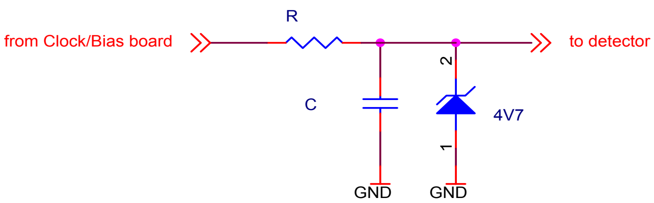

Figure 3.4.1-8 preamplifier protection circuit

Last but not least the detector manual states that there are some protection diodes at the input pads but doesn't reveal any details.

3.4.1.3.9 Troubleshooting - Diagnostics

For troubleshooting purposes there are some built-in diagnostics:

The first diagnostics facility is on the OPTPCI board. The FPGA can be switched to a data generator mode. In this mode errors on the PCI side of the OPTPCI can be discovered.

The second facility is on the AD36 board. The FPGA on this board can also be switched to a data generator mode. In this mode the data transfer mechanism from the ROE to the OPTPCI can be checked.

A device that simulates a HAWAII2RG detector will soon be available. This device has read only memory, 32 DACs and a FPGA onboard. In response to the clocking pattern it outputs a test picture on the DAC outputs and thereby allows to check the complete signal path from thecryogenic preamplifiers to the shared memory.

3.4.2 Control Electronics

3.4.2.1 Requirements

Positioning of filter wheels

Positioning Accuracy: +/- 800µm outer dimension of filter wheel

Motor: 1,8° stepper motor, 200 steps/rev. ,
Driver: microstepping driver, 1,5A RMS, 2,1A peak
Reference mark: micro switch
Feedback: resolver in 16-bit incremental encoder mode
Gear: 10:1 , reduction ratio gear wheel to gear ring

Positioning of optic wheel

Positioning Accuracy: +/- 70µm outer dimension of optic wheel

Motor: 1,8° stepper motor, 200steps/rev, with harmonic drive gear 100:1 reduction ratio
Driver: microstepping driver, 1,5A RMS, 2,1A peak
Reference mark: micro switch
Feedback: resolver in absolute encoder mode with angle accuracy 0,2°

Positioning of field stops wheel

Motor: 1,8° stepper motor, 200steps/rev, with harmonic drive gear 100:1 reduction ratio
Driver: microstepping driver, 1,5A RMS, 2,1A peak
Reference mark: micro switch
Feedback: resolver in absolute encoder mode with angle accuracy 0,2°

Monitoring of temperature inside the cryostat

Temperatur accurancy: Including electronic and sensor accurancy: +/- 1K

Measurement device: 8 channel temperature monitor Lake Shore 218S
Temperatur sensor: Silicon temperature diode DT-670, wide useful temperature range from 1,4K to 500K

Detector temperature controlling (max.fall rise time 0,5K/min)

Temperatur accurancy: Including electronic and sensor accurancy: +/- 0,1K

Controller device: Temperature controller Lake Shore 331S
Temperatur sensor: Silicon temperature diode DT-670, wide useful temperature range from 1,4K to 500K
Heating Element: Power resistor

Quality of vacuum preasure inside the cryostat

Device: Vacuum measurement system dual-channel device pfeifer TPG262 , connection for two gauges, measurement range from 5x10-11mbar up to 55bar .

Transfer of data between serial interfaces and ethernet

Device: Serial device server Nport 5610-xx, up to 16 ports supporting RS232 10/100 Mbps Ethernet, 15kV ESD surge protection for all serial signals

3.4.2.2 General electronics concept

3.4.2.2.1 Overview

The PANIC instrument control electronics is based on the computer infrastructure of Calar Alto. Standarized Calar Alto instrumentation boards and devices are forseen. The connection to the instrument workstation is realized via a Local Area Network. The central process computer for PANIC is a x86 multicore PC. Most of the other function units are independent, intelligent devices. The following table shows the chosen devices and their manufacturers.

Device	Manufacturer
x86 multicore PC	
Nport server Nport 5610-xx	MOXA
Motion Controller	MPIA
Read Out Electronics	MPIA
Temperature Monitor Model 218S	Lake Shore
Vacuum measurement system TPG 261	Pfeiffer Vacuum GmbH
Temperature Controller Model 331S	Lake Shore

Table 3.4.2-1 Summary of electronic devices

3.4.2.2.2 Simplified block diagramm of instrument control electronics

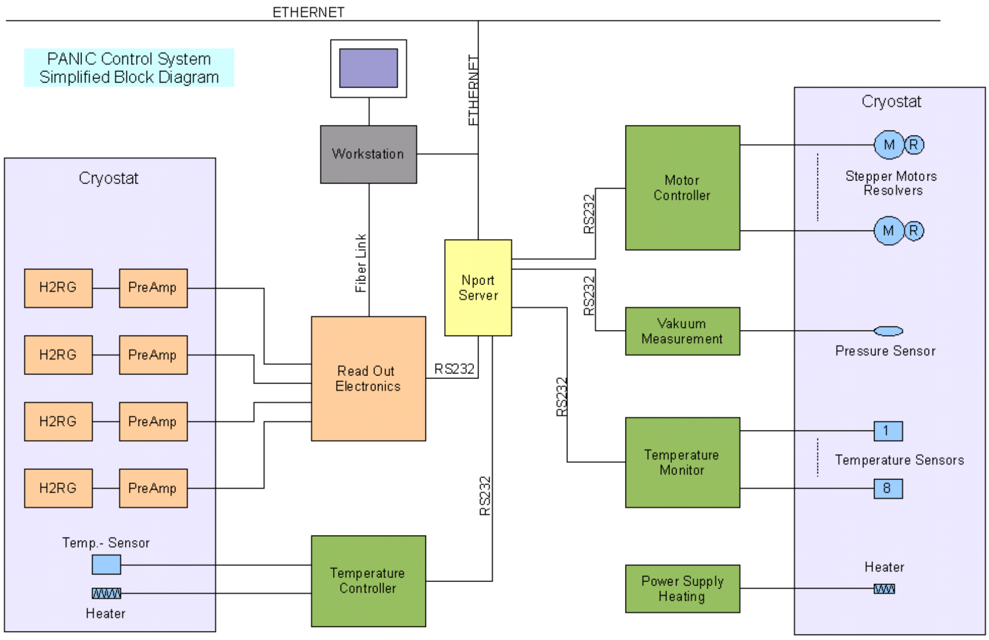

Figure 3.4.2-1 PANIC Control System Simplified Block Diagram

3.4.2.3 Motion control electronics

3.4.2.3.1 General

The heart of the PANIC Motor Controller is the standard MPIA MoCon board with a phyCORE-XC161 Single Board Computer module on it. This MoCon board is a multi-functional device, which is able to control a huge variety of motors. Due to the modular concept, the MoCon electronics is capable to drive stepper motors as well as servo loop motors. Core of the hardware is a 16 bit Infineon Controller, which contains the firmware managing the communication and command functions. For motion controlling the electronics is equipped with two motion processors from Performance Motion Devices.

3.4.2.3.2 Principle of motion control system

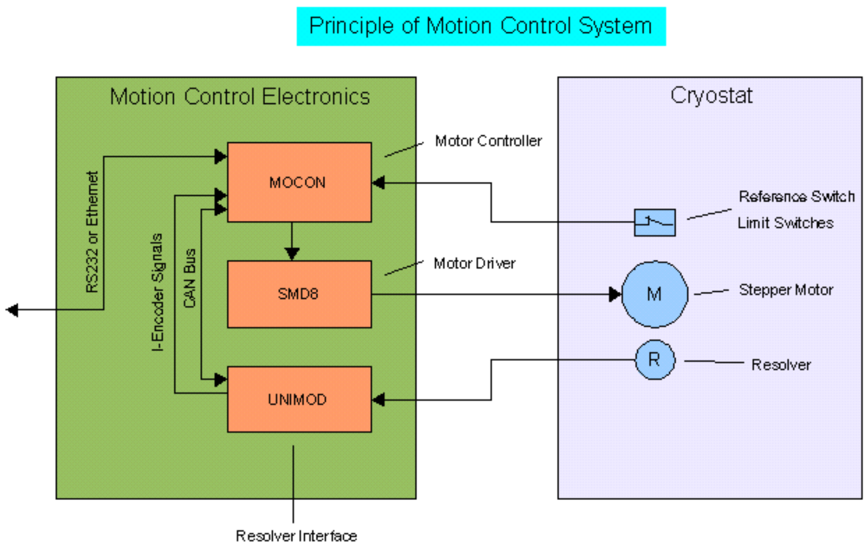

Figure 3.4.2-2 Principle of motion control system

3.4.2.3.3 Motion controller board (MOCON)

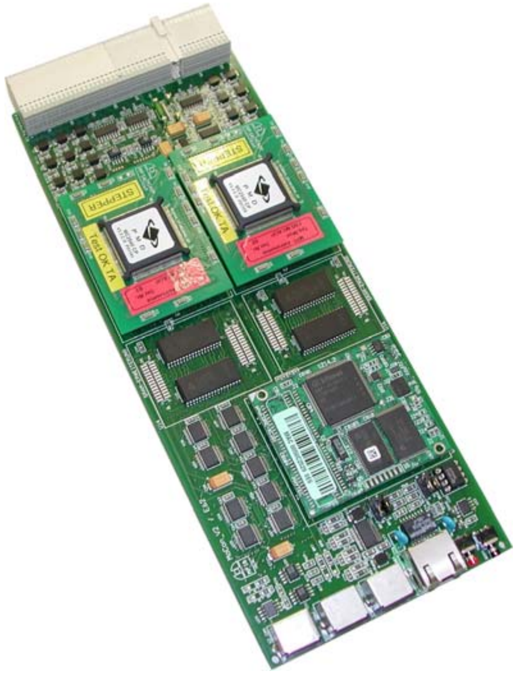

Figure 3.4.2-3 Motion Controller Board

Features:

- Control of up to 8 axes.
- Motion profiles include S-curve, trapezoidal, velocity contouring, and electronic gearing
- Asymmetric acceleration and deceleration to custom program a trapezoidal motion profile
- Incremental encoder quadrature input and parallel input for absolute encoder or resolver for on-the-fly motor stall detection
- Trace capabilities for system performance checks, maintenance and diagnostics.
- Advanced breakpoint capability allows precise sequencing of events.
- Two-directional limit switches, index input, and home indicator per axis.
- Serial Interface (RS232), CAN Bus, Ethernet

3.4.2.3.4 Stepper Motor Driver (SMD8)

Figure 3.4.2-4 SMD8 Board

The stepper motor driver board SMD8 contains the power amplifiers to power the stepper motor coils. The SMD8 board is capable to carry eight IM481H amplifier modules. The IM481H is a PWM chopper type sinusoidal micro step bipolar stepping motor driver. Sinusoidal micro step operation is generated by means of built-in hardware and is outputted for operation by clock signal inputting. The micro stepping rate is selectable from: 1/1 - 1/256-Steps, which enables individual application-related microstep switching, smooth and constant running and reduces considerably system resonance. Current down system eliminates motor power losses and heating during standstil.

3.4.2.4 PANIC motors

3.4.2.4.1 General

Extreme Environment Stepper Motors from the company Phytron will be installed inside the PANIC cryostat. These two-phase hybrid stepper motors are build with special windings, insulating material and adhesive. This motor drives successfully the filter wheels of infrared camera O2000.

Figure 3.4.2-5 Vacuum stepper motor VSS

3.4.2.5 Position and reference marks

3.4.2.5.1 Microswitches

Microswitches will be used to indicate the reference position of all motorized units. The selected switches are manufactured by Saia Burgess AG. This type of switches have been successfully used in past cryogenic projects, for example the infrared camera O2000.

Characteristics:
- Wide range of forces and variants
- Long mechanical and electrical life
- Solder, PCB and faston terminals

Rating:
- 250 VAC, 10 A max.

Dimensions (mm) :
- 19.9 x 9.5 x 6.4

Figure 3.4.2-6 Micro switch

3.4.2.5.2 Resolver

An angular resolver (Type RE-15-1-A14 from LTN Servotechnik) will be mounted on the motor axis of each filter wheel. The resolver monitors the angular position of motor axis.
With a simple rotor modification of LTN Servotechnik this type is suitable for cryogenic projects.

Figure 3.4.2-8 Resolver Type RE-15

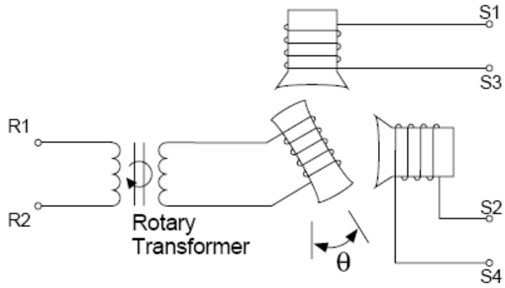

Figure 3.4.2-7 Principle of operation

Operating principle:
A resolver is a rotary transformer that provides information on the rotor position angle θ. The stator bobbin winding is energized with an AC voltage R1-R2. This AC voltage is transferred to the rotor winding with transformation ratio Tr. The AC voltage then induces the voltages S1-S3 and S2-S4 into the two output windings of the stator.The magnitude of the output voltages vary with the sine and the cosine of the rotor position angle θ, because the two secondary windings are shifted by 90°.

3.4.2.5.3 Resolver Module (RESMOD)

Figure 3.4.2-9 RESMOD_V2

The ResMod_V2 is a piggyback-module designed for use with the UniMod board. It contains a resolver to digital converter (RD19230) and a frequency generator to drive the primary side of the resolver. The resolution of the converter can be programmed to 10, 12, 14 or 16 bit. The RD19230 has 3 digital outputs that emulate an incremental encoder.

3.4.2.6 Motion controlled units

3.4.2.6.1 Filter unit

The filter unit has four filter wheels. Each wheel is driven by a stepper motor . The position feedback comes from an angular resolver that is mounted on the stepper motor axis. Each wheel has one fixed reference position. This position is detect by an micro switch.

Part	Motor	Resolver	Ref-Switches
Filter wheel 1	VSS65.200.xx	RE-15-1-A14	1
Filter wheel 2	VSS65.200.xx	RE-15-1-A14	1
Filter wheel 3	VSS65.200.xx	RE-15-1-A14	1
Filter wheel 4	VSS65.200.xx	RE-15-1-A14	1

Table 3.4.2-2 Summary of motion controlled filter wheels

3.4.2.6.2 Optics and field stops wheel

Part	Motor	Reslover	Gear	Ref-Switches
Second Pixel Scale Optic	VSS52.200.xx	RE-15-1-A14	Harmonic Drive 100:1	1
Field Stops Wheel	VSS52.200.xx	RE-15-1-A14	Harmonic Drive 100:1	1

Table 3.4.2-3 Summary

Both wheels are driven by a stepper motor in combination with an 100:1 harmonic drive gear . The detection of a reference position comes from a micro switch.

Harmonic drive gears mounted on Phytron motors have the following advantages:

- High reduction ratio in a small volume
- Very low weight
- Very low mass inertia
- High permissible torque, in comparison to the size
- High drive speed
- Very low backlash in comparison to conventional gears
- High efficiency

3.4.2.7 Resources

3.4.2.7.1 Power consumption and weight

Part	Mains requirement power consumption [VA]	Weight [kg]
Motion Controler (MPIA)	40	10
Temp-Monitor Lake Shore 218S	18	3
Nport Sever 5610	27	4
Pfeifer TPG 262 Dual Gauge	45	2
Read Out Electronic	50	7
Temp-Controller Lake Shore 331S	15-120	5
Compact Rack+Components	-	22
	195-300VA	53kg

Table 3.4.2-4 Summary of power consumption and weight

The calculated power is the maximum power consumption, from manufacturer datasheets, 195-300VA. The calculated weight is 53kg.

We are investigating ahead possibilities exist to reduce the power dissipation, e.g. switching off devices not in use.

3.4.2.7.2 Instrumentation rack

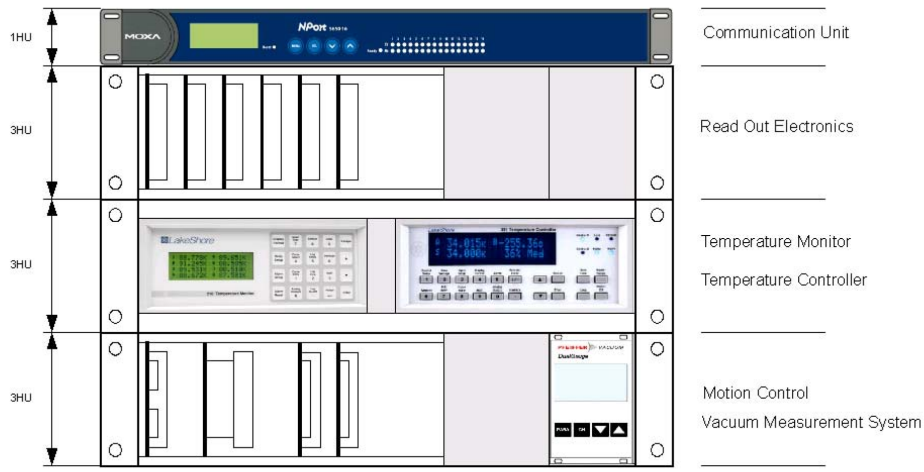

Figure 3.4.2-10 Instrumentation rack

3.5 Software

3.5.1 Summary

This section contains the requirements of the SW of the PANIC instrument and the design report for fulfilment of that requirements. After the introductory part, the requirements for the SW, which were derived from the applicable documents, are presented. This document forms part of the documentation set to be revised by the review panel at the PDR.

3.5.2 Introduction

The PAnoramic Near Infrared camera for Calar Alto (PANIC) is planned as a wide field NIR camera for the 2.2m telescope at Calar Alto Observatory. PANIC will be built by a consortium formed by two institutions with proved experience in R+D developments. These institutions are MPIA (Heidelberg, Germany) and IAA (Granada, Spain).

The PANIC SW is divided into two main parts, the Instrument Control Software (ICS) and Data Handling Software (DHS). The ICS is divided into two systems, GEIRS and the Observation Tool (OT), and the DHS is again divided into the data reduction software (DRS) and the Quicklook.

3.5.3 Requirements

3.5.3.1 Guides to understanding the requirements

3.5.3.1.1 *Use of shall/should*

"Shall" is used for requirements, whereas "should" is reserved for guidelines. Requirements are mandatory and guidelines are not mandatory, although their fulfilment should be strongly pursued.

3.5.3.1.2 Unconfirmed and undefined requirements

A "TBC" or a "TBD" identifies unconfirmed or undefined requirements, respectively.

3.5.3.2 General Requirements

3.5.3.2.1 Parts

The System shall be divided in the following main parts :

1. Instrument Control Software (ICS)
   1.1 GEIRS
   1.2 Observation Tool (OT)
2. Data Handling Software (DHS)
   2.1 Data Reduction Software (DRS)
   2.2 Quick look

3.5.3.2.2 Operating System

All the computer system involved in PANIC (ICS and DHS) shall work on a personal computer (PC) running 64-bit Suse 10.x Linux distribution. This requirement is in compliance with CAHA staff.

3.5.3.2.3 System Log

The errors, faults and warnings shall be logged properly and used as input for system maintenance, giving as minimum the timestamp, code and description of the error.

3.5.3.3 GEIRS

The generic infrared camera software of the MPIA and Calar Alto shall offer the same capabilities for PANIC like for Omega2000 with some extensions and add-ons.

It shall implement all instrument hardware interfaces and shall offer the telescope interface.

It shall still support the previous interactive usage of the camera with GEIRS GUIs and commands.

It shall log all commands and maintenance relevant logging levels with the timestamp.

3.5.3.3.1 Hardware minimum requirements

The computer system (PC) shall

- use a 64bit PCI-data interface for the detector data read out to be able to read the expected max. data rate of 256 Mbytes/sec peak and 250 Mbytes/sec mean. This data speed arises from the number of 16bit data channels (128), the maximal clocking speed (1 MHz) and the subtraction of some overhead (for example line-reset $\leq$ 10 microseconds of 2048 lines per channel)
- have multiple CPU cores on probably at least 2 processor sockets to support the concurrent multiprocessing and multithreading of tasks of all software parts.
- have about 16 to 32 Gbytes of RAM to allow the buffering of a single data sequence, which is done by the detector read out electronic (ROE) with a single trigger, and to have additionally enough space for caching of disk-transfers. The 16 Gbyte RAM will allow to buffer a single integration count of an exposure of double correlated images of about 125 for full-frames (about 340 sec of min. integration time at 100kHz pixel clock) and 11000 for the 36x36 window size (about 11 sec of min. integration time at 1MHz pixel clock) . Always all rawdata from the detectors are buffered.
- not delay the optimal efficiency for the detector usage. This is also supported by the double exposure buffering logic of GEIRS.
- have multiple hard disks as data storage, to allow data saving with full speed of the read-out and the DHS data access. The disks should be RAID protected if that solution is fast enough.

3.5.3.3.2 Interfaces

All interfaces should be provided additionally in simulation.

3.5.3.3.2.1 Instrument Status

GEIRS shall support :

- an instrument status GUI.
- monitoring of all available temperature and pressure sensors of the PANIC dewar.

- and monitoring of external conditions if information is accessible (dry liquid nitrogen protection flow of the entrance window; temperatures of electronic rack houses, etc).
- logging of the temperature and pressure values as history to allow to be checked and visualized at any time by plotting tools.
- writing of the necessary status information (temperature, pressure, other conditions) into the FITS-header.

3.5.3.3.2.2 Control Electronics

The interface to the motor electronics (6 cryogenic motor units controlled by a MPIA motor electronic) shall optimize the moving time and the position reliability for instrument efficiency.

The motor devices shall:

- be configurable as disabled, enabled, fixed-to-position, simulated.
- be configurable for the position of the elements, the element objects and the dependencies defined by the elements (wavelength, focus offset, etc).
- do for each device during home initialization the verification of the configured backlash correction size, which is used for correct positioning.

use a second reference switch additional to the home position switch as backup in case of problems with the single home switch in the not accessible dewar (if no encoders or element position sensors are used for the device).

3.5.3.3.2.3 Readout Electronics (ROE)

GEIRS shall support:

- the new MPIA-PLX-PCI-Interface to the ROE3 using a single device port with 2 data lines (DMA-channels).
- the new Rockwell IR-detector Hawaii-2RG properties according to the requirements for PANIC (100kHz to 1 MHz pixel clock; limited by the used ADCs, read-noise reduced read-out modes, full-frame and sub-window readouts nested with different frame speeds into each other for parallel guiding in the science focus field of view).
- the read-out of 4 detectors simultaneously via the 2 PLX data lines, in full arrays and in fast sub-windows, and combined with the nested guiding readouts.
- the acquisitions in time without losing data, also for small 36x36 frames (until about 200 to 256 Mbytes/sec data rate from the detector)
- the detector engineering and maintenance tasks by allowing detector patterns to be configured and handled by detector engineers during runtime, without recompilation of the control software (detector pattern engineering interface).
- a data protocol added to the frame read-out in front and at the end of a logical pattern clocking frame by the ROE3 via pattern control.

- the handling of the reference pixels which surround the detectors and are automatically clocked together with the data (only 2040 of the 2048 pixels in each detector direction are science data).
- the saving of the 4 detector science data units in an appropriate FITS format.

the guiding processing directly with the science detector in the science FOV (some time after the first light).

3.5.3.3.2.4 Telescope

GEIRS shall provide a telescope interface which:

- allows all necessary telescope commands
- contains a GUI to show and control the telescope activities (focussing, positioning).
- should show the status information of the open dome segment limitation (the dome segment shifting is not done automatically but has to be started manually).
- allows the control of the focus depending on the used optical elements in the beam.

3.5.3.3.2.5 OT

- GEIRS shall provide a complete command interface via external shell commands and/or via the command server interface to the OT.
- GEIRS should provide a status interface, informing regularly about a configurable parameter set on a selectable time base (of the order of seconds).

3.5.3.3.3 Data

GEIRS shall:

- offer a FITS keyword interface, which allows to configure the FITS header keywords specific to the instrument and add externally supplied keywords (about GEIRS does not know the correct entries). This shall be based on a flexible FITS keyword dictionary of the instrument. Telescope and mountain informations from the observatory, the PANIC instrument informations, as well as the PANIC OT and data reduction informations shall be specified in this keyword dictionary and used in the FITS header.
- write the data into FITS-files. Preferred format is a single multi-extensions FITS file per exposure with the integral image of each detector stored as FITS-image extension.
- write each resulting data file name and information into a data log file which might be used for accessing data files from software parts outside GEIRS.

store the data files alternating on multiple hard disks in parallel, if speed of a single disk (or RAID-partition) is a limiting factor.

3.5.3.3.4 Filter focus

The different telescope focus offsets for each filter shall be characterized and available to the instrument control system. The GEIRS shall focus the telescope secondary mirror automatically when a new filter is selected by the user.

3.5.3.3.5 Guiding

Due to the telescope tracking performances and planned observing modes, guiding shall not be needed at first light, but it should possible to implement after first light.

Although guiding will not be necessary for most observations because typical exposure times are on the order of a few tens of seconds, narrow band imaging clearly requires guiding. At least in the beginning, it is sufficient to select the guide star manually by clicking on it, an automatic routine might be implemented later on. The guide star should not be lost during a dithering sequence and guiding should continue automatically on the new position.

3.5.3.4 Observation Tool (OT)

3.5.3.4.1 Functionality

The OT should allow access to all of the astronomical observing functionalities of the instrument. i.e., for normal astronomical observing it should not be necessary to access any engineering functionality of any other system.

3.5.3.4.2 Hardware requirements

The OT shall have a PC with enough CPU to run the Java Virtual Machine, at least 1 GByte of RAM and a hard disk with at least 20 GByte of available space. The OT should be able to run on the same GEIRS PC.

3.5.3.4.3 External Interfaces

3.5.3.4.3.1 Graphical User Interface (GUI)

The OT shall be a PANIC high level control based on a GUI which shall allow the users to make the observations in a simple and user friendly way.

3.5.3.4.3.2 Hardware Interfaces

No hardware interfaces are required for OT.

3.5.3.4.3.3 Software Interfaces

3.5.3.4.3.3.1 GEIRS Interface

OT shall have a well defined interface with GEIRS. This interface will be based on the current GEIRS command server interface. Likely some new internal commands between GEIRS and OT will be needed.

3.5.3.4.3.3.2 Telescope Interface

The interface of the OT with the telescope shall be provided through the GEIRS interface.

3.5.3.4.3.3.3 On-line star catalog

Remote communication between OT and on-line star catalogs shall be carried out via http.

3.5.3.4.4 Display

The frames coming from the camera shall be shown in GEIRS real time display tool; the OT shall not show them, it has no own frame display.

3.5.3.4.5 Observing definition

The OT shall allow the definition of all observing information. This shall include, but not be limited to:

- Science program information (PI, observer, program title, email, …)
- observation constraints (seeing, airmass, distance from moon, time intervals, …)
- target coordinates and epoch
- scale mode (0.45arcsec/pixel or 0.25 arcsec/pixel)
- filter
- detector setup
- dithering pattern (for sparse fields or extended objects)
- exposure time each position
- number of cycles
- readout mode
- saving mode (separate disk FITS files for each exposure, integrated image, only a multi-extension FITS file, …)
- guiding stars (TBC)

3.5.3.4.6 Calibration definition

The OT shall allow the definition of calibrations observations. This shall include, but not be limited to:

- calibration series : darks
- dome flat-fields with a fixed lamp power and filter, providing automatic exposition time calculation.
- twilight/sky flat-fields (with recommended sky flat fields)
- focus test (with recommended focus fields)

3.5.3.4.7 Survey/Mosaic definitions

The OT shall allow to define a sequence of observations to make a survey/mosaic observation.

3.5.3.4.8 Templates

The user can choose some of these templates or define his/her own template for the observation. In any case, the observer can always do the observation without any specific defined template. In this case, he/she will handle the observation with the

GEIRS control GUI or with the command line commands available also into GEIRS : dither, read, save, focus or other macros as in Omega2000 and new ones.

The OT shall provide a set of predefined observation templates. There shall be at least three types of templates:

- calibration templates: darks, dome/sky flat fields
- science templates : source and calibration objects
- test templates : used for technical maintenance of the instrument (not available to users)

3.5.3.4.9 Dome segments shift

The dome segments shifting during an observation shall not be managed by the OT. The OT shall only show a warning about these kind of events if they are provided by the telescope control system to GEIRS.

3.5.3.4.10 Validation

The OT shall check that the observation program specified by the user complies with the operational instrument rules, avoiding wrong parameters values or nonsense sequences. In any case, the checking process should not block user entries, it should only warn about them.

3.5.3.4.11 Execution Control

Once the observation is defined by the user and validated, the OT shall allow users to execute, pause, resume or abort the observation sequence at any time.

3.5.3.4.12 Output scripts

For each observation defined, this tool shall produce a list of GEIRS instructions/commands [1] to carry out the planned sequence, but they should not be managed directly by the user.

3.5.3.4.13 Extra keywords

The OT shall provide a set of extra info keywords to write in FITS files. In that way, we can ensure that the quicklook tool and the pipeline will work in an appropriate way. These extra keywords should also facilitate the data archiving and subsequent data searching.

3.5.3.4.14 GEIRS Functionalities

The OT should provide the same GEIRS functionalities and new ones with higher abstraction level for the observer.

(In one way, the aim of this tool is to “replace” the current O2k MIDAS scripts and GEIRS commanding and provide and enhanced graphical tool to edit and build new observation scripts using GEIRS command via a well defined TCP interface.)

3.5.3.4.15 Secondary mirror focusing

OT should provide an item to program a focus sequence, but it shall not calculate best focus offsets for the secondary mirror for each filter, it shall be done by quicklook utilities. Besides, GEIRS shall include offsets for each filter into its configuration parameters, but the calibration of the focus offsets for each optical element should be a maintenance-calibration template.

3.5.3.4.16 Simulation

It should be possible to use the OT in two simulation modes:

1. GEIRS (and therefore the camera and telescope) is not present. In this mode, it should be possible to carry out a observing sequence simulation.

2. GEIRS is present and in simulation mode too, so a full testing of the OT can be done.

3.5.3.4.17 Observing Modes

It shall be possible to execute PANIC observations in-situ and in service mode. A remote mode (outside CAHA) should only be available via ssh-X-tunneling for engineering support.

3.5.3.4.18 Efficiency

The OT shall not compromise the efficiency of the observations, it shall only improve the efficiency of the observations.

3.5.3.4.19 Flexible

The OT shall be flexible enough to allow running of different types of scientific programs and engineering tests.

3.5.3.4.20 On/Off-line

The OT shall work online by the astronomer at CAHA control computers and off-line at astronomer computer. When offline the user will be only able to define, pre-plan and save them for a further execution.

3.5.3.4.21 Timeline Calculator

The OT should generate a estimation of the time required for the observation sequence defined by the user, taking into account the overheads and delays. That estimation should be available before any start of observation at the instrument.

3.5.3.4.22 Exposure Time Calculator

The OT should integrate an exposure time calculator in order to estimate exposure times. The total integration time should be taken and automatically divided into several exposures.

3.5.3.4.23 Engineering support

The OT should provide templates and observation blocks for engineering purposes during the different stages of the instrument development (integration, commissioning, maintenance). The necessary engineering tests should be packed at commissioning time into maintenance OBs for easier verifications.

3.5.3.4.24 Errors & Warnings

The OT should handle errors reported by the systems controlled by it. It will pause the observation in execution in response to such errors, and report the error to the user. Warnings shall only be reported to the user in a suitable way.

Both Errors and Warnings shall be written into the log file.

3.5.3.4.25 Repository

The OT should allow to submit the observation definitions and user defined templates as XML files to a repository through the net. A submitted observation could be retrieved and modified later.

3.5.3.5 Quicklook Tool

3.5.3.5.1 General requirements

The quicklook operations shall be all accessible from an GUI with a display tool. There must be communication with the image display for the purposes of specifying positions with the cursor, and for overlaying graphics. The general requirements are:

3.5.3.5.1.1 Quick feedback

The quicklook shall be able to provide quick feedback on the quality of the raw data to the user.

3.5.3.5.1.2 Quality control

The quicklook system should be able to provide the Quality Control required to monitor the quality of the data. That should include: mean sky brightness, sky noise, image detection threshold, average FWHM seeing, average stellar ellipticity and average saturation level.

3.5.3.5.2 Observing Utilities

3.5.3.5.2.1 Focus

A utility to enable determination of best focus from a series of frames taken at different focus positions shall be provided by the quicklook.

3.5.3.5.2.2 Seeing

A utility to enable determination of seeing from a frame should be provided by quicklook.

3.5.3.5.3 Data reduction tasks

The quicklook pipeline shall do the data reduction tasks defined in the quick pipeline mode.

3.5.3.5.4 Extensions

The quicklook pipeline could be extended to produce coloured images (with different filters) or mosaic images if possible.

3.5.3.5.5 Quick data persistence

Quick look reduced data should only be kept until the beginning of the next observing night.

3.5.3.6 Data Reduction Software

3.5.3.6.1 Quick pipeline

The quick pipeline mode shall be operative at first light, providing the following main features:

3.5.3.6.1.1 Dark current subtraction

Dark current frame shall be scaled to the real integration time and be subtracted from the flat field images.

3.5.3.6.1.2 Flatfielding

By dividing the science image through a normalized flatfield image, the sensitivity variations across the detector shall be corrected.

3.5.3.6.1.3 Bad pixel correction

The bad pixel values have to be replaced by a representative count level determined from good pixels in the local neighborhood. The defect pixels shall be flagged in a bad pixel mask by a value 1, whereas the position of good pixels shall be indicated by 0.

3.5.3.6.1.4 Raw sky modeling

The high background from the environment and the sky, with additional temporal and spatial variability of the latter, produce the main background signal. A fast computing of sky modeling shall be computed and it shall be subtracted later from the science images.

3.5.3.6.1.5 Shift and align

Since the images will be shifted by the dithering offsets, they shall have to be aligned prior to the summation.

3.5.3.6.1.6 Fast Astrometry

The quicklook should provide the possibility to make a fast (raw) astrometry of the images.

3.5.3.6.2 Science pipeline

The following tasks should be provided after first light by the science pipeline mode, but the software team will try to have some of them ready at first light.

3.5.3.6.2.1 Master calibration frames

The science pipeline shall compute, maintain and update a series of master calibration frames (darks, flats, skys, hot/bad pixels masks) to provide a basic instrumental signature removal for the *quick* pipeline.

3.5.3.6.2.2 Dark current substraction

Dark current frame shall be scaled to the real integration time and subtracted from the science image.

3.5.3.6.2.3 Flatfielding correction

The pipeline shall divide the science image through a normalized flatfield image to correct the sensitivity variations across the detector.

3.5.3.6.2.4 Bad/hot pixel removal

The bad pixel values (dead, hot and cold pixels) shall be replaced by a representative count level.

3.5.3.6.2.5 Fringe correction

It is not clear that PANIC will have fringes, but in case it has, they should be removed by the pipeline. Fringing correction should be considered at the commissioning stage.

3.5.3.6.2.6 Cosmic rays removal

When present, the cosmic rays shall be removed using a suitable algorithm.

3.5.3.6.2.7 Sky modeling

The high background from the environment and the sky, with additional temporal and spatial variability of the latter, produce the main background signal. A fast computing of sky modeling shall be computed and it shall be subtracted from the science images.

3.5.3.6.2.8 Shift and align (Dithering and Stacking)

Since the images will be shifted by the dithering offsets, they shall have to be aligned prior to the summation (image stacking). This should be done with choice of several schemes (drizzle, SWARP, MONTAGE, …).

3.5.3.6.2.9 Gap elimination

The detectors will be spaced about 147 pixels on focal plane, so the DRS shall eliminate that gap in the full image when enough frames are taken with the suitable dither offsets.

3.5.3.6.2.10 Scale Modes

The two different pixel scale modes shall be considered into the data reduction software, both quick and science pipeline mode.

3.5.3.6.2.11 Astrometry Requirements

3.5.3.6.2.11.1 Absolute Astrometry

Absolute astrometry accuracy shall be ≤ 0.3 arcsec rms for any processed multi-frame.

3.5.3.6.2.11.2 Relative Astrometry

Differential astrometry accuracy shall be ≤ 0.1 arcsec rms for any processed multi-frame.

3.5.3.6.2.11.3 World Coordinate System (WCS)

Final astrometry calibration from the catalogue with an appropriate and agreed World Coordinate System (WCS) shall be written in all FITS headers.

3.5.3.6.2.12 Photometric Requirements

3.5.3.6.2.12.1 Absolute Photometric in J, H, Ks

Absolute photometric accuracy should be ≤ 0.02 mag in J, H, K_s bands with pixel size of 0.25 arcsec and (0.04 mag with pixel size of 0.45 arcsec. It will depend on the quality of the input data.

3.5.3.6.2.12.2 Absolute Photometric in Y,z

Absolute photometric accuracy should be (0.03 mag in Y, z bands with pixel size of 0.25 arcsec and (0.05 mag with pixel size of 0.45 arcsec. It will depend on the quality of the input data.

3.5.3.6.2.13 Ghosts

The reduction pipeline shall remove the ghost images created the different filters. To do that, it will be necessary that they are characterized.

3.5.3.6.2.14 Field distortion

The reduction pipeline shall correct the field distortion. To do that, it will be necessary that it is characterized. The corrected images shall be suitable for mosaicing.

3.5.3.6.2.15 Image stability

The reduction pipeline shall correct the image motion by the instrument during an exposure run. To do that, it will be necessary that it is previously characterized.

3.5.3.6.2.16 Catalog generation

The pipeline shall provide a basic catalogue generation including astrometric, photometric, shape and data quality information.

3.5.3.6.3 Hardware Requirements

The DRS should run on a fast system based on Linux PC, with multi-CPU, at least 16-32 GByte of RAM and using disk RAID arrays for local storage with at least 4 TB of capacity for about 30 full operation nights.

3.5.3.7 Data Collection And Data Rates Requirements

3.5.3.7.1 Data volume

PANIC control system shall be able to handle an average data volume of 100GBytes per night, and a peak of 200GByte per night.

3.5.3.7.2 Data storage

3.5.3.7.2.1 Disk

The data should be copied to the data reduction system from the data acquisition computer. The data reduction system should have a minimum total capacity of 4 TeraBytes (about 30 full operation nights).

3.5.3.7.2.2 Access

Raw data, monitor data, calibration data, and images shall be easily accessible to the users for copy to DVD , USB disk or any other removable supports.

3.5.3.7.3 Delivering format

FITS shall be the default format for delivering the results to the scientific community, so both raw and final data shall be FITS files.

3.5.3.7.3.1 FITS headers

One separate document shall specify contents of FITS headers. The CAHA FITS document of Mr. Roeser (MPIA) shall be taken into account.

3.5.3.7.4 Saving Modes

Data files shall at least not exceed the 2 Gbytes size limit, to allow data storage and handling of data also on 32bit-limited file systems. Therefore a configuration shall be available to limit the max. FITS-file size to a proper size and the software shall split larger exposure files into multiple files.

For a single exposure buffer of 125 full size images the storage size as 16bit-data is ≥ 125*32Mbytes = 4000Mbytes = 3.9 Gbytes.

In the fast photometrie mode, a 15 minutes continuous run of 1 kHz of 36*36 pixels the single subwindow alone has 2.2 Gbytes of data; when stored together with a second window of another detector channel area as sky saving, it is already 4.4 Gbytes.

3.5.3.7.4.1 Data type size

Single images are in GEIRS always the correlated result of 1, 2 or more single frames, which are based first on a reset and then read-out non-destructive.

An integral image is the summation of 1 or more single images acquired in the same exposure sequence.

GEIRS

- shall write an integral image of all selected single images of the exposure. The resulting depth will be stored at least as 32bit data type.
- shall write single images as FITS standard BITPIX=16, which is a signed 16bit data type. Because there is no unsigned 16bit format in FITS available, it involves using the FITS keywords BZERO=32768.0 and BSCALE=1.0 according to the equation

  real-value = fits-value * BSCALE + BZERO.

Data types shall be selected in a way to minimize the needed storage space.

The BITPIX=16 format is not 100 percent data type safe for a double correlated image: Normally the subtraction of a 16bit-unsigned reset-frame from the 16bit-unsigned integrated-frame results in an unsigned 16bit. But it might happen by bad pixels or very short images or integrations of less then the noise level or strange first-reset images, that the single image might have already some negative results.

This problem should be solved either by adapting BZERO, if the range of minimum and maximum is still in the range of 16bit, or by storing the data in a data type of 32bit width.

3.5.3.7.4.2 File structure

GEIRS shall store an exposure, independent of single image or integral image saving, in a single FITS file.

But PANIC will have 32 Mbytes or 64 Mbytes of data per full detector-array field and should ensure that the resulting file sizes does not get too large to handle. GEIRS shall allow to configure the maximal size of a data-file (e.g. 1 GByte-size limit) and split larger exposure results into multiple files.

The preferred default file structure shall be the integral images of each detector stored as distinguished image extensions into a single multi extensions FITS-file format. But this implies proper quality in all single images without artefacts in one of them.

On request, it shall also allow to store the exposure image(s) into single FITS files or FITS cubes (FITS files with NAXIS > 2).

GEIRS shall write

– single extended FITS file in the multiple extensions format (MEF):

  Each single or integral image is written in a single FITS header-data-unit (HDU). Each extension has its own FITS-header, but might inherit the primary FITS header. This allows to add any count of HDUs to the file. The order of the written HDUs are the same like above:

  x*y-HDU, window, detector, time

– single standard FITS-file with 2, 3, 4 or 5 dimensions (axis):

  x * y [* windows-of-identical-size] [* detector] [* time]

  In case of multiple windows of different sizes, multiple FITS-files are created, each of the according window size x * y [* detector] [* time].

– as special case the original raw-data, as buffered in the shared memory, can be dumped directly into a '<name>.dump' file. An header file is also be written in the FITS-header format as '<name>.info'-file.

All these file structures have the advantage of easy writing the FITS file immediately and parallel to the incoming data, arriving in the same order.

In a FITS-file should only be data of a single exposure. That means, dithered data will not be in a single FITS-file, because each dithering is a new tele-position and a new exposure.

3.5.3.7.5 Archive and VO

3.5.3.7.5.1 Archiving

Following Scientific Advisor Committee (SAC) recommendations, the PANIC data should be compliant with the future CAHA Archive, implementing when the Archive is defined, the necessary modules to support it and to allow data retrieval and data queries in concordance with the pipeline outputs.

3.5.3.7.5.2 Virtual Observatory

The PANIC Archive should be VO-compliant.

3.5.3.7.5.2.1 VO data model

A data model for PANIC should be defined for VO integration.

3.5.3.8 Caha Sw Requirements

The section 3.6.3 about CAHA technical requirements includes some specific requirements concerning the software. So, they complete the software requirements. However, some of those software requirements should be revised after PDR.

3.5.4 Design Report

The software architecture of PANIC shall be divided in two main packages: the Instrument Control Software (ICS) and the Data Handling Software (DHS). Each one is composed as follows:

3.5.4.1 Instrument Control Software

- **GEIRS**: It is an already existing GEneral InfraRed instrument Software once intended to control all MPIA/CAHA in-house infrared cameras. It shall control all PANIC hardware like in other CAHA instruments and the telescope interface. The main part shall be the control of the detector and the data readout.
- **Observation Tool (OT)**: This software package will allow high level control of the instrument based on a GUI. This tool shall provide a higher level of abstraction to the user in order to allow an easier observation procedure. It will provide a set of predefined observation templates with some parameters to be set by the user. The user can choose some of these templates, define his/her own observation template or control directly the observation using high/medium level commands.

3.5.4.2 Data Handling Software

- **Data Classifier (DC)**: It will be composed of two main tasks, the data receiver and the data collector. The aim of these packages is to inspect the FITS headers and classify the data files using a set of predefined rules. In this way, the classified data will be processed more easily by the quicklook tool and the on/off-line pipeline.
- **Quicklook Tool (QT)**: This tool shall provide a fast preview of the data being acquired by GEIRS. It will perform a rough and ready data reduction to the observation at the telescope and shall allow to check that the right objects are being observed. This package will use some parts of the pipeline procedures (quick reduction mode).
- **Data Reduction Software (DRS)**: The data produced by the observation run shall be calibrated and processed in a on/off-line (TBC) pipeline. Automatic pipeline reduction of the instrument data is predicated on the assumption of a well defined set of observing protocols that supply the relevant meta-data of the pipeline reduction system. These meta-data should be provided by the Observation Tool to GEIRS to be saved in FITS headers. Besides, the pipeline will not only delivered a product with scientific quality product but also provides feedback on the health of the camera.

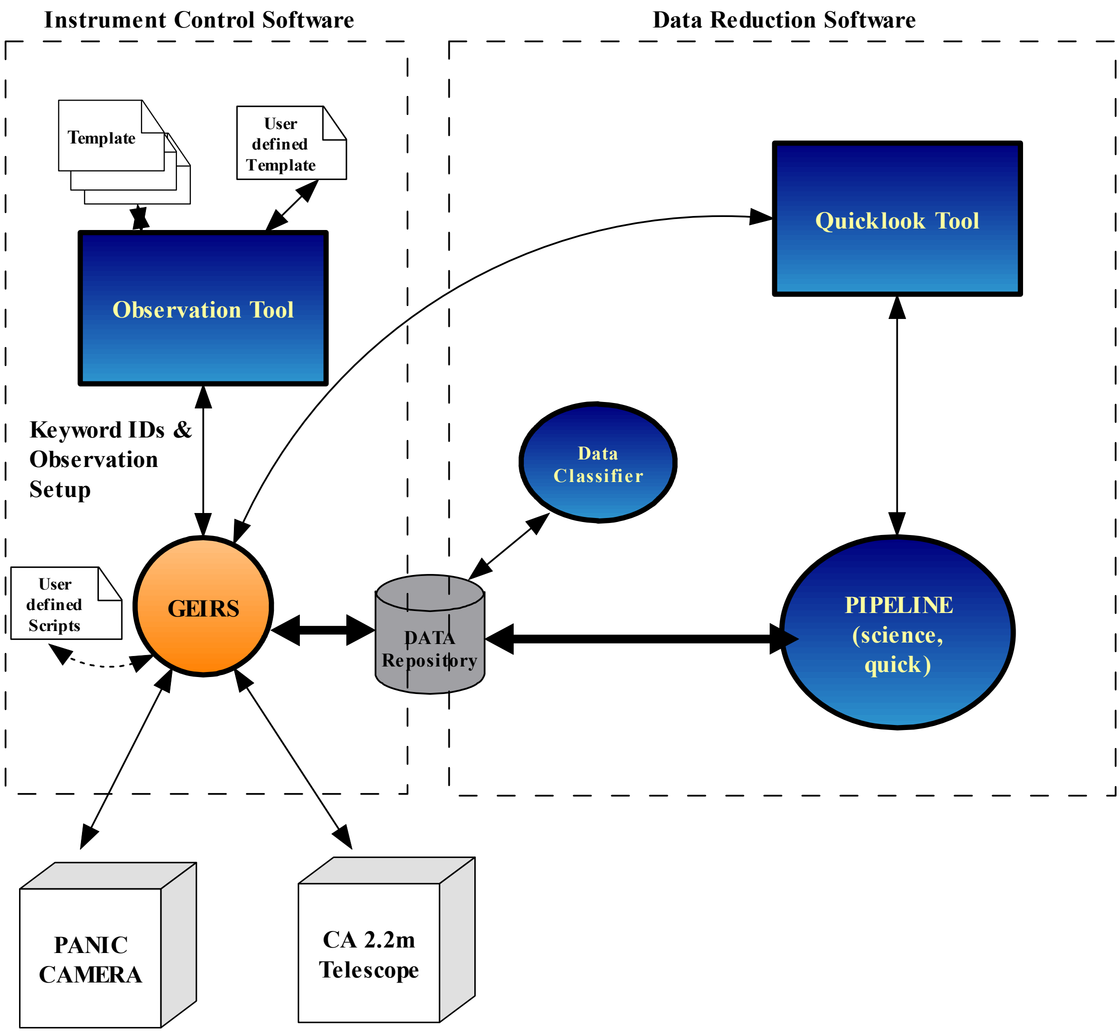

Figure 3.5.4-1 Software architecture

3.5.4.3 Network Layout

In regard the layout of the main parts of the system, there will be tree main areas properly network connected: the telescope are where the instrument will be, the computer room next to the telescope area, and the control room that is where the user will handle the instrument using a Thin-Terminal connected to the ICS workstation. The data reduction workstation will also be in the Control Room with a fast network link to the ICS data storage unit. A general overview of the network layout is described in the next figure:

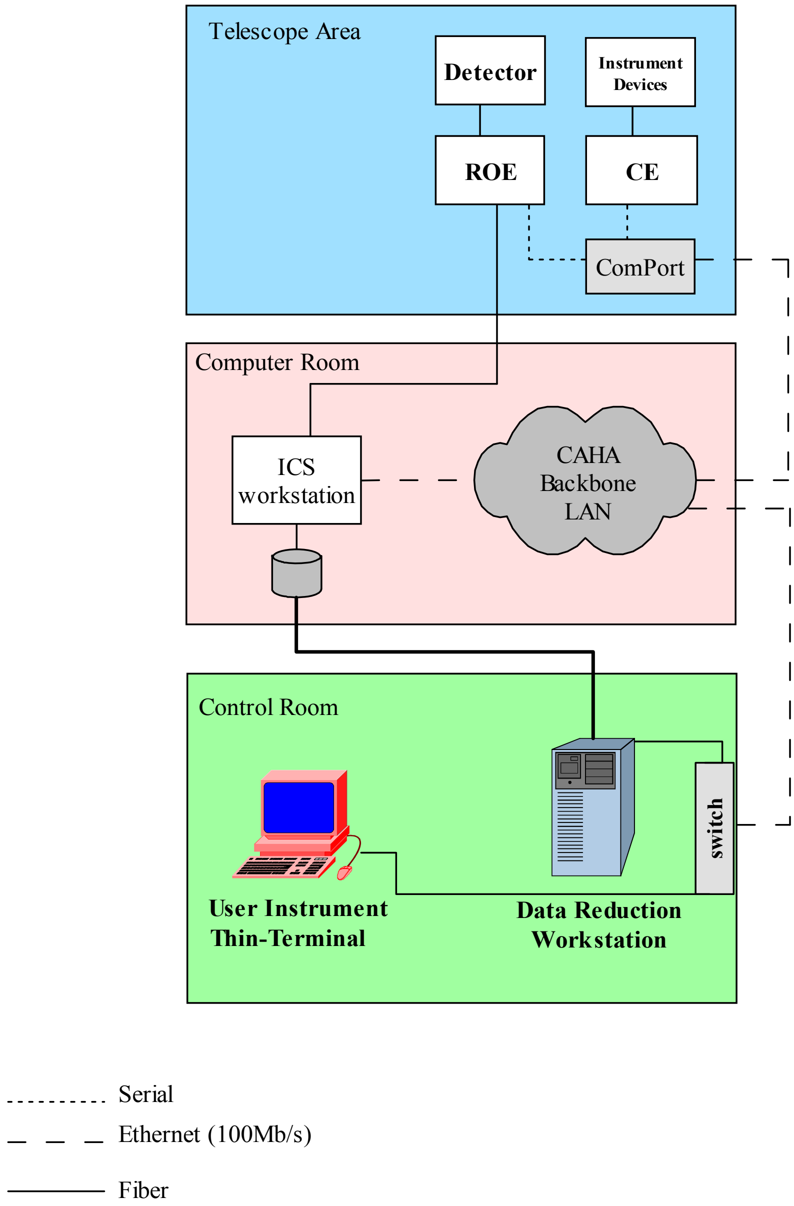

Figure 3.5.4-2 Network layout

3.5.4.4 Computer Architecture

The PANIC software will be divided in two main systems, one for the Instrument Control Software and other for the Data Reduction Software. Both systems will be Linux-PC based with multiple-CPU, enough RAM and a fast network links.

For the data storage a system based on local disk RAID arrays to prevent data losses, as well as a DAT/DVD for backup, should be installed by Calar Alto staff as archive server.

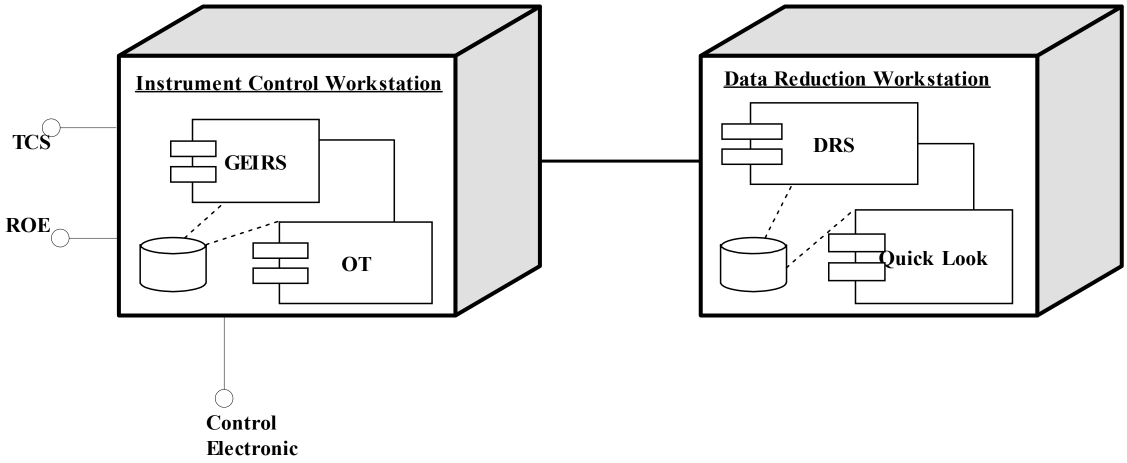

Figure 3.5.4-3 Computer Architecture

3.5.4.5 GEIRS Design description

For general GEIRS description see the manual of Omega2000 (AD1), or other IR-instrument manuals using GEIRS.

This description concentrates on the specific functionality of PANIC and its requirements.

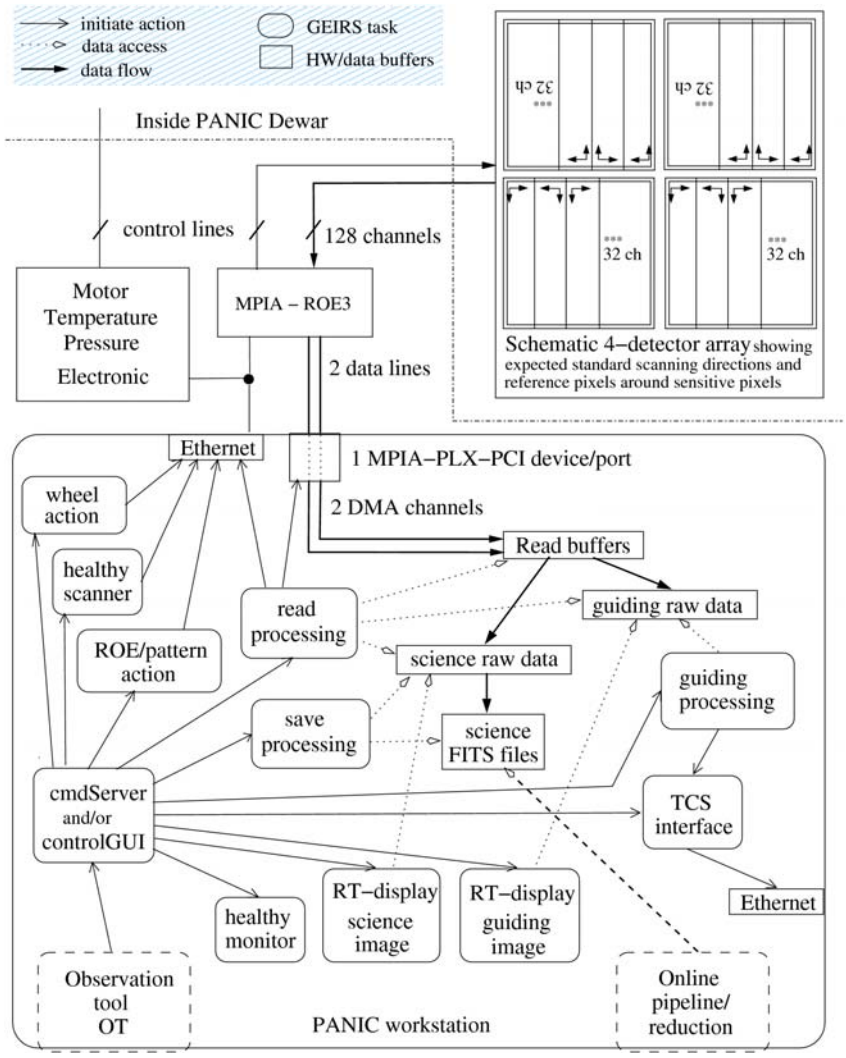

Figure 3.5.4-4 Overview of the PANIC control software tasks, the access to data, the data flow, the connection to the hardware and to Observation Tool and to the on-line pipeline reduction software

3.5.4.5.1 GEIRS integration time and data specifications

GEIRS most important expressions and how they shall be interpreted are

● ***exposure*** is the result of a single "start read-out" command sent to the ROE. This will result in the execution of cycle-repeat times of cycle-type executions by the ROE.

● ***exposure time*** is the sum of the pixel integration time in all cycle-types done as result of a single "start readout" command sent to the ROE.

● ***integration type*** for the HAWAII2-RG, this is always the 'integration-while-read' type (IWR). To start with a well defined detector state (new IWR cycle), the detector is normally reset pixel by pixel or line by line or in the 2RG eventually also frame wise.

● ***integration time*** is the time that each pixel of a single cycle type image is exposed to photons. Because of the IWR property of the detector this is

for single correlated images:

the time between the reset of the pixel and the readout of the pixel

for double correlated images:

the time between the 1st readout and the 2nd readout of the pixel
for multiple correlated images:
the time between the 1st readout and the correlated readout of the pixel
(different behaviour for 'msr' and 'sar') (see AD1).

● ***cycle type*** (also called ***read-out cycle/mode/type***) is a specific read-out pattern of clocking logic. The result of a single read-out is normally a single image, but the read-out raw-data might consist of multiple frames (exception 'msr', which has multiple images as result of a read-out cycle).

● ***cycle time*** is the time of the total cycle type pattern. It is always larger or equal to the integration time.

● ***single correlated image*** means that the read-out type produces no time-correlated read-out frames, but only a single read-out frame (normally after a detector reset), which still contains typical detector properties.

● **double or multiple correlated image**

means that the read-out type produces two or more read-out frames correlated in time, which are used to get rid of the pixel dependent time and offset properties. Only amplification dependencies of the pixels and imaging dependencies of the instrument or photonic sources as well as some kind of noise remain in the correlated images.

3.5.4.5.2 Read-out with high speed

The detector shall be clocked at minimum speed with 100kHz pixel clock rate.

Additionally it shall be clocked with a faster maximal speed, because a 1 kHz image rate for a sub-window of the size of about 35x35 pixels is required in [Ad2].

To prevent edge effects to the rest of the detector the pixel count for this requirement is increased by an additional pixel read around the wanted sub-window (36x36). In the multi-channel mode of the detector it should be possible to reduce the necessary reading time by centering the sub-window on the edge between 2 channels. The table below summarizes some expected image rates for the different cycle read types.

The fast sub-window 36*36 results in a maximal data rate out of the ROE of about 200Mbytes/sec to 250Mbytes/sec in the mean in the multichannel read-out mode:

1 MHz * 128 channels * 16bit – (2048 line-resets ≤ 10 microseconds) ≈ 250 Mbytes/sec.

The science data to store in that small sub-window case will be much less (~2 Mbytes/sec), if there is no interest at the additional data of the other detectors or channels in terms of cheap sky references.

A maximum of 250 Mbytes/sec shall be in principle achievable as read-out speed as first tests of the MPIA-PLX-interface in a 64bit/66MHz PCI-slot showed, which is the data interface for the ROE3, using data read tests from a data generator on the interface itself.

Fast small single frames or data units should be possible at maximal speed of about 10kHz frame rate over each of the 2 DMA-channels of the PLX-board in parallel (the interrupt reaction speed of the low-level driver itself).

pixel clock	cycle type (efficiency between single images)	32 channel output/detector		1 channel output/.detector	
		100 kHz	**1 MHz**	**100 kHz**	**1 MHz**
full size	single frame-rate	0.74 Hz	7.14 Hz	0.024 Hz	0.24 Hz
subwin 36x36 inside area of a single channel	single frame-rate	75.2 Hz	588 Hz	75.2 Hz	588 Hz
	lir (ieff=100%)	37.6 Hz	294 Hz	37.6 Hz	294 Hz
	dcr (ieff>=50%)	37.6 Hz	294 Hz	37.6 Hz	294 Hz
	msr* (i eff=100%)	75.2 Hz	588 Hz	75.2 Hz	588 Hz
subwin 36x36 centered on the edge between 2 channels	single frame-rate	139 Hz	1000 Hz	-	-
	lir (ieff=100%)	69.4 Hz	500 Hz	-	-
	dcr (ieff>=50%)	69.4 Hz	500 Hz	-	-
	msr* (ieff=100%)	139 Hz	1000 Hz	-	-

* msr looses 1 frame-time at each cycle-restart in a cycle-repeat loop

Table 3.5-1 Expected image rates compared for the subwindow size of 36x36 read pixels asked for in [AD 2]

3.5.4.5.3 Read noise reduction

For small narrow band filter observations of faint stars a read noise reduction with non destructive read-outs should be available. The table below lists the expected read noise and integration times, based on Rockwell's general specification of the Hawaii-2RG, depending on the correlation of nondestructive reads.

pixel clock	multi correlated reads [n]	single pixel multi samples (~1MHz)	Expected expected Read Noise (e-)	Overhead Read min. exp. time* (sec)	Usage
100 kHz	1	1	~15	~1.35	high background/bright objects
100 kHz	1	16	~4	~1.5	medium background/ medium-bright objects Exposure ~10-30s
100 kHz	16	16	~1.5	~26.4	low background/faint objects/ narrow band filters Exposure >30s
~1 MHz	1	1	~50	~0.14	high background/very bright objects
~1 MHz	1	16	~12	~0.44	better to use a 100 kHz read
~1 MHz	16	16	~3	~7.0	not recommended, use 100 kHz read

Table 3.5-2 Table with expected read noise suppression, in case of limitation by read noise instead of background.

3.5.4.5.4 Guiding

Guiding requirements shall be supported by the development of the ROE and the pattern development for the read-out modes. The extensions of the Hawaii-2RG allow to use 2 nested clockings without skipping needs and the possibility to reset only a part of the detector. But the clocking is not parallel and the photon sensitive pixels are accessed by both clocks.

The 2 nested clocked data output from the detector shall be splitted by GEIRS into 2 independent data streams.

The guiding processing part should be implemented after commissioning of PANIC itself, but shall be foreseen and the ROE shall be in principle prepared for these nested clocking patterns, and first tests shall be done.
Software modules for CCD cameras already exist to calculate the centroid of the guide star (e.g. LAICA).

always 100 kHz clocking	# of wins	each of win-size [x*y]	total pixel count	maximal guide-win-rate	minimal full-science time	fix win-rate	minimal full-science time
				wins done each full-line		wins done at fix rate	
full frame size	-	-	-	-	1.31 s	-	-
+ single win	1	8*8	64	418 Hz	4.9 s	10 Hz	1.34 s
+ single win	1	8*8	64	418 Hz	4.9 s	70 Hz	1.5 s
+ multi wins	2	8*8	128	329 Hz	6.2 s	70 Hz	1.6 s
+ multi wins	16	8*8	1024	83 Hz	24.6 s	70 Hz	7.3 s
+ single win	1	36*36	1296	68 Hz	30.1 s	50 Hz	4.55 s
+ single win	1	36*36	1296	68 Hz	30.1 s	10 Hz	1.53 s
+ multi wins	4	36*36	5184	18.7 Hz	109.8 s	10 Hz	2.8 s
+ multi wins	8	36*36	10368	9.5 Hz	215.9 s	4 Hz	2.3 s

Table 3.5-3 Some estimated timings for (multiple) guiding windows embedded between normal full-frame read-out lines

3.5.4.5.5 Parts

- GEIRS source package
- GEIRS control configuration files for PANIC
- GEIRS ROE engineering configuration files for PANIC
- GEIRS FITS configuration files for PANIC

- PANIC read-out electronic including fibers and cables (serial line (NPORT terminal server) and data lines) or running PLX data generator or running in data simulation.
- MPIA-PLX-PCI-64bit/66MHz interface, PLX driver extensions running in multi-threaded code, or running in data simulation.
- Linux-PC system to run GEIRS (multiple-CPUs, enough RAM)
- Connection to PANIC-instrument IP-network

Expected additional software: gnuplot X(for installation: g++, X, subversion). All this is available in the standard openSuSE distribution.

3.5.4.6 Observation Tool description

3.5.4.6.1 Purpose

The aim of the OT is to provide a higher abstraction level for the users of PANIC at the observatory, providing easier observation procedures and a set of extra keywords to be saved on FITS headers to be used by the data reduction software (DRS).

The OT will allow the astronomical users to specify the observations in a user-friendly way, avoiding to remember large commands or building complicated scripts. They should choose a predefined observing template or build their own observation template using high level commands to PANIC. It is intended to be the sole instrument user interface (at the telescope as well as remotely), capable of configuring and sequencing instrument and telescope motions and of integrating the data processing pipeline with data acquisition. Once a observation is defined, it will be executed by astronomers or/and operators (users) when they believe that the conditions are most favourable.

3.5.4.6.2 Observing strategies

A typical observing strategy carried out with an infrared camera like PANIC is shown bellow:

1. **Instrument setup**: this includes read mode (RRR, CDR, Fast …), saving modes (FITS cubes, individual, integrated,…), saving paths, filenames, log files, etc
2. **Darks**: before starting observations we take dark images using several integration times and coadds.
3. **Twilight/dome flat-fields**: we take flat images for each filter that we are going to use during our observation.
4. **Focus**: we measure the focus in one filter (for the other filters the telescope computes the focus using the programmed offsets). Usually, the GUI provides different fields for focus, and the user select a field close to the zenith. During the night we can check the seeing and repeat the focus procedure if needed.
5. **Calibration stars**: That loads the standard object list and observes the standard stars in each filter we are going to use. Then a dithering sequence for these observations (number of positions and offsets) is selected.
6. **Target fields**: That loads project objects list and perform an observation of each field with each of the desired filters and then a dithering sequence for these observations (number of positions and offsets) is selected. Each filter and field may require a different observing setup, like exposition time, coadds or dithering sequence.

7. **Twilight/dome flat-fields**: At the end of the night, we can take flats for each of the filter that have been used during our observation

8. **Data storage:** The data should be copied from the data repository to a removable device.

3.5.4.6.3 Data Entities

In order to get a set of accurate and unambiguous PANIC observation programs that allow to follow the general observing strategies described before, we consider a hierarchical structure of the observation program with the following main entities shown in the next figure:

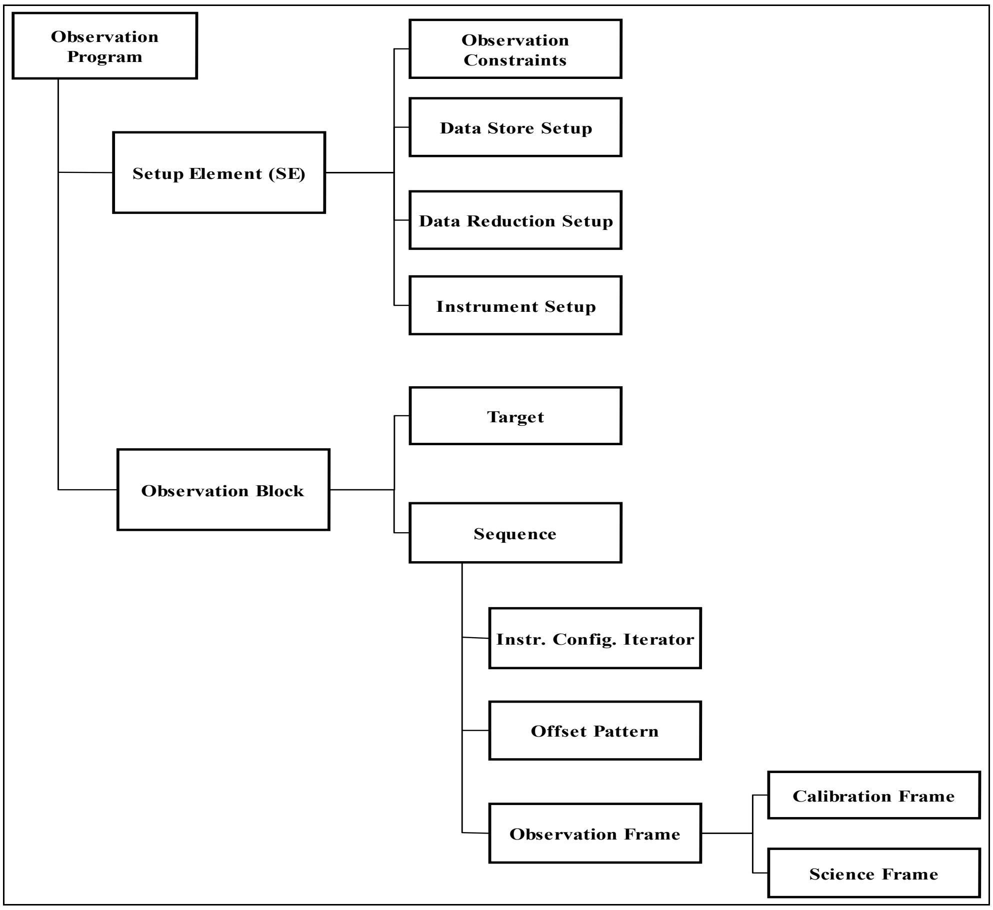

Figure 3.5.4-5 Data Entities

where each entity is defined as follow:

- **Observation Program**: An Observation Program (OP) is defined as a full set of observations that the observer sets up to achieve the scientific goal. It contains most of the information associated with one proposal. Each OP consists of multiple Setup Elements (SE) and Observation Blocks (at least one). An OP shall be also completed with the following fields:
  - Name of the OP
  - Purpose

  - Name or the PI
  - Institution
  - E-mail
- **Setup Element (SE)**: A SE contains the information associated with one of the following subjects :
  - Observing Constraints:
    - Site quality (sky background, seeing, …)
    - Schedule data (airmass, elevation constraints, …)
  - Data store Setup:
    - File name prefix
    - Save mode (raw, FITS cube, integrated, individual, …)
  - Data reduction Setup
    - Reduction Mode: No reduction | Quick | Science
    - Quicklook display: True | False
  - Instrument Setup
    - Readout mode/cycle type: CDS, LIR, MSR, …
    - Scale Mode: 0.45 arcsec or 0.25 arcsec
    - Frame size : Full, subwindow
    - Integration Time (IT): is the single integration time for a single image result; it is time that each pixel of a single cycle type image is exposed. This parameter is to be optimized for each filter to allow background limited observations.
    - Repeats (cycle repeat count): number of single integration (single images) done. They can be added up in memory before the final single image (with an *exposition time* of *IT*Repeats* seconds) is saved on disk or otherwise they can be saved each single integration individually.
    - Positions (P): number of images with an exposition time of *IT*Repeats* seconds. This parameter determines the total exposition time for the target and the final limiting magnitude of the pointing. *P Positions* images are taken at different dither positions.
    - Number of Exposures (N): Perhaps we need for the same dither position also a repeat of exposures, at least for the shorter wavelengths where we do not need to get often the current sky sampled multiple exposures at the same dither position will be faster then often dithering and more sure than a very long exposure time.

      It is expected, that it should be interesting for a field of acquisition, which has also saturated stars, to be able to do multiple (and perhaps different) exposures for the same position to get different dynamic ranges, and be able to use it for the resulting deep image result.
    - Filter : the selected filter

- **Observation Block:** An Observation Block (OB) is the smallest entity that contains all the information necessary to obtain a "single" observation. The changes to one of the parameters of a OB in a given OP do not affect all OBs of the OP. Each OB consist of :
  - Target
    - Name
    - Type
    - Epoch
    - RA (hr:mm:sec)
    - Dec (dec:arcmin:arcsec)
    - Proper motion
      - RA (milli-arcsec/year)
      - Dec (milli-arcserc/year)
  - Sequence
    - Instrument Configuration Iterator: To perform any complex observations, iterators are required. They are placed into a sequence of an observation and are used to define the series of actions that will be performed to collect the data. It will allow you to change in a single step any configurable attributes of an item. For instance, with an iterator we can set up a series of iteration steps each of which simultaneously changes the selected filter, readout mode, integration time, repeats and positions as defined for a instrument setup.
      - Filter
      - Scale Mode (0.45 arcsec or 0.25 arcsec)
      - Readout mode
      - Integration Time (IT)
      - Repeats (R)
      - Positions (P)
    - Offset Pattern (dithering pattern, mosaic pattern)
      - Number of points
      - Offset (p, q)
    - Observation Frame (dark, sky flat, dome flat, focus seq, science)
      - Number of Exposures (N)

An Observation Program (OP) can be defined using a notation described below . This description aims to show all the possibilities feasible with the OT.

OP::= {Setup_Element} [Target] { Observing_Block}+

Setup_Element::= <Observation_Constraint> | <Instrument_Setup> | <Data_Store_Setup> | < Data_Reduction_Setup>

Observation_Block ::= <Target>{ Sequence }+

Sequence::= [Instrument_Config_Iterator] [Offset_Pattern] <Observation_Frame>

Observation_Frame::= <dark> | <flat> | <focus> | <science>

Flat::= <sky_flat> | <dome_flat>

where

::= meaning "is defined as"

{} is a optional set of elements (0-N),

{}+ is a optional set of elements, but at least one element (1-N),

[] mean single and optional element (0,1)

| meaning "or"

< > angle brackets used to surround obligatory entities

3.5.4.6.4 Workflow

Firstly, the observer shall define the observation program according to his/her scientific program proposal. It can be done on-line or off-line using the OT. After the observer has defined his/her observation program with the OT Editor, it should validate it to ensure that it is compliant with the operational instrument rules, avoiding wrong parameters values or nonsense sequences. Then OT shall generate a script (commands sequence) that shall be sent to GEIRS command server over a socket connection. If these commands are accepted by GEIRS it will execute them and reply to OT about the success or failure of them. So, on the OT side there is a listening event handler that manages the GEIRS reply commands. The OP can also be submitted to the observation repository for a further execution.

The general workflow of the OT is presented in the next figure:

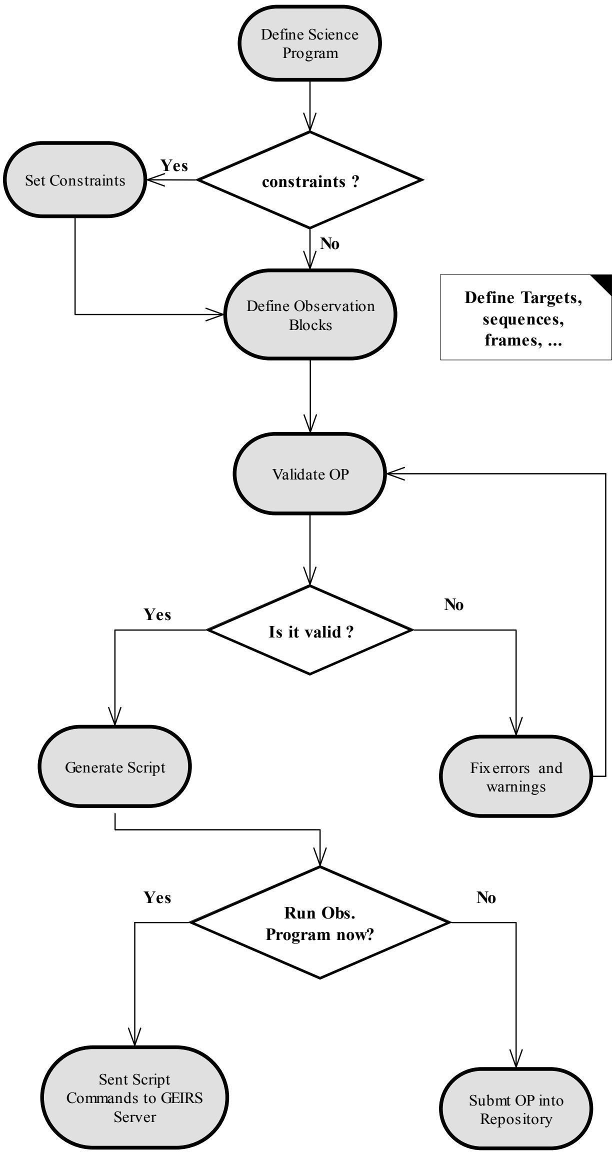

Figure 3.5.4-6 OT Workflow

3.5.4.6.5 The Observation Tool Editor

As a main GUI component, the observation tool editor will be implemented containing three main areas: a button frame on the left side, a navigator area on the middle which shows the components in a hierarchical structure and editors for each observation component on the right side. This seems to be a natural design since a OP has a hierarchical structure. This structure is show in the next figure.

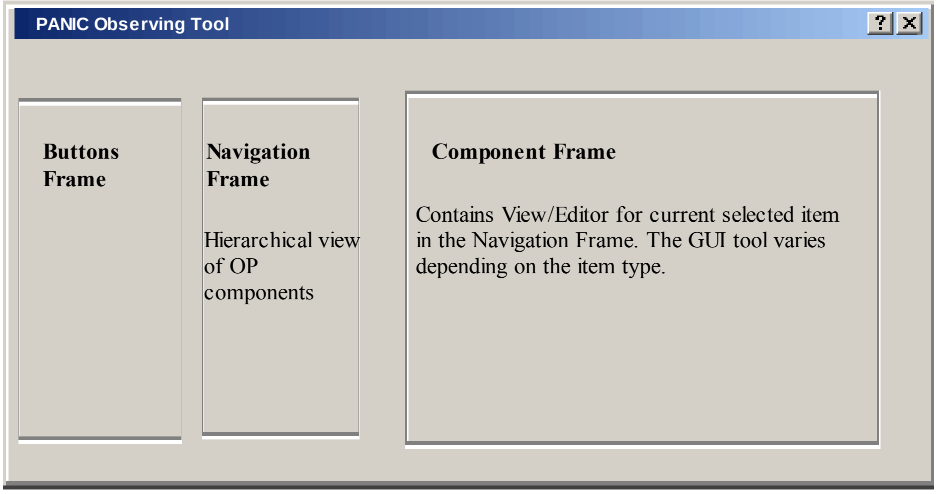

Figure 3.5.4-7 Browser interface Conceptual Diagram

3.5.4.6.6 Programming language and components

The programming language will be the Java language based on the Java Virtual Machine, which has a great deal of power and flexibility. The Observing Tool will extensively use the classes that are part of the JSky (Java Components for Astronomy) Project started at ESO. That tool is freely available for the community.

3.5.4.7 Quicklook description

3.5.4.7.1 Purpose

When observing with infrared instruments, it is often necessary to reduce the images in real-time to adapt to varying conditions and to adopt the correct observing strategy.

The quick-look facility is intended to allow a fast examination of raw frames and pre-processed images. It will be used to visualize sets of images and monitor in real-time the observation. It shall offer a wide variety of graphical resources, as well as preliminary inspection tools specific to the observation mode, such as simple statistics, zooms, cuts, radial profiles, among others.

Therefore a quick-look data reduction mode will be implemented into PANIC DRS, specifically designed to reduce in a fast mode the infrared observations. The quick-pipeline will allow the observer to clean-up the images cosmetically using a set of calibration files (darks, flat fields, etc.), to examine the images in many modes, to compute image quality parameters (FWHM, SNR, …) and to put various images together (in mosaics or shift and add). Furthermore, the quick-look pipeline shall accept data acquired with various observing techniques (dithering, separate sky exposure, etc.).

3.5.4.7.2 Implementation

The quicklook will be based on display tool like SkyCat or DS9. They are freely available and provide a powerful programming interface for our purposes.

3.5.4.8 Data reduction software description

3.5.4.8.1 Purpose

The high background in infrared data must be carefully estimated to retrieve the science information. In imaging mode, the observations are done in *dither* mode, with small offsets around a central position for each exposure, to allow to estimate the sky background variations directly by filtering the images, and separate astronomical from sky signal. Apart from this difficult sky estimation, the frames are recombined with some cross correlation techniques to precisely determine the offsets between the images.

The main role of the Data Reduction Software (DRS) will be this data reduction. For this purpose, an on/off-line pipeline will be considered.

Automatic pipeline reduction of PANIC data is predicated on the assumption of a well-defined set of observing protocols that forward the relevant meta-data to the pipeline reduction system. Besides, the pipeline should not only deliver science-quality products but also provide feedback on the health of the camera and on the overall data quality.

The DRS will have two main operational modes, *quick* and *science*. The *quick operational mode* is used for quick look purposes and for on-site quality control. It will process all raw data sequentially, i.e. as they arrive from the instrument. It produces calibration products and reduced science data, but will usually not obtain the best possible results. This is due to the sequential operation: post observation day-time calibrations are not available during night-time.

The *science operational mode* becomes possible when all data of a night including the associated day-time and twilight calibrations have been collected. Then the calibration data are sorted and assessed independently of their timestamp. The best possible master calibration data are created. Their quality is checked. They are finally applied to the science data of a night.

In this report, both the first after light and after first light requirements will be considered for the preliminary design description, however, for first light only OT and quicklook shall be operative.

3.5.4.8.2 Data Flow

The next figure shows how the data flows in the system from the ROE to the data repository after the data processing into the DRS. The data quickly reduced will be able to show in the quicklook display tool. The main tasks of the data receiver and the data collector are detailed bellow:

<u>Data Receiver</u>:

1. Detect when new data arrive from the data acquisition system (ICS)
2. Inspect the data header, classify the data and put it into the corresponding directory (calib, science, tests, …). Some new keywords may be inserted into the header and/or file conversion could be done (Multi extension FITS cubes to single FITS or whatever).
3. If quicklook is activated by the user, run the quick reduction mode pipeline with the new science data as they arrive.
4. Provide the new data (calib and science) to the science reduction mode pipeline.
5. Remove periodically the old quick reduced data and temporary files created.

<u>Data Collector</u>:

1. Detect when new quick reduced data are produced and send them to the quicklook display tool and save them into the quick data temporary directory.

2. Detect when new science reduced data are produced and save in the data repository in the corresponding directory for data delivery.
3. If data archiving is working in CA, insert new data (raw and reduced) into the archive.

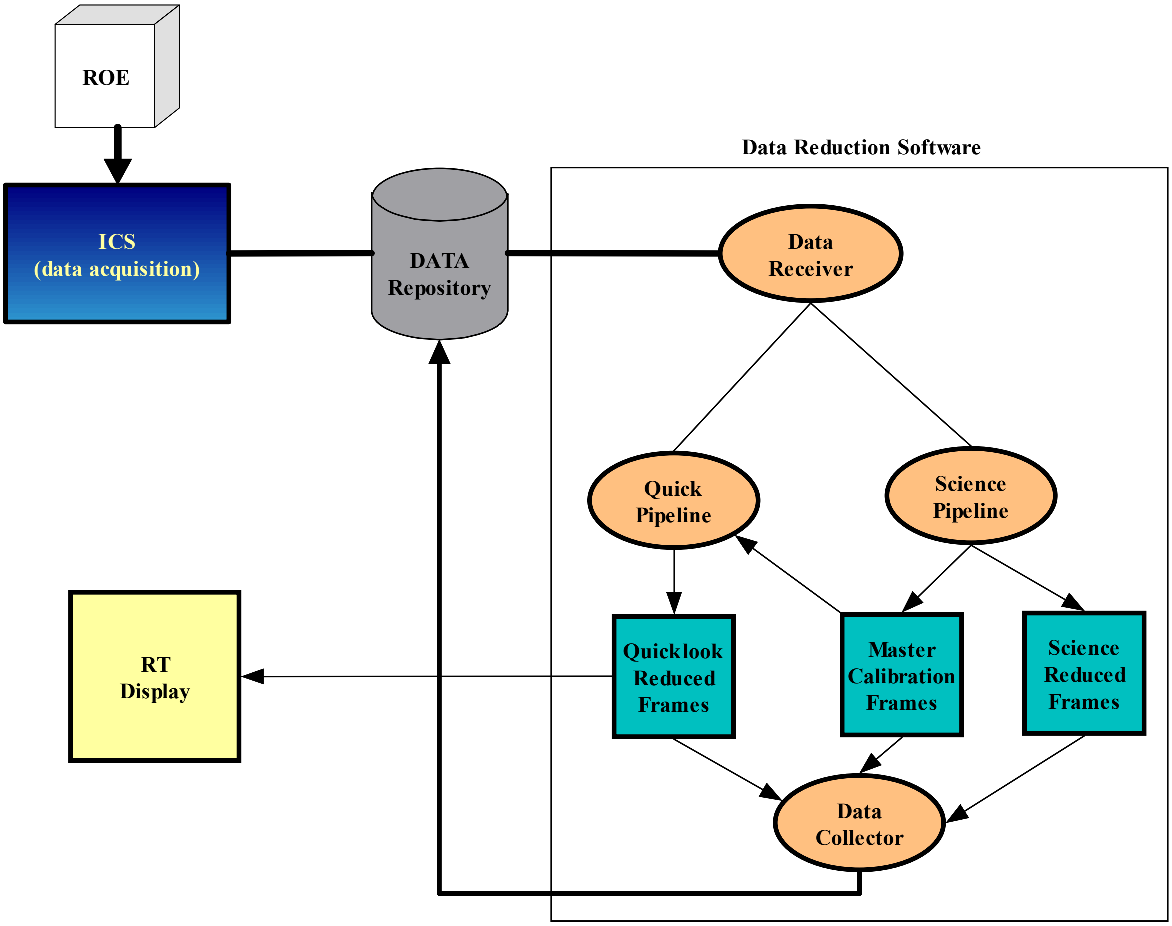

Figure 3.5.4-8 Data flow

3.5.4.8.3 General data reduction schemes

3.5.4.8.3.1 Main steps

The standard IR image reduction process involves several steps from the raw frames to the reduced image, which contains the calibrated astronomical signal. The data reduction software will implement the following processes:

1. Detector calibration, for instrument signature removal
   a. Linearity correction
   b. Dark subtraction
   c. Flatfield division
   d. Bad pixel correction mask frame

2. Fringing correction
3. Sky modelling and extraction
4. Shift and align
5. Electronic Crosstalk correction
6. Optical ghosts removal
7. Field distortion correction
8. Mosaicing
9. Astrometry
10. Photometry

3.5.4.8.3.1.1 Detector Calibration:

It includes the following processing to remove the detector signature:

1. **Linearity correction:** The data obtained from NIR arrays may be strongly non-linear, although the linearity curve can be derived through observations of a stable "light source" for a range of exposure times (e.g. a sequence of dome flats). Potentially, because each PANIC detector is read out in 32 parallel channels (64x2048 pixels each), 32 separate linearity correction functions may be needed for each detector. At the moment of writing this document we do not know what effect non-linearity will have, but in case a noticeable effect exists (>1%), the suitable correction should be implemented into the GEIRS correlated image result-function due the readout mode; that is, the resulting image pixel we get as raw image pixel is already a subtraction of (pixel(integration-frame)-pixel(reset-frame)), where depending from the light the reset-frame might already have a significant level, which means we might have a pixel value of 100 as result of (43100-43000) or as result of (1100-1000).
2. **Dark subtraction** from target and calibration frames. Darks will be routinely computed from the daily observations, by combining as many darks as are generally available for each exposure time and readout mode. If a particular combination is not available the nearest suitable calibration dark frame from nearby nights will be used instead. If this still does not produce all the required darks to process a night's data, a suitable combination of closely related dark frames will be created and used instead.
3. **Flatfield division**, in order to correct for pixel response non-uniformity in the detector. Twilight or dome flatfields can be routinely taken from the daily observations, by combining as many flats as are generally available for each time and readout mode. Also weekly flatfield sequences can be taken, dark corrected and then stacked to form intermediate master flats.
4. **Bad Pixel Correction:** The bad pixel values (dead, hot or cold pixels) will be replaced by a representative count level determined from good pixels in the local neighbourhood. The defect pixels will be marked in a bad pixel mask by a value 1, whereas the position of good pixels shall be indicated by 0.

3.5.4.8.3.1.2 Fringing

At the time of writing, we have no way of knowing what effect fringing will have on data from PANIC. Some infrared detectors are badly affected by it and some are not affected at all (WFCAM). It appears to depend upon the final f-ratio of the optical system, the properties of the top layer of material in the detectors and the presence or not of atmospheric emission lines in a particular waveband. It is also true that a background sky correction may remove any fringing that is present if the sky estimate is sufficiently local both spatially and temporally.

First we note that fringing is an additive effect, so if removed as part of a procedure that used night sky data as a flat field source, this would introduce a systematic error in the photometry. To perform sky fringe removal effectively requires the flat fielding to be decoupled from the defringing by, for example, using twilight sky exposures to construct the flat-field frames, where the contribution from sky emission lines is negligible.

The basic method to remove fringing from images is to fit the fringe pattern from a library fringe frame to that of an observation frame by iteratively minimising the median absolute deviation of the difference of the two images. This should work in principle so long as the fringe pattern is stable with time. However, experience shows that this is not the case. The flux of the emission lines that lead to the fringe patterns can vary in a complex temporal manner which means the relative intensity of parts of the fringe pattern will also alter with time.

The way to get around this problem is to use data from the night in question to form mean fringe frames rather than to rely on a library frame which may be days or even weeks old. As this can only be done once the whole night of data has been at least partially reduced, this method of fringe correction will only be possible in the science pipeline.

3.5.4.8.3.1.3 Sky modelling and extraction

The principle of the sky extraction is the following: Several dithered images are stacked in the pixel coordinate system, i.e., the values in the third dimension of the image cube all result from the same detector pixel. Due to the small telescope offsets in between the image sequence, the astronomical objects are slightly shifted from image to image. Thus, the pixel columns, the values for the same pixel in the different images, contain mostly sky signals even at the position of a stellar object in one image. A suitable value for the actual sky level in such a pixel column is the median. The median is a less sensitive function concerning outliers than the average and is thus less influenced by a high star signal. An accurate sky frame is obtained by determining the median for each pixel column of the image. Besides a real median process, other techniques can be applied to extract the best local sky value for a pixel.

3.5.4.8.3.1.4 Shift and align

After the background contribution has been removed and the individual image is fully reduced, all frames belonging to the same pointing have to be added up in order to create a master image with an improved signal-to-noise ratio. When summing N images with a given SNR of an object, the signal-to-noise ratio of the superimposed frame will be improved by a factor $\sqrt{N}$. For the detection of very faint objects, a large number of images has to be co-added in order to reach a sufficiently high SNR.
Since the images were taken at slightly different positions, shifted by the dithering offsets, they have to be aligned prior to the summation. The approximate offsets can be calculated from the observing position stored in the image header or directly from the

known dither pattern used. For high quality images, the alignment precision should be on a sub-pixel scale, which is beyond the pointing accuracy of the telescope. The exact shifts of the images can be obtained by matching the positions of corresponding point sources in the frames. Once the offsets are known, the frames can be superimposed to the master sum frame in different ways. Well sampled images can just be summed with integer pixel shifts, whereas in the under-sampled case a more elaborate summation process, e.g., the DRIZZLE [RD7] algorithm for the PSF reconstruction might be more appropriate. Both methods will be implemented in the pipeline system.

The summation process also offers the possibility to effectively eliminate cosmic ray events in the data. Since cosmics usually affect individual pixels and are statistically distributed in the different images, they can be removed by filtering high pixel count levels that are detected in a single frame only.

3.5.4.8.3.1.5 Electronic Crosstalk correction

Images from one detector channel may produce secondary images (ghosts) on other channels either positive or negative in sign and may also even cross from one detector to another. In a stable environment, it is feasible to measure the contribution of crosstalk from one channel to another by using bright point-like sources, and thereby define a comprehensive crosstalk matrix $C_{j,k}$. Since this is environment specific, determining the final form of this matrix will be one of the commissioning tasks, although earlier laboratory-based measurements will be used to characterise its likely impact and to investigate ways of minimising the effect. Providing the cross-talk terms are small (i.e. <1%, the most likely scenario), then the following simple single-pass additive correction scheme will be used to correct for this problem,

$$I'_j=I_j-\sum_{k\neq j}I_jC_{j,k}$$

where I_j is the observed frame and I'_j the corrected version.

3.5.4.8.3.1.6 Optical ghosts removal

At the time of writing this document, we have no way of knowing what effect ghost images created by the different filters will have on the data from PANIC. However, if they are present and they shall be characterized and available to the data reduction pipeline to remove them.

3.5.4.8.3.1.7 Field distortion correction

Due the large field of view of PANIC, it is supposed that a field distortion correction will be needed. To do that is necessary the field distortion created by the optics is characterized and available for the data reduction software.

3.5.4.8.3.1.8 Mosaicing

As the focal plane of PANIC is populated with detectors spaced 147 pixels, for projects needing contiguous coverage and analysis of large areas of sky it is necessary to take dithered images with offsets of ~167 pixels (~75.15 arcmin) or greater. In such cases, the reduction software will implement an algorithm to generate a large area image removing the cross between each detector. SWARP software and algorithms from Terapix might be used into the pipeline.

3.5.4.8.3.1.9 Astrometry and Photometry

Since astrometry and photometry are not a requirements at first light, methods will be defined further on. However, a raw astrometry, based on distortion parameters determined from the optical design, should be ready at first light.

3.5.4.8.3.2 Quick look Mode

The quick look mode will have the following main tasks:

1. Detector calibration, for instrument signature removal
    a. Dark subtraction
    b. Flatfield division
    c. Bad pixel correction mask frame
2. Sky modelling and extraction
3. Shift and align
4. Mosaicing

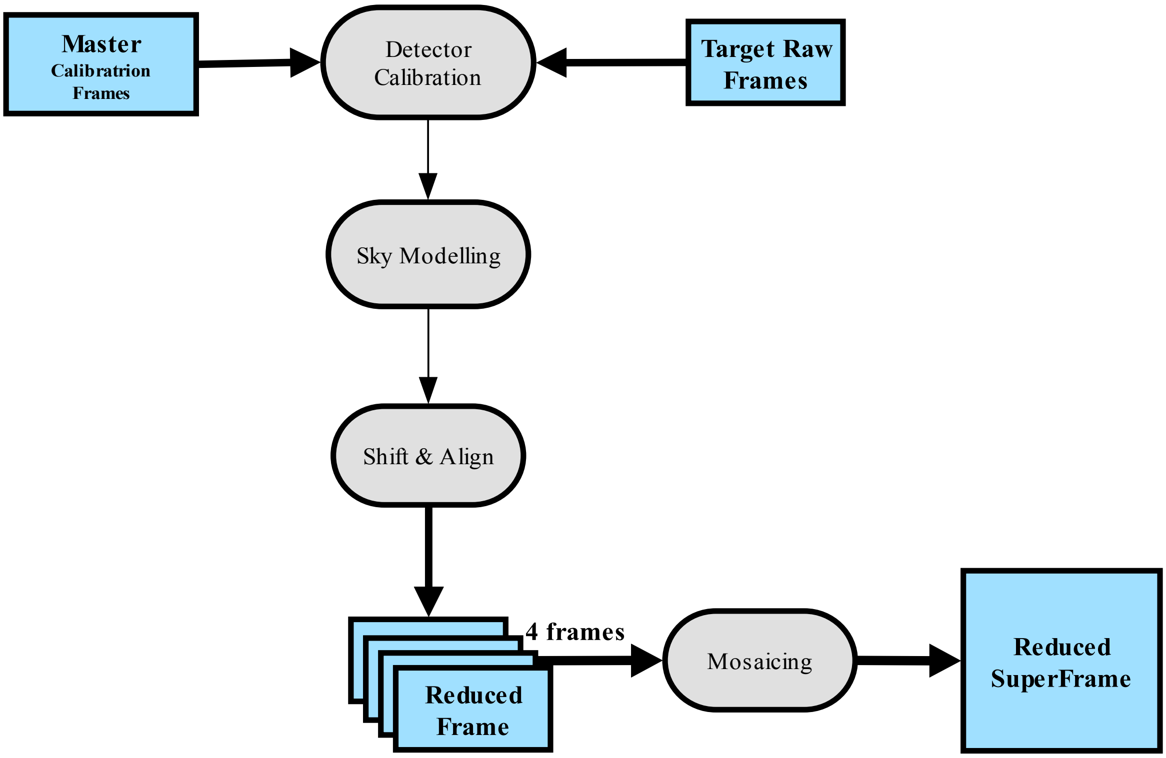

Figure 3.5.4-9 Quick reduction scheme

3.5.4.8.3.3 Science Mode

The science mode will have the main tasks described in *3.5.4.8.3.1Main steps* as shown in the next figure:

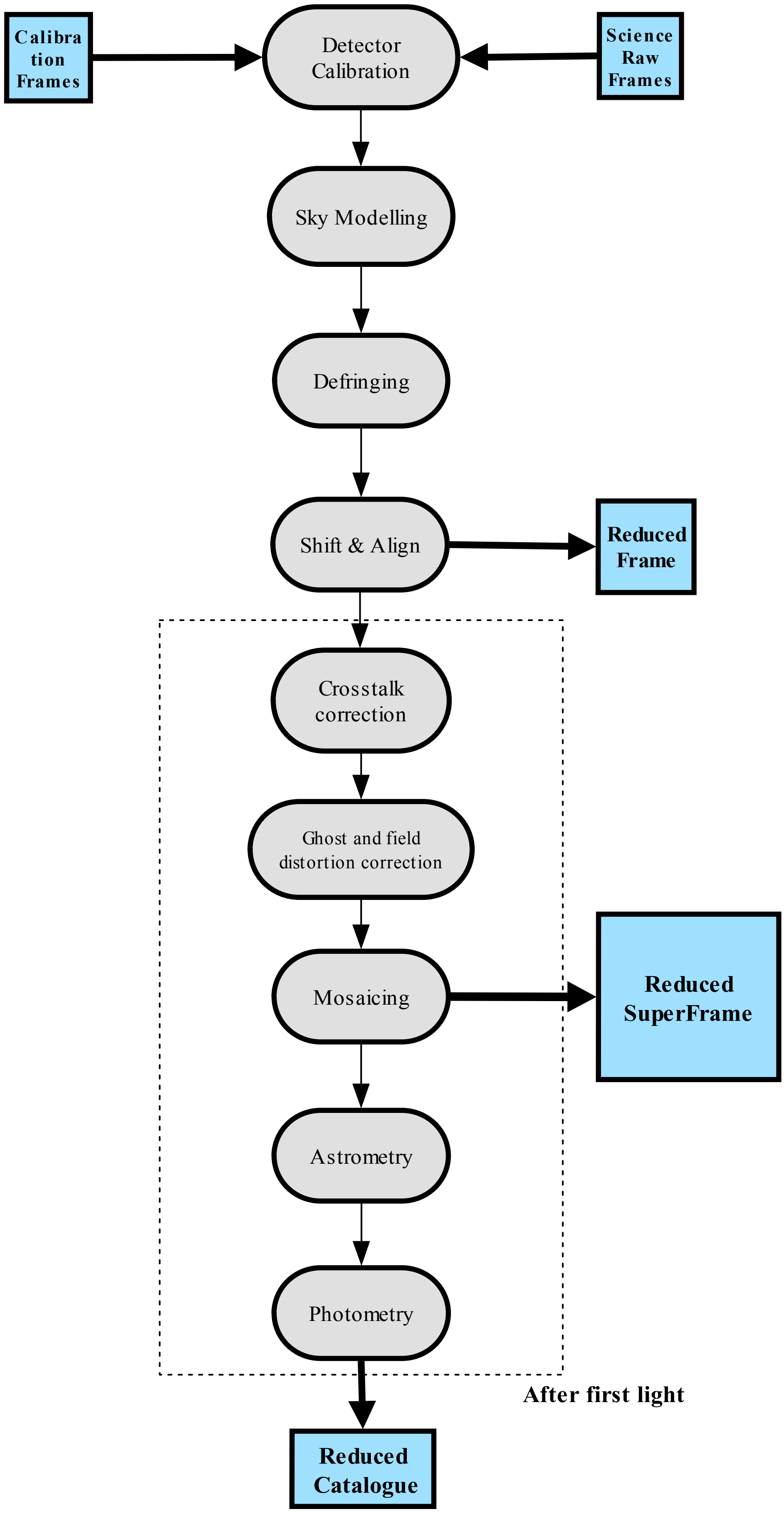

Figure 3.5.4-10 Science mode scheme

3.5.4.8.4 Implementation overview

For the implementation of the DRS we will use already publicly available software modules wherever possible and others will be own implemented. Some of the main pillars of our pipeline will be the following software modules:

- TERAPIX software: SExtractor, SCAMP, SWarp, SkyMaker, MissFITS
- CFITSIO library for FITS file manipulation
- Eclipse, *ESO C Library for an Image Processing Software Environment*
- Others common libraries

3.6 Maintenance / Operation

3.6.1 Summary

This document will present Calar Alto Technical requirements and Operations for the Panic instrument.

3.6.2 Introduction

The main reason for this part of the document is to guarantee the best integration for Panic in the Calar Alto Observatory and its standards. As known, Panic will be operated in the 2,2m Telescope at Calar Alto, and in order to guarantee the best possible operation and integration in the instrument park, and at the telescope, the instrument needs to be as compatible as possible with the rest of the instruments.

In item 3 (Technical requirements) you will find all what we consider important to obtain the best results and the best possible service in case of problems, separated in 4 different sections, these are mechanics, electronics, software, optics and cryogenics. This is a copy from the "CAHA Technical requirements for PANIC" prepared by Calar Alto staff and the Calar Alto director. This document will be revised by the PDR

In item 4 (Operation) we describe how we will prepare the instrument for the observation, and what we will do in case of technical problems.

3.6.3 Technical Requirements

CAHA Technical requirements for PANIC

3.6.3.1 Synopsis:

This document presents CAHA's technical requirements for the PANIC instrument. Science operations requirements are not part of this document.

3.6.3.2 Mechanics:

2.1.The maximum measurements for PANIC including transportation car are limited by the elevator dimensions, namely: 190 cm wide, 130 cm deep, and 200 cm high.
2.2.Maximum height at the telescope flange is 165 cm (without car).
2.3.Filling and vacuum pipes should face North.
2.4.The vacuum valve should be similar to the one used on Omega2000.
2.5.Transport car requirements:
2.5.1.Inflatable wheels, for a smoother transport.
2.5.2.Hydraulic elevation system for an easier mounting at the telescope.
2.5.3.Good access to vacuum and N2 filling pipes.
2.5.4.Good access to electronic plugs for diagnostics in the lab.
2.5.5.Possibility to tilt the instrument is desirable.
2.6.Maximum weight for PANIC is 400Kg.
2.7.The instrument must adapt to the telescope flange. Specifications can be found in the Engineering Book where the flange drawings are numbered as: 563951, drawings 1 to 3.

3.6.3.3 Electronics:

3.6.3.3.1 The electronics Rack can be mounted under the mirror cell, independent of the cryostat. This means that the cable length between the electronics rack and the cryostat will be about 4m.

CAHA requirements for PANIC, August 2007

3.6.3.3.2 To guarantee the best technical support CAHA needs a full spare electronics set.

3.6.3.3.3 Before first light, Calar Alto staff needs a full documentation set (in English).

3.6.3.3.4 Regarding electronics the documentation should include:

3.6.3.3.4.1 Block schematics for cabling between different electronic units.

3.6.3.3.4.2 Block schematics for each electronic board.

3.6.3.3.4.3 Detailed schematics for each electronic board.

3.6.3.3.4.4 Detailed electrical cabling for each electronic subsystem.

3.6.3.3.4.5 Cabling through the telescope to be decided together with Calar Alto staff.

3.6.3.3.4.6 Documentation about non standard components.

3.6.3.3.4.7 Documentation about test programs and adjusting procedures.

3.6.3.3.4.8 Extended users manual with all necessary for trouble shooting including serial and parallel port configuration.

3.6.3.3.5 The maximum acceptable power dissipation under the mirror cell will be 100W. If more is needed, a cooling system should be implemented.

3.6.3.3.6 .Before first light, at least 2 technicians from Calar Alto staff need a complete training about the electronics and software.

3.6.3.3.7 For at least the first year Calar Alto needs a contact person to solve the unforeseen problems that will appear until the system is stable and Calar Alto staff has a complete knowledge of the instrument. This contact person should be reachable also during vacations and occasionally, but rarely, during the night and weekends.

3.6.3.3.8 The first PANIC observations will be done during instrument commissioning and in contact with the hardware and software designers (if possible present at Calar Alto).

3.6.3.4 Software:

3.6.3.4.1 The disk organization will be as follow:

3.6.3.4.1.1 One disk for the system installation (/boot, swap, and / partitions).

3.6.3.4.1.2 One disk for the whole instrument software (/disk-a).

3.6.3.4.1.3 One or more disks for data (/disk-b …).

3.6.3.4.1.4 Filesystem ext3.

3.6.3.4.2 The system installation will be done by Calar Alto staff according to its own standards, SuSE Operating system, and Pc based computer.

3.6.3.4.3 Before first light Calar Alto needs a full backup of all necessary software installed in the computers necessary for the normal operation. This backup system will be tested before first light. CAHA requirements for PANIC, August 2007

3.6.3.4.4 Any non standard part in the Pc shout be acquired together with a spare part.

3.6.3.4.5 Regarding software the final documentation should include:

3.6.3.4.5.1 Disk structure.

3.6.3.4.5.2 Directory structure for the software.

3.6.3.4.5.3 Start and user scripts.

3.6.3.4.5.4 Test scripts, help programs and debug.

3.6.3.4.5.5 Description about Log files.

3.6.3.4.5.6 Changes done in the standard operating system.

3.6.3.4.5.7 Normal programs installed in the system.

3.6.3.4.5.8 Description for the different versions if available.

3.6.3.4.5.9 Description about the network structure.

3.6.3.4.5.10 Hardware and software fail procedures (How-to's).

3.6.3.4.6 In case it will be needed by CAHA staff, training of software operation will be required.

3.6.3.4.7 It is recommendable to have a RAID system to prevent data losses, as well as a DAT unit.

3.6.3.4.8 If possible the hardware should be acquired in Spain for warranty issues.

3.6.3.5 Optics and cryogenics:

3.6.3.5.1 In case that the optical fine adjustments will be done on Calar Alto, it would be desirable to mount a clean room. This room can later be used for filter changes, and all works to be done on the cryostat.

3.6.3.5.2 Transmission curves (including red leaks beyond 2.5 µm) for all filters and the other optical elements should be supplied in paper and electronic (ASCII) format.

3.6.3.5.3 The drawings of the optics shall be delivered in electronic form in a format agreed upon with CAHA.

3.6.3.6 Acceptance:

Fulfillment of all these technical requirements, together with fulfillment of science operations requirements (separate document) and successful commissioning, are necessary conditions for final CAHA acceptance.

PANIC Acceptance and Commissioning Team Calar Alto, August 2007
CAHA requirements for PANIC, August 2007
Approved by CAHA director on 17 of October of 2007

3.6.4 Operation

Before first light CAHA needs to know how much Nitrogen will be needed for normal operation, but it's assumed that the actual Nitrogen production is good enough for the Panic needs.

A few days before Panic comes to the telescope, Calar Alto staff will make the necessary vacuum, and will cool down the instrument with the Nitrogen produced in the 3,5 Telescope to its nominal values. For that purpose Calar Alto will use its own vacuum pumps.

On the day when the instrument comes to the telescope it will be properly cooled down, and the mechanics group will mount it and prepare the telescope (balance) for observation.

After installing Panic at the telescope the Electronics group will make all necessary connections and a functional test to ensure the correct working conditions from all motors and detectors.

After this the Astronomers group will prepare the instrument for the observer and if necessary they will give an introduction.

The normal operation place will be the remote observation room situated in the laboratory building.

The observer will have a backup possibility for copying his files to an appropriate data media, which must be decided in future.

During the normal operation, the instrument will be filled with Nitrogen at least once a day.

When the observing run is over, and if it will not be used, it will be stored in the Coudé room, in the 2,2m Telescope.

In case of technical problems during the observing run, the Calar Alto staff will try to solve this problems by themselves (if necessary during the night) with the possibility to change the whole electronics rack. After this emergency repair they will try to solve the problem in the lab, and if they need help, they will contact the appropriate engineers at MPIA Heidelberg, or at IAA Granada.

System backup copies will be made by the informatics group on DAT tapes, or any other media if necessary, as often as necessary, normally once per month. Programs backup will be made when there is a new program version.

The idea is to use the instrument computers (pc) only for Panic operation, other activities like data reduction should be done on other computers, and on separate disks, in order to avoid interferences in the instrument operation.

In case that operating system patches must be installed, Calar Alto staff will make a system backup before installing patches, especially if they include the kernel.

In case that the Panic cryostat must be opened, Calar Alto staff will take the maximum possible care to ensure a clean and electrostatic sure environment, in consideration that actually there is no clean room available.

4. MANAGEMENT

4.1 Summary

In this document we describe management issues - how the project is split into work packages, how assembly and integration are planned, cost, manpower and schedule.

4.2 Work Packages

Since PANIC is build by two institutions it is necessary to split the whole project into well separated, well defined work packages, in order to minimize internal friction and traveling. We have also assigned the work packages according to the experience of each institution. The project was split into the following work packages:

- *Optics:* the optics calculations are done by IAA under guiding by MPIA since this is new to IAA. IAA will also contact the manufacturers, monitor the test protocols during fabrication, and will also take care of specifying and ordering of the filters. Since MPIA has more experience in these affairs, MPIA will be contacted and informed at each step.

- *Mechanics:* MPIA will make the design of the whole instrument, detail the drawings of the cryostat as required by industry and take care of fabrication of the cryostat by local industry. Wheels and lens holders will be designed and manufactured at MPIA. IAA has already participated in the design process and has interest to continue.

- *Instrument hardware and detector control*: Will be included in MPIA GEIRS software. MPIA will also take care of testing and optimizing the read-out of the detectors.

- *Read-out electronics*: The read-out electronics is build at MPIA, based on previous systems. This includes also firm/software to store the data in the computer memory so there is a clear-cut division to the data retrieval software.

- *Control electronics*: This includes temperature and pressure sensors, temperature controller for the detector, controller for the wheels. This will be build by MPIA.

- *Integration, lab tests:* MPIA has the facilities for this, so these work packages will be done at MPIA. IAA will participate.

- *Observation tool, data retrieval, pipeline, archiving:* this will be developed by IAA.

The experience during the first year of cooperation is excellent and shows that this division is very reasonable.

4.3 The panic team

The following people form the PANIC team:

Mathias Alter	Control Electronics
Harald Baumeister	Design
Concepcion Cardenas	Optics
Josef Fried	PI
Jens Helmling	Calar Alto feedback
Jose Miguel Ibanez	Software
Julio Rodriguez	Project Management
Werner Laun	Cryotechnique
Ulrich Mall	Read Out Electronics
Marcos Ubierna	Design
Matilde Fernandez	CoPI, Science
Jose Ramos	Read Out Electronics
Ralf-Rainer Rohloff	Design
Clemens Storz	Software
Vianak Naranjo	Detectors
Karl Wagner	Electronics

Former team members: Lourdes Verdes Montenegro and Bernhard Grimm.

4.4 Assembly and integration

The logical place for lab-tests, assembly and integration of PANIC is clearly MPIA, since the hardware is build and/or assembled here. Thus we will have the support from MPIA's well equipped mechanical and electronics shops. In addition, MPIA has laboratories suited for such purposes, and a large park of all kinds of equipment, both electronical and mechanical.

For the tests of detectors, MPIA has a test dewar which is large enough to house the FPA. Influence of gravity on the instrument (functionality of movable parts, optical quality) can be checked by means of a mechanical mounting system, which allows the instrument to be moved in any direction.

We intend to hire a student in the lab test phase, probably also for the commissioning runs. IAA will participate in this phase.

4.5 Manpower

In the following table we list the manpower required for the progress of the project according to the schedule in units of man-months. The numbers for 2006 and 1/2007 are really allocated time, the rest of the table estimates. The listing corresponds to the departments at the institutes. Instrumentation group at MPIA comprises participation in the grand design of the cryostat, test of the detectors individually and optimization of the read-out process for the array. Software MPIA includes read-out of the array and hardware control. Design IAA means participation of Marcos Ubierna during design and integration.

	2006 2	2007 1	2007 2	2008 1	2008 2	2009 1	2009 2	2010 1	2010 2	2011 1	2011 2	total
Optics	6	6	6	7	2	2	6	4	3			42
Design MPIA		2	3	3	1	2						11
Design IAA		0.75	0.75	0.5	0	1.5	1.5	0.5	1.5			7
Mech.shop					12	12						24
Electronics			5	9	9	6	6	3				38
Instr.group		1	1.5	2	3	4	4	1.5	1.5	1	0.5	20
Software MPIA		2	2	2	2	2	2	2				14
Software IAA	1	3	4	4	6	6	6	6	4	3	2	45
Management MPIA	1	3	3	3	2	4	4	4	4	2	1	31
Management IAA	3	3	3	3	3	3	3	2	1	1	1	26

Total	11	20.75	28.25	33.5	40	42.5	32.5	23	15	7	4.5	258

4.6 Cost and Financial plan

The cost listed below is exact for detectors and electronics. First offers for filters are $10000 each. Only crude estimates can be made at this stage for cryostat and optics. *This table does not include cost for man power.*

Detectors	1,050,000 (= $1,490,000)
Optics	260,000
Filter	150,000
Cryostat	150,000
Electronics	30,000
Computers etc	10,000
miscellaneous	30,000
Travel expenses	30,000
Total	**1,710,000**

According to the schedule, this results in the following financial plan:

2007	255,000	250,000 detectors 5,000 travel
2008	765,000	550,000 detectors 150,000 cryostat 60,000 electronics, misc. 5,000 travel
2009	680,000	250,000 detectors 260,000 optics 150,000 filters 10,000 computers 10,000 travel
2010	10,000	10,000 travel

The dates of the rates for the detectors are as requested by Teledyne in their offer. The other expenses have to be distributed over the years 2008 and 2009; if these are outside the budget, one might consider to buy only a subset of the filters or aim at delivery of filters early 2010.

4.7 Schedule

The schedule is shown on the next page. An important date is the assembly of the instrument early 2009. This requires that the cryostat, including all interior parts, is finished, and the detectors and the read-out electronics are working, at least in a non-optimized way. For integration of the whole system and laboratory tests we have foreseen 1 year. Since MPIA has much experience gained from the Omega2000 project, we are confident that the cryostat and the wheels will not cause major problems. So most of this time will be devoted to optimization of the read-out. First light will be in 2010, and we plan to optimize the instrument during about 3 commissioning runs, so that it will be available for the astronomical communities in 2011.

The schedule rests on three assumptions: (i) the manpower required is actually allocated to the project (ii) the time of delivery of the detectors is 18 months as promised by Teledyne in their offer and (iii) the detectors fulfil the specifications.

Assumption (i) may be optimistic, since the design office at MPIA is currently overbooked by a factor of about 2. The schedule assumes that the design of the cryostat to the level required by industry can be finished until about march 2008, and the design of the interior parts (lens holders, wheels, mirror mounts) is finished during summer, so that the manufacturing of these parts can start in September and be finished early 2009, so we can proceed with the assembly and integration of the instrument. Any delay here clearly leads to a delay of the whole project.

Assumption (ii) is delivery of the detectors until February 2009, as promised by Teledyne. Past experience, however, has shown that this might be optimistic. Furthermore, it is also very important that *all* channels of *all* detectors work well (assumption iii). Past experience, however, has shown that this, too, might be optimistic.

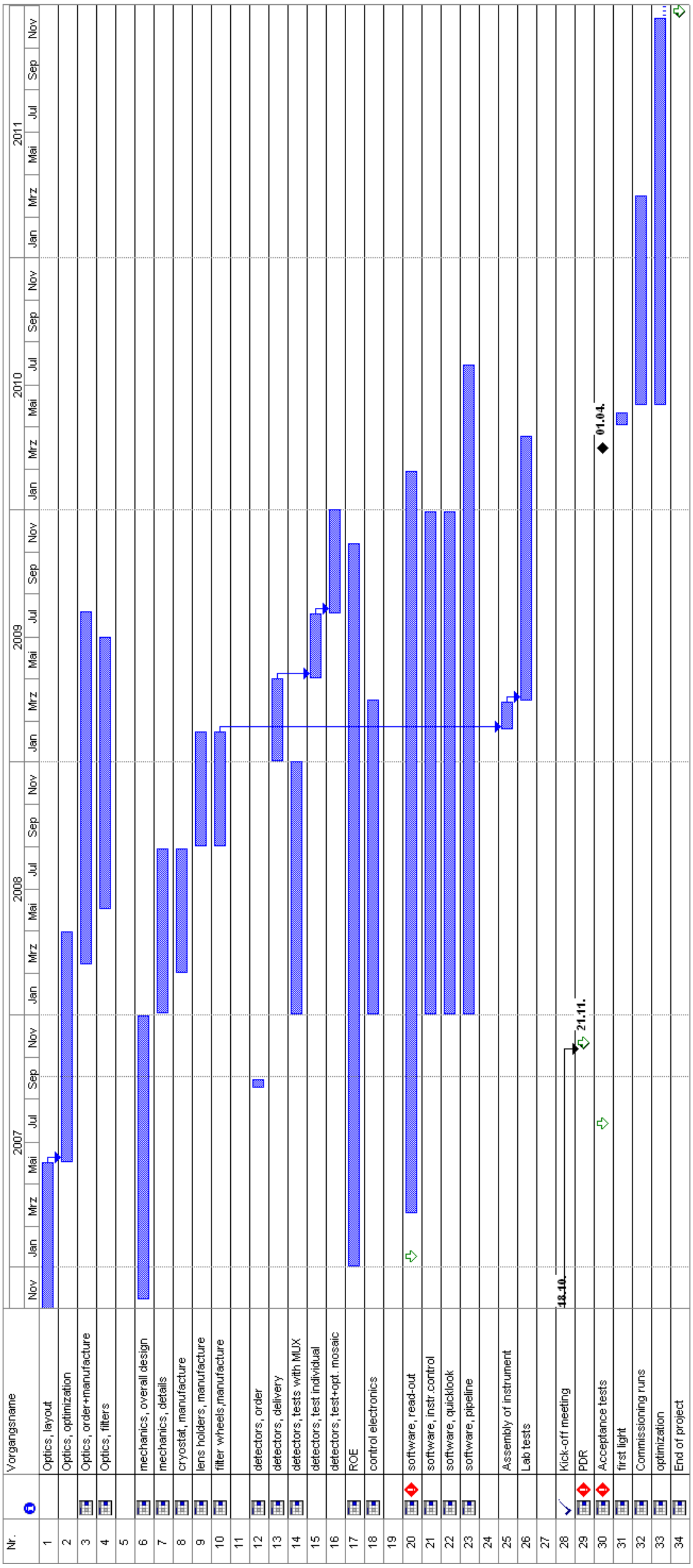
Nr.
Vorgangsname
1 Optics, layout
2 Optics, optimization
3 Optics, order+manufacture
4 Optics, filters
5
6 mechanics, overall design
7 mechanics, details
8 cryostat, manufacture
9 lens holders, manufacture
10 filter wheels,manufacture
11
12 detectors, order
13 detectors, delivery
14 detectors, tests with MUX
15 detectors, test individual
16 detectors, test+opt. mosaic
17 ROE
18 control electronics
19
20 software, read-out
21 software, instr.control
22 software, quicklook
23 software, pipeline
24
25 Assembly of instrument
26 Lab tests
27
28 Kick-off meeting
29 PDR
30 Acceptance tests
31 first light
32 Commissioning runs
33 optimization
34 End of project
2007
2008
2009
2010
2011
Nov
Jan
Mrz
Mai
Jul
Sep
18.10.
21.11.
01.04.